TEXTILE RESEARCH JOURNAL

VOL. XXII, No. 10 October, 1952

Relation Between Certain Defects in Dyed Fabrics and Mechanical Damage in Wet Processing*

D. M. Cates,† K. S. Campbell, and Henry A. Rutherford

Department of Textile Chemistry and Dyeing, School of Textiles, North Carolina State College, Raleigh, North Carolina

Introduction

One type of physical damage to cloth which is encountered all too frequently in certain branches of the textile industry is that produced by abrasion or related mechanical distortion. The effect of such action may become evident in marks on the surface of the fabric; these marks have been termed "lay marks," "rub marks," "crease marks," "chafe marks," "rope marks," "bruise marks," etc. Apparently, they may result whether the physical action to which the fabric is subjected is simple creasing or rubbing, or actual abrasion, resulting in easily observable fiber damage. Physical distortion or destruction of this sort may occur in almost any wet-processing stage after the yarn has been made into cloth, but ordinarily does not become a problem before the dyeing operation; in fact, except for the effect produced in dyeing, it would probably be considered of no importance or go unnoticed altogether. This is because the marks left on undyed cloth may not readily be visible to the eye except when viewed carefully from the proper angle. The photographs in Figure 1, showing the same piece of undyed abraded cloth held at different angles, illustrate this. (This specimen was obtained from actual mill production.) These are two photographs of a piece of cloth stretched on an embroidery hoop. In the top photograph, the cloth is turned about 90° from its position in the lower photograph. The chafe marks in this case outline a more or less triangular area. When such a fabric is dyed, the abrasion mark is usually much more apparent to the eye; its appearance depends upon the contrast with the unabraded area, and it can be related to the different ways in which the two dyed surfaces (*i.e.*, abraded and unabraded) reflect light. This phenomenon is among those discussed in the review entitled "Luster and Cotton," by Buck and McCord [6]. It can easily be demonstrated that an abraded area in a fabric which has been dyed to equilibrium can be made to range from slightly darker to considerably lighter than the background by turning the fabric at different angles to the light. This effect, obviously, is optical in nature. As such, it constitutes one factor which must be considered in any discussion of this subject. Previous work in this laboratory by Jenkins and Keels [11] showed that

* Presented in part at the Spring Meeting of The Fiber Society at Clemson, S. C., Apr. 17, 1952.

† Present address: Textile Research Institute, Princeton, N. J.

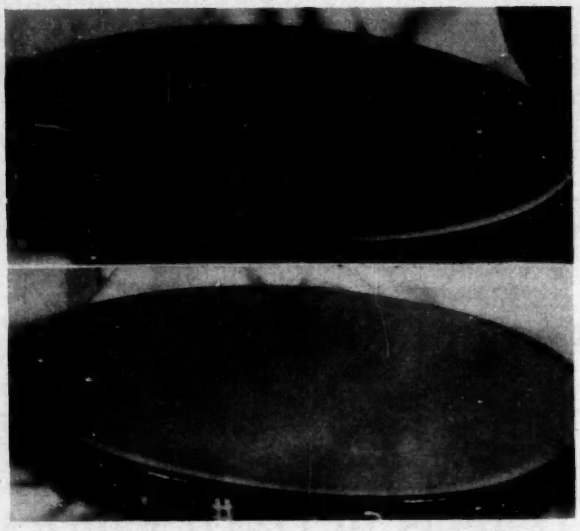

FIG. 1. *Abraded fabric from two angles of view. In the top photograph the ring is turned about 90° from its position in the lower photograph.*

with many abraded samples, however, there was definitely more than an optical effect involved, as evidenced by a striking color contrast between abraded and unabraded portions when the specimen was dyed according to the differential dyeing technique of Goldthwait and coworkers [9]. The explanation of this behavior involves the second and, we believe, more important factor in the problem and the one with which we are immediately concerned—namely, a differential rate of dyeing. Its importance arises from the fact that in many cases in commercial dyeing it is uneconomical and otherwise impractical to dye to equilibrium. When a fabric is dyed and removed from the dye bath before equilibrium is reached, the abraded area is often found to be much darker than the background, regardless of the direction of the incident light or the viewing angle. This effect is utilized in the Clegg test [7], in which the dye Congo red, when applied for a limited time to cellulose fibers which previously had been swollen in sodium hydroxide, stains the damaged areas in marked contrast to undamaged areas, thus identifying and locating mechanical and chemical breakdown of the fiber. Such contrast between damaged and undamaged portions in this test, or in commercial dyeing, is, in reality, a differential rate of dyeing effect, and is the subject of the present paper. The purpose of this work has been to gain some fundamental knowledge of the mechanism involved in uneven dyeing attributable to mechanical damage, with the hope that such knowledge might lead to practical corrective measures.

Materials and Methods

The fabrics used in this study were cotton, viscose, Bemberg, acetate, and Fortisan—all plain-weave fabrics, except for the cotton, which was a five-harness sateen. All of the regenerated fibers were continuous filament, with the exception of the viscose, which was staple fiber. The mechanically damaged specimens for study were obtained in several ways. Some of the samples were abraded by placing them on the moving peg of the standard A.A.T.C.C. Crockmeter [1] and subjecting them to three strokes against very fine sandpaper. This was considered a very light treatment. Some samples were abraded with sandpaper by hand to a point just short of complete destruction of the weave. Treatments such as this could not be duplicated closely, but the intent was primarily to find out whether a differential rate of dyeing between the abraded and unabraded portions would exist under various conditions of dyeing. Other samples were abraded to various degrees on the Schiefer Abrasion Machine [15] in order to determine the influence of extent of abrasion.

The method used for preparing dewaxed and depectinized cotton was essentially that of Mease and Worner [18]—that is, an alcohol extraction followed by successive boilings in 1% sodium hydroxide.

The so-called "differential dyeing" procedure described by Goldthwait, Smith, and Barnett [9] was used, and the individual dyes called for in this procedure were also employed alone throughout this work since they were ideally suited for minimizing or maximizing rate-of-dyeing differences. These two dyes were Diphenyl Fast Red 5BL (Geigy) and Chlorantine Fast Green BLL (Ciba). According to Boulton [4], their "times of half-dyeing"—an excellent measure of the comparative diffusion rates under practical dyeing conditions—are 0.88 min. for the red and 55 min. for the green dye, a ratio of nearly 63 to 1. The molecular weight of the green dye is about twice that of the red.

The rate of dye exhaustion was determined on ½-g. samples dyed in 0.5% salt solution at a liquor-to-goods ratio of 50 to 1. In one series 0.65% Chlorantine Fast Green BLL was used, and in another 1.25% Diphenyl Fast Red 5BL. Dyeing was

carried out for 2 hrs., except in some cases where the duration was extended to allow equilibrium to be reached. The amount of dye left in the dye bath was determined spectrophotometrically in the usual manner. For the dyeings using alcohol, a saturated solution of Congo red in 95% alcohol was made up. This, in turn, was diluted with water and alcohol so as to give dye solutions in which the dye concentration was kept constant but in which the amount of water was varied in a succession of steps from 5% to 80%. In experiments using alcoholic solutions of dye, the samples were first dried at 110°C for 20 hrs. They were then immediately transferred to the dye solution, dyed 2 min., rinsed 2 min. in 95% alcohol, and dried.

Results and Discussion

Figure 2 (top) shows an abraded spot on cotton which had been dyed differentially by the Goldthwait technique. The abrasion was accomplished with three strokes of the Crockmeter against fine sandpaper. There is no question about the location of the abraded area.

The differential dyeing method depends for its effect upon the widely variant diffusion rates of the component dyes to exaggerate inherent differences in dyeability within the material being dyed. The positive result obtained on abraded cotton fabric is good evidence that mechanical damage alters the rate of dyeing. The problem, therefore, concerns the nature of and the reasons for this change in dyeing rate.

Simultaneous dyeings were made on cotton fabric which had not been abraded and on cotton which had been abraded over the greatest part of its surface, using the rapid-dyeing red dye in one series and the slow-dyeing green dye in another series. Figure 3 shows the percent exhaustion (determined from the amount of dye left in the dye bath) of each dye on both abraded and unabraded fabric plotted against time at 93°C. (It is difficult to estimate the percentage of abraded fiber surface in a sample, but in this case it was probably less than 50%.) As indicated by the curves of Figure 3, there is little doubt that in the case of the slow-dying green dye a difference in dyeing rate exists for the abraded and unabraded fabric, but that for the rapid-dyeing red dye under the conditions of this experiment the difference is insignificant. However, if the temperature is lowered, we get the effect shown in Figure 4, which

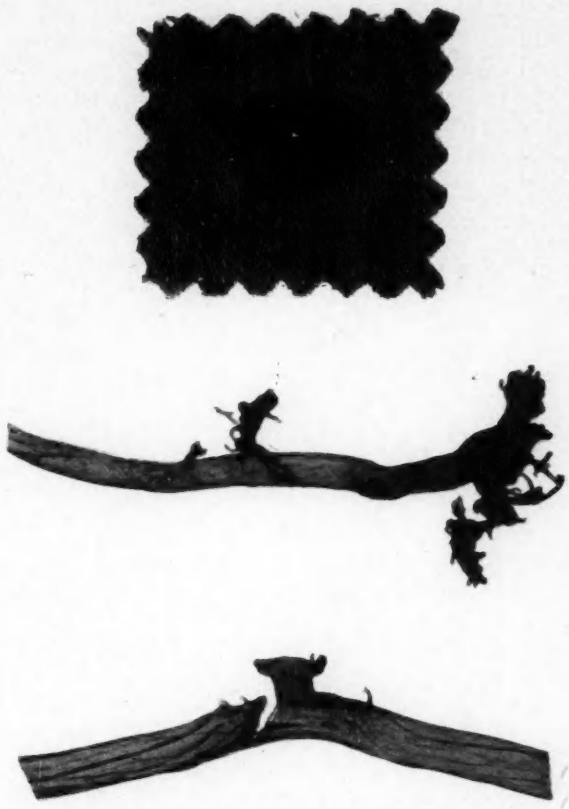

FIG. 2. Top—*Cotton fabric, abraded, then differentially dyed.* Middle—*Cotton fiber taken from abraded differentially dyed fabric (magnification, 375 ×).* Bottom—*Viscose fiber taken from abraded differentially dyed fabric (magnification, 375 ×).*

shows the difference in exhaustion of the red dye at three different temperatures on abraded and unabraded material. It is plain that a difference in dyeing rate due to abrasion is much more marked at lower temperatures. The importance of the temperature effect in practical dyeing is obvious.

Since the curves shown are all more or less parallel in the later stages of dyeing, it is apparent that the rate differences occur in the initial stages. The amount of Chlorantine Fast Green BLL actually adsorbed at or close to equilibrium is virtually the same for both abraded and unabraded portions, as shown in Table I. Presumably, this result would also be true for other dyes.

The contrast between abraded and unabraded areas is dependent upon two factors. These are: (*a*) the magnitude of the initial rate difference; and (*b*) the nearness of approach to equilibrium dyeing. Figure 5 should make this clear. Note that as dyeing is

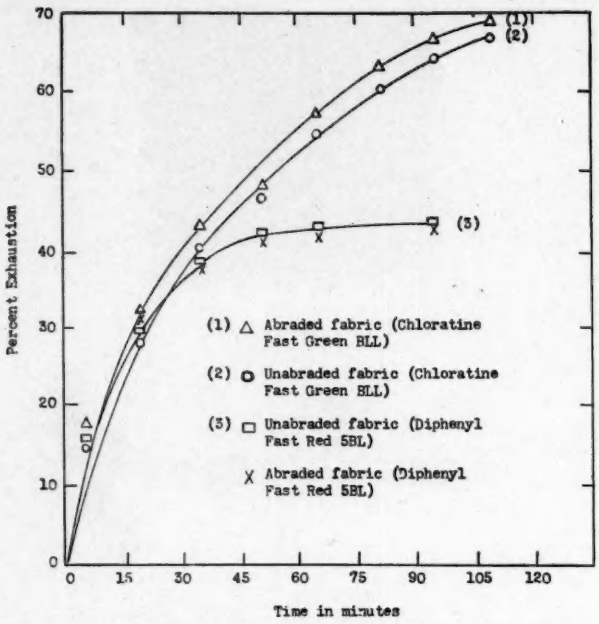
Percent Exhaustion
Time in minutes
(1) △ Abraded fabric (Chloratine Fast Green BLL)
(2) ○ Unabraded fabric (Chloratine Fast Green BLL)
(3) □ Unabraded fabric (Diphenyl Fast Red 5BL)
X Abraded fabric (Diphenyl Fast Red 5BL)

FIG. 3. *Exhaustion of Chloratine Fast Green BLL and Diphenyl Fast Red 5BL on abraded and unabraded fabric at 93°C.*

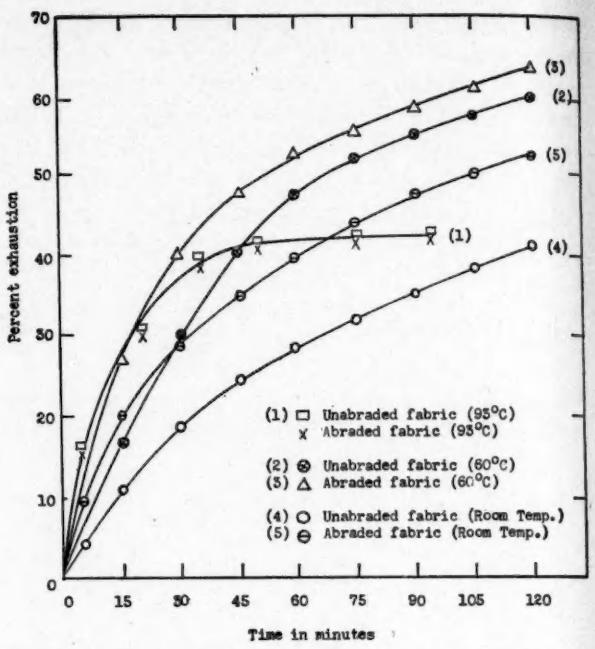
Percent exhaustion
Time in minutes
(1) □ Unabraded fabric (93°C)
x Abraded fabric (93°C)
(2) ⊛ Unabraded fabric (60°C)
(3) △ Abraded fabric (60°C)
(4) ○ Unabraded fabric (Room Temp.)
(5) ⊖ Abraded fabric (Room Temp.)

FIG. 4. *Effect of temperature on the exhaustion of Diphenyl Fast Red 5BL on abraded and unabraded fabric.*

continued—*i.e.*, as equilibrium is approached—the contrast between the abraded area and the background becomes much less marked. After a dyeing time of 48 hrs., the difference in appearance can be considered purely an optical one, since, as the sample containing the abraded spot is moved about so as to change the angle of viewing and of the incident light, the contrast can be either light against dark or dark against light. From most angles, however, the abraded area will appear lighter than the background; incidentally, while this latter effect can be obtained by abrading an already dyed sample, the opposite effect—a dark abraded spot against a light background—cannot be obtained in this way. Figure 6 shows the transition of contrast with time of dyeing much more clearly because the sample was held in such a manner as to accentuate the contrast to the fullest possible extent.

In all of the above tests it was observed that although the abraded fabric always adsorbed more dye than unabraded fabric before equilibrium was reached, if special care were not taken, the magnitude of the differences between abraded and unabraded

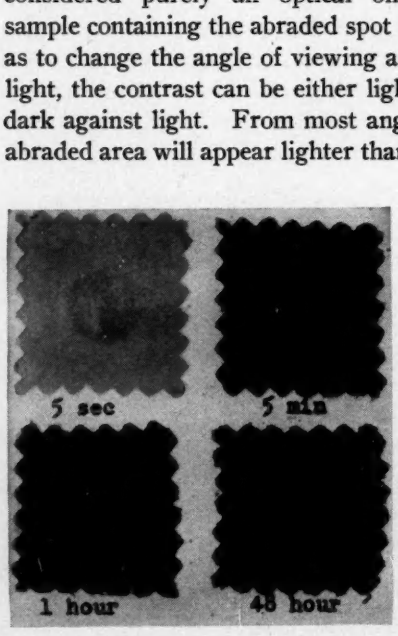

FIG. 5. *Abraded cotton, showing differential rate of dyeing.*

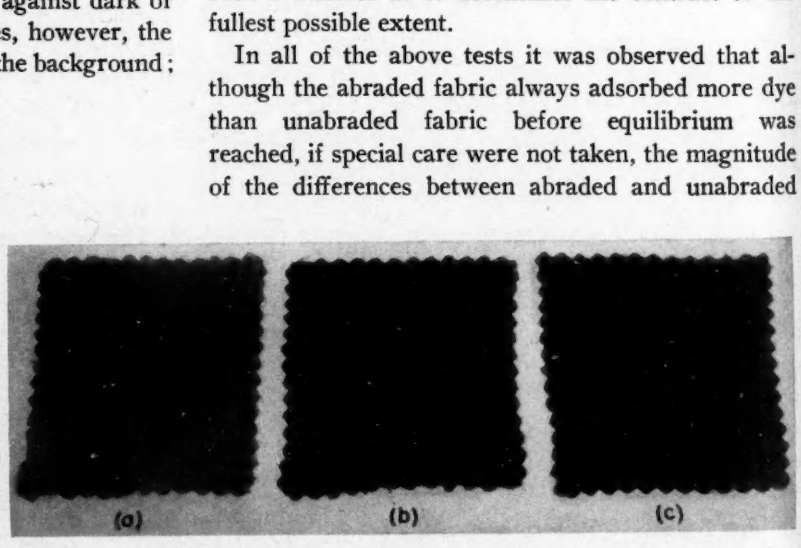

FIG. 6. *Transition of contrast with time of dyeing on abraded cotton.* (a) *5 min.* (b) *1 hr.* (c) *48 hrs.*

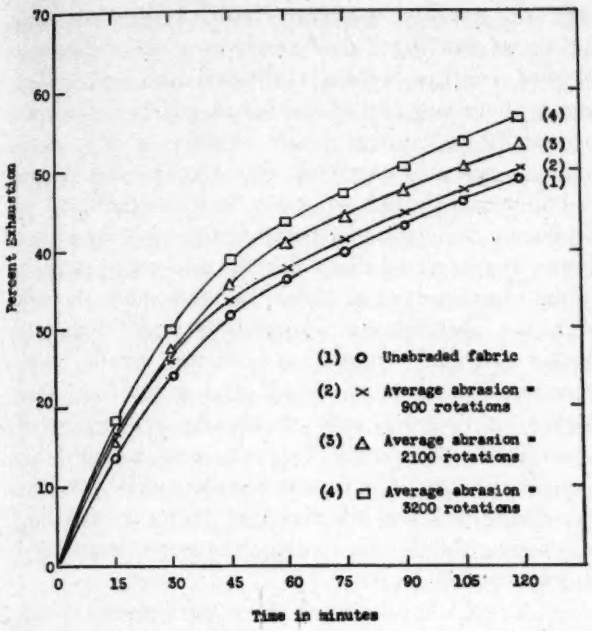
Percent Exhaustion
Time in minutes
(1) Unabraded fabric
(2) Average abrasion = 900 rotations
(3) Average abrasion = 2100 rotations
(4) Average abrasion = 3200 rotations

FIG. 7. *Effect of degree of abrasion on rate of dye adsorption.*

areas in replicate samples would not be constant. This is believed to be due to differences in the degree of abrasive action. In order to determine the effect of the extent of abrasion, samples were abraded to varying degrees by means of the Schiefer Abrasion Machine, dyed with the green dye, and the exhaustion was plotted against time, as before. The results are shown in Figure 7. It is plain that the degree of abrasion suffered can materially affect the rate of dye adsorption.

An attempt was next made to discover the causes of the dyeing behavior which has been described. The first experiment was carried out to determine whether the mechanical abrasive action removed wax and pectin, which are known to be concentrated in the outer or primary wall of the cotton fiber, thus possibly permitting greater local adsorption of dye. Samples were carefully dewaxed, depectinized, and then abraded; on dyeing, the samples showed practically identical contrast with specimens which were not so purified. This proved that this possibility is without foundation.

TABLE I. AMOUNT OF CHLORANTINE FAST GREEN BLL* ADSORBED BY ABRADED AND UNABRADED FABRIC AFTER 2 DAYS AT 93°C

Milligrams of dye absorbed per gram of fabric		
Abraded fabric	Unabraded fabric	Ratio
5.97	6.00	1.00
5.76	5.66	1.02
4.65	4.63	1.00
4.28	4.28	1.00
2.76	2.79	.99

* Different initial concentrations of the dye were used.

The factor of increase in surface area must be given serious consideration. A number of workers [5, 17] have pointed out the importance of available surface area in determining the dyeing rate. Armfield and Boulton [2] have shown that differentially dyed rayon becomes greener with decreasing denier. The amount of surface which is immediately available to dye is increased by abrasion in two ways: by the creation of what might be called "fuzz fibers," by severing and raising or napping fibers that make up the yarn; and by roughing up and tearing the individual fibers. The raised fibers in a differentially dyed specimen can easily be seen under the low-power microscope to be somewhat darker green than the yarns from which they were raised, so that this extra surface must undoubtedly be a factor. However, the yarns beneath are also distinctly green in comparison with unabraded yarns. This can be observed visually and demonstrated easily by removing the fuzz fibers from the surface with an electric razor. The question is whether the roughness of the fibers represents enough increased surface to account for the preferential dyeing with green dye. Abraded yarn and fibers under the microscope do not appear, by visual estimate, to have increased impressively in surface area, and it seems doubtful that this alone contributes appreciably to the effect. Furthermore, it was observed in the microscopic examination of fibers which had been removed from differentially dyed abraded fabric that the green dye not only showed up strongly in the area where the fiber wall was ruptured, but also apparently had diffused into the fiber for a considerable distance adjacent to the point of rupture. These results, together with the experiments which followed, led to the conclusion that, in itself, increase in surface area due to abrasion plays a relatively minor part in the phenomenon being studied.

Figure 2 (middle) shows what an abraded differentially dyed cotton fiber looks like under the microscope. It is apparent that the physical disruption of the outer portion of the fiber has affected the ease with which the dye diffuses into the fiber in areas ex-

tending for some distance around the actual point of damage.

At this point, it may be desirable to review briefly certain aspects of the structure of cotton and rayon fibers, especially with regard to their outer walls and their swelling properties. The fine structure of the cotton fiber has been studied by a number of workers. It seems generally agreed that the primary wall is very thin—0.2μ or less—and that the fibrils or component members of this wall are arranged in a fine interwoven network structure. In turn, the outer layer of secondary thickening, referred to by Hock, Ramsay, and Harris [10] as the "winding," lies just beneath the primary wall. It, too, is extremely thin. Because of its similarity to the primary wall, Rollins [14] has referred to the two together as the "fiber sheath." As such, they enclose the central areas, the component fibrils of which lie much more nearly parallel to the long fiber axis than do the structural members of the sheath. In fact, the fibrils of the central area—which area comprises 90% or more of the fiber—apparently lie perpendicular to the crystalline strands of the winding and at a large angle to whatever crystalline cellulose exists in the primary wall [3]. Because of these angular relationships, it is to be expected that the sheath would have considerable influence upon the swelling characteristics of the cotton fiber. The formation of beads or balloons when the fiber is swelled in cuprammonia, and the inversion of cross sections of purified fiber in cuprammonia, as reported by Hock, Ramsay, and Harris [10], have been attributed to the differential swelling brought about under certain conditions by the restrictive influence of the winding and primary wall on the lateral expansion of the main body of the fiber.

The ability of a fiber to swell is recognized as being essential to the dyeing of the fiber; the more hydrophobic a fiber, the less the fiber swells and the more difficult it is to dye. By the same token, a variation in the degree of swelling at various points in the same fiber should exert considerable influence upon the rate of dyeing at these points. When portions of the outer wall are removed by mechanical action, unrestricted swelling of the cellulose beneath is permitted, and the rate of dye diffusion into this area is much more rapid than into adjacent restricted areas.

If these statements are correct, and the degree of swelling is vital in the dyeing variation between abraded and unabraded areas, then a series of dyeings on abraded material under controlled conditions of swelling should result in a series showing *marked* contrast between abraded and unabraded areas where swelling is maximum, grading down to practically no contrast where swelling is at a minimum. Such an experiment was made, using Congo red in alcohol-water solutions so constituted as to produce a systematic decrease in the swelling of the fiber. It was found that while the unabraded portion of the samples dyed to about the same shade in each case, the abraded area progressed from definitely darker to slightly lighter, as compared to the background, decreasing in depth and giving a lesser degree of contrast with decreasing proportion of water in the dye bath. This was only a qualitative experiment, but it gave considerable weight to the hypothesis that the difference in degree of swelling was responsible for the dyeing differences in abraded and unabraded areas.

Dyeings made on viscose rayon gave results which were similar to those obtained on cotton fabric. An abraded area on viscose fabric dyed green in the Goldthwait differential dyeing method, and to an initially darker shade when a single dye was used.

Morton has reported [19] that alcoholic solutions of direct dyes fail to color viscose. However, experiment showed that when abraded viscose was placed in an alcoholic solution of Congo red for 2 to 4 days, the abraded areas were dyed. In this period of time the cut edges of the fabric were also stained, indicating that if the outer portion of the viscose fiber could be by-passed in some way, dyeing could take place.

An examination of the differentially dyed viscose fibers under the microscope revealed that the dye is preferentially adsorbed in damaged areas, just as was observed in cotton fibers. Figure 2 (bottom) shows one of these viscose fibers.

Sufficient information is available so that it seems safe to say that this behavior of viscose rayon is due to a difference in density between the skin and the core of the fiber. Preston [13], Schramek [16], Morehead and Sisson [12], and Elöd [8] are among those who have worked on this subject. Morehead and Sisson have shown that in water the core of a viscose fiber swells about 40% more than the skin. This greater swelling capacity evidently gives the core a potentially higher rate of dye adsorption.

Elöd [8] showed that swelling ability decreases with an increase in density, and that the radial

density of both rayon nad cotton decreases in the direction of the center of the fiber, resulting in relatively greater swelling in the interior portions.

Elöd also pointed out that in the case of Cuprama fiber (cuprammonium staple) the radial density varies in an opposite direction to that in viscose, the density being slightly greater in the interior. This suggested that a fabric of cuprammonium rayon should not show the differential rate of dyeing effect which is characteristic of viscose and cotton, since exposure due to abrasion of denser, inner cellulose of lower swelling capacity should have little effect upon the dyed appearance. It was found, however, that abraded cuprammonium rayon fabric did exhibit the differential dye effect, although the effect was much less pronounced than for viscose or cotton under the same conditions. It was not learned until later that "Cuprama" referred only to staple cuprammonia; filament was used in the experiment, and this may have affected the result.

Experiments made using Fortisan fabric showed that when the damage done by abrasion was sufficiently extensive, the differential dye effect shown with viscose could be obtained; under these conditions, the abraded areas also dyed darker when a single dye was used.

When dyed with dispersed acetate dyes, abraded cellulose acetate material was also found to show a differential rate of dyeing very much like that of viscose and cotton. The effects noted on Fortisan and acetate are somewhat surprising inasmuch as the techniques which were used to show the presence of a skin on viscose did not indicate a skin on Fortisan, nor apparently has any evidence been reported in the literature of a radial variation in structure for either the Fortisan or acetate fiber. Nevertheless, in view of the fact that they do show a differential rate of dyeing when abraded, a radial variation is apparently a possibility.

As an alternate hypothesis, it may be that mechanical distortion or stress applied to the fibers, whether it brings about permanent visible damage or not, can produce enough change in the amorphous area of the fiber to affect its affinity for dye at the site of such distortion. Such an hypothesis has the advantage of accounting for nonuniformities in dyeing where no actual mechanical wear has taken place. It is unlikely, however, that existing methods would be able to measure changes in crystalline-amorphous ratios of this order.

Summary and Conclusions

In summary, it has been shown that mechanical damage by abrasion on the surface of cotton, viscose, Fortisan, and acetate fibers results in an increase in the initial rate of dyeing at the damaged area. This produces an abraded area appearing darker than the undamaged background up to the point where the amount of dye actually adsorbed is approximately the same in both areas. This point may occur in a matter of minutes or hours, depending upon the nature of the dye, the degree of abrasion, and external conditions; when both areas contain approximately the same amount of dye, any apparent difference in depth of shade between the two areas is optical in nature, and it is most common for the abraded portion to appear lighter.

It is believed that the initial more rapid adsorption in the damaged areas is due in large part to a greater degree of swelling brought about by partial removal of restricting outer layers of the fiber. The increased swelling means more rapid diffusion into the fiber and adsorption of the dye in those areas.

Alternately, it can be postulated that mechanical stresses of various types increase the amount of amorphous area in the fiber, with consequent increase in dye affinity in localized areas.

Based on the observations described, any measures taken to minimize abrasion marks in dyeing already damaged fabric must involve careful selection of dyes, proper consideration of time and temperature effects, and no small amount of good luck.

Literature Cited

1. American Association of Textile Chemists and Colorists, "Year Book 1944," New York, Howes Publishing Co., p. 192.
2. Armfield, W., and Boulton, J., Application to Viscose Rayon of the Differential Dyeing Test for Cotton Maturity, Textile Research Journal **19**, 212 (1949).
3. Berkley, E. E., Cotton—A Versatile Textile Fiber, Textile Research Journal **18**, 71 (1948).
4. Boulton, J., The Importance of Dyeing Rate—An Interpretation for the Practical Dyer of Recent Research in Direct Dyeing, *J. Soc. Dyers Colourists* **56**, 145 (1944).
5. Boulton, J., and Morton, T. H., The Dyeing of Cellulosic Materials: A Review of the Physics and Chemistry of the Dyeing Process, *J. Soc. Dyers Colourists* **56**, 145 (1940).
6. Buck, G. S., and McCord, F. A., Luster and Cotton, Textile Research Journal **19**, 715 (1949).

7. Clegg, G. G., The Examination of Damaged Cotton by the Congo Red Test: Further Developments and Applications, *J. Textile Inst.* **31**, T49 (1940).
8. Elöd, E., Influence of Fiber Structure of Rayon on Swelling and Radial Density, TEXTILE RESEARCH JOURNAL **16**, 432 (1946).
9. Goldthwait, C. F., Smith, H. O., and Barnett, M. P., New Dye Technique Shows Maturity of Cotton, *Textile World* **97**, 105 (1947).
10. Hock, C. W., Ramsay, R. C., and Harris, M., Microscopic Structure of the Cotton Fiber, *J. Research Natl. Bur. Standards* **26**, 93 (1941).
11. Jenkins, K. A., and Keels, H. F., The Effect of Abrasion on the Dyeing Characteristics of Cotton, *Am. Dyestuff Reptr.* **39**, 660 (1950).
12. Morehead, F. F., and Sisson, W. A., Skin Effect in Viscose Rayon, TEXTILE RESEARCH JOURNAL **15**, 443 (1945).
13. Preston, J. M., Skin Effect on Viscose Rayon, *J. Soc. Chem. Ind. (London)* **50**, 199 (1931).
14. Rollins, M. L., Applications of Nitrogen Dioxide Treatment to the Microscopy of Fiber Cell Wall Structure, TEXTILE RESEARCH JOURNAL **15**, 65 (1945).
15. Schiefer, H. F., Crean, L. E., and Krasny, J. F., Improved Single-Unit Schiefer Abrasion Testing Machine, TEXTILE RESEARCH JOURNAL **19**, 259 (1949).
16. Schramek, W., and Helm, J., The Dependence of the Dye Adsorption Power of Regenerated Cellulose Fibers on Their Inner Structure, *Kolloid-Z.* **88**, 291 (1938).
17. Vickerstaff, T., "The Physical Chemistry of Dyeing," London, Oliver and Boyd, 1950, p. 248.
18. Worner, R. K., and Mease, R. T., Effect of Purification Treatments on Cotton and Rayon, *J. Research Natl. Bur. Standards* **21**, 609 (1938).
19. Morton, T. H., Dyeing of Cellulose with Direct Dyestuffs: The Importance of Colloidal Constitution of the Dye Solution and of the Fine Structure of the Fiber, *Trans. Faraday Soc.* **31**, 281 (1935).

(Manuscript received August 1, 1952.)

Studies on Cellulose Acetate

Part III: Combination of Sulfuric Acid During the Acetylation of Cellulose and the Mechanism of Acetylation*

Tsunao Araki

Government Chemical Industrial Research Institute, Tokyo, Japan

ALTHOUGH numerous catalysts for the acetylation of cellulose have been proposed in the patent literature, sulfuric acid is one of the most effective. Commercial acetylations are usually carried out with this catalyst.

The disadvantage of using sulfuric acid as the catalyst is that it enters into combination with cellulose during the acetylation; the stability of the acetate so produced is decreased so that the cellulose ester requires a stabilizing treatment such as the removal of sulfate groups or salt formation with metallic ions.

The combination of sulfuric acid during acetylation has been reported by Caille [3], Cross and Bevan [4], Ost [7], Malm, Tanghe, and Laird [6], and others, but the behavior of sulfuric acid throughout the acetylation has not been interpreted adequately.

In Part I of this series [1] the present author reported on the behavior of sulfuric acid throughout the course of acetylation, and indicated that a large amount of sulfuric acid is taken up chemically by cellulose at the beginning of acetylation and then gradually split off from cellulose, showing that the sulfuric acid group is gradually replaced by acetyl.

Such behavior of sulfuric acid suggests that catalysis by sulfuric acid in the acetylation of cellulose is more complicated than expected according to the theory of normal catalysis due to proton activity supported by Krueger *et al.* [5].

In the present work, the relationship between the amount of combined sulfuric acid and the acetylation

* Parts I and II, respectively, appeared in *Cellulosechemie* **18**, 109 (1940) and *Cellulosechemie* **19**, 137 (1941).

TABLE I. ANALYSIS OF TREATED SAMPLES

	(1) Pptd. in water: Pptd. very slowly		(2) Pptd. in 20% NaCl	(3) Pptd. in benzene-ether	(4) Pptd. in alcohol
Acetylating bath neutralized (*A*)					
CH_3COOH (%)	—	49.2	49.3	49.3	49.6
H_2SO_4 (%)	—	10.68	11.07	11.01	10.72
Acetylating bath not neutralized (*B*)					
CH_3COOH (%)	56.1	53.5	49.5	49.3	54.4
H_2SO_4 (%)	2.61	8.27	10.89	10.75	5.94

conditions as well as the behavior of sulfuric acid radicals in acetic acid and acetic acid anhydride are studied, and the mechanism of acetylation is discussed.

Method

Acetylations were carried out according to the following schedule, using 10 g. of purified cotton (moisture content of about 5%) for each acetylation.

Pretreatment

Cellulose samples were steeped in water for 30 min., squeezed and pressed to a weight of 30 g., then steeped in 85% acetic acid, pressed to a weight of 30 g., steeped in approximately 100% acetic acid, pressed to a weight of 30 g., and fluffed out.

Acetylation

Acetylation conditions are noted in the description of each experiment.

Precipitation

Samples were taken at intervals, precipitated in 20% sodium chloride solution, washed with water to neutrality, and dried in vacuum at room temperature. Some of the samples that were high in sulfuric acid content were very gelatinous and soft in saturated sodium chloride solution; these were collected through linen cloth, squeezed by hand in cloth bags, and washed with 85% ethanol. Some of the samples that were the most rich in sulfuric acid were soluble in water and could not be precipitated in saturated sodium chloride solution; these were precipitated in cold benzene-ether mixture (2:1), neutralized with sodium acetate alcoholic solution, washed with 85% ethanol, and dried in vacuum at room temperature.

Acetic Acid Content

To a 1-g. sample in a flask were added 20 cc. of 75% ethanol and 25 cc. of *N* NaOH; the system was kept overnight at 25°C. The contents of the flask were then back-titrated with *N* H_2SO_4, and the acetic acid content was calculated as % CH_3COOH.

Sulfuric Acid Content

A 1-g. sample was dissolved in 20 cc. of fuming nitric acid, kept overnight at 25°C, and then evaporated almost to dryness. 150 g. of water were added, the solution was heated nearly to boiling, and then 10 cc. of 2*N* $BaCl_2$ were added. The precipitated barium sulfate was estimated in the usual manner, and the sulfuric acid content was calculated as % H_2SO_4.

Preliminary Experiment

As it was thought to be of importance to confirm that there is no hydrolysis of the sulfate or the acetyl group in precipitating the cellulose acetate-sulfate in 20% NaCl or in benzene-ether mixture, the following preliminary experiments were carried out.

Ten grams of cotton were pretreated and then acetylated in the acetylating mixture containing 120 g. of acetic acid anhydride, 80 g. of acetic acid, and 3 g. of sulfuric acid at 25°C for 35 min. After dividing the acetylating bath into two equal parts and adding to one part enough sodium acetate (as acetic acid solution) to neutralize the sulfuric acid present, both parts were precipitated and washed in the following manner: (*1*) precipitation in water, treatment in 5% NaCl, and washing in water; (*2*) precipitation in 20% NaCl, followed by washing with 20% NaCl and water; (*3*) precipitation in benzene-ether mixture, neutralization in sodium acetate alcoholic solution, and washing with alcohol and water; (*4*) precipitation in alcohol, treatment with sodium acetate alcoholic solution, and washing with alcohol and water.

Analyses of the samples were carried out. The analytical data for sulfuric acid and acetic acid content are summarized in Table I.

From the results shown in Table I it is seen that the sodium salt of cellulose acetate-sulfate ($NaSO_4^-$) is fairly stable, and the analytical values for acetic acid content and sulfuric acid content are nearly identical, regardless of the method applied (acetylating bath *A*).

On the other hand, it is observed that the acidic ester of cellulose acetate-sulfate (HSO_4^-) is very unstable in precipitating in water and in alcohol, and the analytical values obtained are dependent upon the time of precipitation and the washing treatment (acetylating bath *B*).

However, in spite of the instability of the acidic sulfate radical (HSO_4^-), it is shown by the data that precipitation in 20% NaCl or in a benzene-ether mixture followed by neutralization with sodium acetate gives results almost identical to those for the sodium salt of cellulose acetate-sulfate. This may indicate that in the precipitation of cellulose acetate-sulfate in a large amount of concentrated sodium chloride aqueous solution, the following ion-exchange reaction occurs:

$$\text{Cell—SO}_4\text{H} + \text{NaCl} \rightarrow \text{Cell—SO}_4\text{Na} + \text{HCl},$$

and the stabilization of acetate-sulfate takes place.

In general, it may be said that the sodium salt of a sulfate ester is considerably stable, as, for example, sodium cellulose sulfate, and is scarcely hydrolyzed in the process of precipitation and washing. For example, the calcium or sodium salt of cellulose acetate-sulfate (with 8.76% sulfuric acid content and 50.9% acetic acid content) is scarcely altered in composition by treatment with 50% or 70% acetic acid at 25°C for 20 min.

From these observations it is concluded that precipitation in 20% NaCl or in a benzene-ether mixture followed by neutralization with sodium acetate solution can be applied as a method of precipitating cellulose acetate-sulfate from solution. The best way of precipitating cellulose acetate-sulfate without hydrolysis may be the neutralization of sulfuric acid with sodium acetate-acetic acid solution followed by precipitation in 20% NaCl. Sodium chloride may serve as an ion-exchange and salting-out agent.

Results

Effect of the Ratio of Cellulose to Acetylation Bath

The effect of the ratio of cellulose to acetylation bath on the combination of sulfuric acid with cellulose was studied. Ten grams of pretreated cotton were acetylated at 25°C using the acetylation mixture

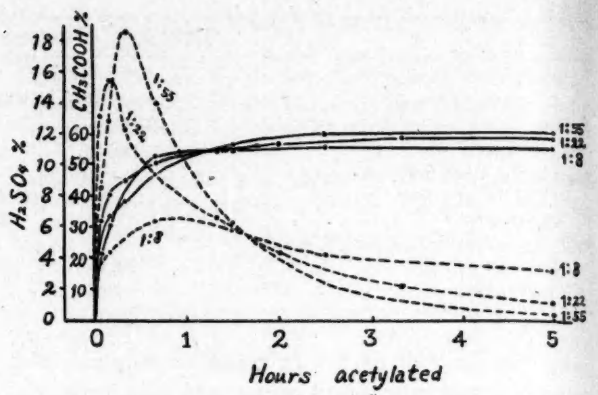

FIG. 1. *Effect of the ratio of cellulose to acetylation bath.* (---- *sulfuric acid content;*——*acetic acid content.*)

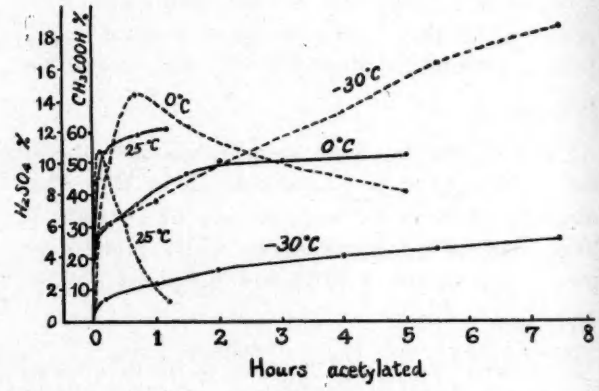

FIG. 2. *Effect of the acetylating temperature.* (---- *sulfuric acid content;*——*acetic acid content.*)

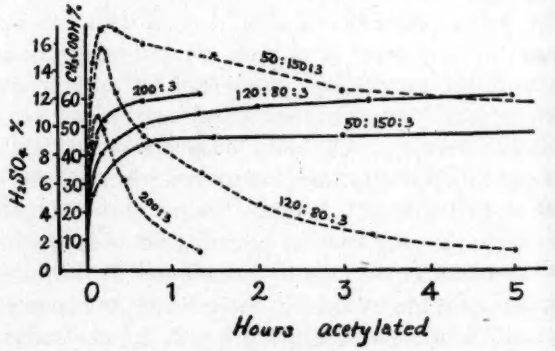

FIG. 3. *Effect of the composition of the acetylating mixture.* (---- *sulfuric acid content;*——*acetic acid content.*)

TABLE II

(*i*) *Cellulose:acetylation mixture = 1:8*

Minutes acetylated	5	10	40	90	150	300
CH_3COOH (%)	19.5	30.1	51.4	54.7	55.3	57.4
H_2SO_4 (%)	3.99	4.21	6.22	5.66	4.15	3.23

(*ii*) *Cellulose:acetylation mixture = 1:22*

Minutes acetylated	4	10	20	40	80	120	200	300
CH_3COOH (%)	32.6	40.5	44.3	50.8	53.7	57.3	59.3	61.0
H_2SO_4 (%)	13.03	15.61	12.30	9.21	6.52	4.42	2.24	1.31

(*iii*) *Cellulose:acetylation mixture = 1:55*

Minutes acetylated	5	10	20	40	90	150	300
CH_3COOH (%)	21.3	32.5	37.8	46.0	55.8	59.6	62.3
H_2SO_4 (%)	8.49	13.01	18.80	14.02	6.11	2.28	0.33

TABLE III

(*i*) *Acetylating temperature, 25°C*

Minutes acetylated	1	4	7	12	25	40	80
CH_3COOH (%)	22.8	37.0	45.7	52.3	56.7	58.9	60.4
H_2SO_4 (%)	5.96	8.81	10.72	9.95	6.34	3.81	1.35

(*ii*) *Acetylating temperature, 0°C*

Minutes acetylated	5	15	40	90	180	300
CH_3COOH (%)	28.7	31.5	36.2	47.3	50.6	53.3
H_2SO_4 (%)	6.04	10.83	14.34	12.34	10.15	8.26

(*iii*) *Acetylating temperature, −30°C*

Minutes acetylated	20	60	120	240	330	450
CH_3COOH (%)	6.9	11.8	16.8	20.6	24.0	27.4
H_2SO_4 (%)	6.09	7.36	10.26	13.47	16.72	19.20

TABLE IV

(*a*) Loc. cit. *Table III*, (*i*)

(*b*) Loc. cit. *Table II*, (*ii*)

(*c*) *$(CH_3CO)_2O$, 50 g.; CH_3COOH, 150 g.; H_2SO_4, 3 g.*

Minutes acetylated	5	10	20	40	90	180	360
CH_3COOH (%)	26.4	30.5	39.3	43.6	46.5	47.7	49.1
H_2SO_4 (%)	14.57	16.86	16.82	15.85	15.08	12.58	11.68

$(CH_3CO)_2O$: CH_3COOH: H_2SO_4 = 120: 100*: 3 in amounts 8, 22, and 55 times that of cellulose. The results are shown in Table II and Figure 1.

Effect of the Acetylation Temperature

The effect of the acetylating temperature on the combination of sulfuric acid with cellulose was studied. Ten grams of pretreated cotton (including 20 g. of pretreated acetic acid) were acetylated at 25°C, 0°C, and −30°C in the acetylation mixture containing 200 g. of acetic acid anhydride and 3 g. of sulfuric acid. The results are shown in Table III and Figure 2.

Effect of the Composition of the Acetylating Mixture

Ten grams of pretreated cotton were acetylated at 25°C in the following acetylating mixtures: (*a*) acetic acid anhydride, 200 g., and sulfuric acid, 3 g.; (*b*) acetic acid anhydride, 120 g., acetic acid, 80 g.,* and sulfuric acid, 3 g.; (*c*) acetic acid anhydride, 50 g., acetic acid, 150 g.,* and sulfuric acid, 3 g. The results are shown in Table IV and Figure 3.

* Including CH_3COOH introduced from the pretreatment.

* Not including CH_3COOH introduced from the pretreatment.

TABLE V

(a) *Acetylation with acetylating mixture I*

Hours acetylated	0.5	2	7	23
CH_3COOH (%)	14.5	20.6	24.8	31.6
H_2SO_4 (%)	19.28	22.89	22.76	21.35

(b) *Acetylation with acetylating mixture II*

Hours acetylated	0.5	2.5	6	22	30
CH_3COOH (%)	11.3	14.0	17.4	23.3	27.1
H_2SO_4 (%)	22.32	22.89	25.87	27.24	34.75

TABLE VI

(i) *Addition of sulfuric acid after 1 hr. of acetylation*

Minutes after addition	0	5	20	60	240
CH_3COOH (%)	51.4	52.4	54.7	58.6	61.0
H_2SO_4 (%)	8.18	10.37	6.49	4.58	0.86

(ii) *Addition of sulfuric acid after 5 hrs. of acetylation*

Minutes after addition	0	5	30	60
CH_3COOH (%)	61.8	62.0	61.9	62.1
H_2SO_4 (%)	0.47	0.54	0.43	0.29

TABLE VII

(a) *Reaction temperature, 25°C*

Minutes reacted	0	10	30	60
CH_3COOH (%)	50.2	57.1	60.3	63.0
H_2SO_4 (%)	9.95	4.12	1.21	0.23

(b) *Reaction temperature, 15°C*

Hours reacted	0	0.5	1	4
CH_3COOH (%)	51.7	57.9	60.4	61.2
H_2SO_4 (%)	10.23	3.34	0.96	trace

(c) *Reaction temperature, 0°C*

Hours reacted	0	0.5	1	4
CH_3COOH (%)	49.7	51.7	52.2	56.7
H_2SO_4 (%)	10.62	8.01	7.78	4.23

TABLE VIII

(a) *Reaction temperature, 25°C*

Hours reacted	0	0.5	1	4
CH_3COOH (%)	47.4	49.7	52.0	53.6
H_2SO_4 (%)	11.38	8.16	6.60	3.03

(b) *Reaction temperature, 50°C*

Hours reacted	0	0.5	1	4
CH_3COOH (%)	52.7	57.8	58.2	58.7
H_2SO_4 (%)	10.23	1.82	0.08	trace

TABLE IX

Water (%)	0	0.5	1	2	4	6	10
H_2SO_4 (%)	1.19	0.49	0.31	0.05	0.21	0.67	0.86

Acetylation of Cellulose with Acetylating Mixtures Rich in Sulfuric Acid

Ten grams of pretreated cotton were acetylated at 5°C in the following mixtures rich in sulfuric acid: (*I*) $(CH_3CO)_2O$, 120 g., and H_2SO_4, 70 g.; (*II*) $(CH_3CO)_2O$, 120 g., and H_2SO_4, 100 g. The results are given in Table V.

Effect of Adding Sulfuric Acid During the Acetylation of Cellulose

Ten grams of pretreated cotton were acetylated in the acetylating mixture containing 120 g. of acetic acid anhydride, 80 g. of acetic acid, and 3 g. of sulfuric acid at 25°C. After 1 hr. or 5 hrs. of acetylation, 5 g. of sulfuric acid were added to the acetylation bath, which was thoroughly mixed and kept at 25°C. Samples were then taken in intervals, precipitated, washed, and analyzed. The results of the experiments are given in Table VI.

Behavior of Sulfuric Acid Radical in Acetic Acid Anhydride and Acetic Acid

Behavior in acetic acid anhydride.—Ten grams of pretreated cotton were acetylated at 25°C in the acetylating mixture containing 120 g. of acetic acid anhydride, 80 g. of acetic acid, and 3 g. of sulfuric acid for 40 min., precipitated, washed in cold benzene, and dried under blown air. 5 g. of this product (containing approximately 10% sulfuric acid) were dissolved in 20 g. of acetic acid anhydride. The behavior of the sulfuric acid radical was studied at 25°C, 15°C, and 0°C. The results are shown in Table VII.

Behavior in acetic acid.—Fifteen grams of cellulose acetate-sulfate containing approximately 10% sulfuric acid (prepared as above) were dissolved in 99.7% acetic acid. The behavior of sulfate radicals

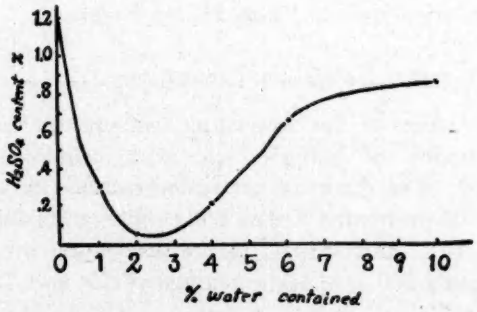

FIG. 4. *Behavior of sulfuric acid group in acetic acid containing water.*

at 25°C and 50°C was studied. The results of the experiments are given in Table VIII.

Behavior in acetic acid containing water.—Cellulose acetate-sulfate containing 1.79% sulfuric acid was treated in acetic acid containing various amounts of water at 20°C for 20 hrs. The sulfuric acid contents of the products were determined. The results of the experiments are shown in Table IX and Figure 4.

Discussion

From the results shown in Table II and Figure 1 it is seen that by increasing the ratio of acetylation bath to cellulose, the amount of combined sulfuric acid rises to 19%, indicating that the combination of sulfuric acid is influenced mainly by the quantity of sulfuric acid present.

The effect of acetylating temperature on the combination of sulfuric acid is also very striking (Table III and Figure 2). By lowering the acetylating temperature to —30°C, the maximum sulfuric acid content of the product rose to 19%–20%; that at 25°C was 10.7%. This suggests that the sulfation of cellulose proceeds fairly well even at very low temperatures, whereas the replacement of sulfate radical by acetyl decreases under such conditions.

Table IV and Figure 3 concern the effect of the composition of the acetylating mixture. These results show that lowering the concentration of acetic acid anhydride—*i.e.*, raising that of acetic acid—favors the combination of sulfuric acid with cellulose, indicating that the acetylation of cellulose and the replacement of sulfate radical by acetate are dominant if the acetylating mixture is rich in acetic acid anhydride.

When the acetylation of cellulose is carried out with an acetylating mixture containing a large amount of sulfuric acid ($(CH_3CO)_2O:H_2SO_4 = 120:100$—*i.e.*, nearly equivalent ratio) (Table V), the sulfuric acid content of the product increases gradually; finally, a product with a sulfuric acid content of approximately 35% and an acetate acid content of 27% is obtained. The fact that considerable acetylation takes place even in this case shows that there is an equilibrium between acetic acid anhydride and sulfuric acid—namely,

$$(CH_3CO)_2O + H_2SO_4 \rightleftarrows CH_3CO \cdot SO_4H + CH_3COOH. \quad (1)$$

A considerable amount of free acetic acid anhydride present in the mixture thus favors acetylation.

It is of interest to know the behavior of the sulfate radical when the sulfuric acid concentration is raised or lowered suddenly during the acetylation, since it may give some indication of the reactivity of sulfuric acid with cellulose. The addition of sulfuric acid after 1 hr. of acetylation resulted in a rapid rise in the amount of combined sulfuric acid and then a fall to the same level as for those without sulfuric acid addition, while addition after 5 hrs. of acetylation (in this stage, cellulose is nearly triacetylated) gave no rise in sulfuric acid content (Table VI). These results show that sulfuric acid reacts even with a small amount of hydroxyl group remaining intact in acetyl cellulose, but does not possess the ability to replace the acetyl group.

As mentioned previously, the acetylation of cellulose is promoted in the presence of numerous catalysts, such as sulfuric acid, perchloric acid, sulfonic acid, pyridine, zinc chloride, etc. The mechanism of acetylation by these catalysts has been discussed by many authors; the theory of normal catalysis by proton activity [5] has been generally accepted as the most probable. However, there exists some speciality in the mode of acetylation of macromolecular substances such as cellulose, starch, agar-agar, etc., in which the formation of a sulfate ester intermediate is observed. The fact that a large amount of sulfuric acid is taken up by cellulose at the beginning of acetylation and then split off in the course of it suggests that catalysis by intermediate formation should also be taken into consideration. Since sulfuric acid is a strong acid in acetic acid and acetic acid anhydride mixture, sulfation of cellulose may proceed in such a low concentration as is used in acetylation. Thus, the sulfation of cellulose may be written as follows:

$$Cell—OH + H_2SO_4 \rightarrow Cell—SO_4H + H_2O. \quad (2)$$

The behavior of sulfuric acid in acetic acid anhydride and acetic acid is of significance with respect to the interpretation of the catalytic mechanism of acetylation. Since a remarkable increase in acetic acid content and a rapid decrease in sulfuric acid are observed in the reaction of cellulose acetate-sulfate with acetic acid anhydride (Table VII), it is apparent that the sulfate group is replaced by acetyl in the reaction with acetic acid anhydride. The reaction

may be represented by the following equation:

$$\text{Cell—SO}_4\text{H} + (\text{CH}_3\text{CO})_2\text{O} \rightarrow \text{Cell—OCOCH}_3 + \text{CH}_3\text{CO}\cdot\text{SO}_4\text{H}. \quad (3)$$

As regards the reaction with acetic acid, the replacement of the sulfuric acid group by acetyl is very doubtful. From the results shown in Table VIII, it can be seen that the splitting off of the sulfuric acid group is retarded in almost anhydrous acetic acid at 25°C, although there is a slow rise in acetic acid content which may be attributed to the weight decrease of the acetate due to the splitting off of sulfate groups—in other words, no rise in the degree of acetylation is observed. Such behavior is more apparent from the results given in Table IX—that is, the cleavage of sulfuric acid groups occurs most readily in approximately 98% acetic acid and is retarded in higher or lower concentrations.*

Considering that the sulfuric acid group undergoes cleavage in the presence of a very small amount of water, it is difficult to build up such an anhydrous condition as to test the possibility of a reaction between sulfuric acid group and acetic acid. At any rate, it would be more likely to consider that there is scarcely a possibility of replacing the sulfuric acid group by the treatment with acetic acid, at least under usual conditions. Hence, the replacement reaction may be written as follows:

$$\text{Cell—SO}_4\text{H} + (\text{CH}_3\text{CO})_2\text{O} \rightarrow \text{Cell—OCOCH}_3 + \text{CH}_3\text{CO}\cdot\text{SO}_4\text{H}. \quad (3)$$

* From this result, it is supposed that the afteracetylation reported in Part II of this series [2] may be a hydrolysis reaction of sulfuric acid groups accompanied by an elevation of acetic acid content due to the weight decrease of the acetate, and the optimum of this reaction may lie in the neighborhood of 98% CH_3COOH concentration.

As discussed previously, reaction (2) may proceed readily even at low temperatures, whereas reaction (3) occurs very slowly under such conditions.

Thus, under usual conditions, the acetylation through reactions (2) and (3) and through reaction (4) may take place competitively:

$$\text{Cell—OH} + (\text{CH}_3\text{CO})_2\text{O} \xrightarrow{\text{H}^+} \text{Cell—OCOCH}_3 + \text{CH}_3\text{COOH}, \quad (4)$$

and the rate of the contributions of both reaction courses may be decided by acetylation conditions.

Summary

1. The effects of the acetylating conditions on the amount of combined sulfuric acid in acetylcellulose were studied.

2. The behavior of the sulfate radical in acetic acid and in acetic acid anhydride was examined with respect to the interpretation of the mechanism of acetylation.

3. The mechanism of the catalysis in the acetylation of cellulose, using sulfuric acid as catalyst, was discussed.

Literature Cited

1. Araki, T., *Cellulosechemie* **18**, 109 (1940).
2. Araki, T., *Cellulosechemie* **19**, 137 (1941).
3. Caille, A., *Chimie & industrie* **12**, 441 (1924).
4. Cross, C. F., and Bevan, E. T., "Research on Cellulose, 1900–1905," London, Longmans, Green and Co., 1906, 83 pp.
5. Krueger, D., and Roman, W., *Angew. Chem.* **47**, 58 (1934); Henk, H. J., *Melliand Textilber.* **19**, 184 (1938).
6. Malm, C. J., Tanghe, L. J., and Laird, B. C., *Ind. Eng. Chem.* **38**, 77 (1946).
7. Ost, H., *Z. angew. Chem.* **32**, 66, 76, 82 (1919).

(*Manuscript received April 16, 1952.*)

Cotton Defoliation and Fiber Maturity*

Mary Anna Grimes†

Texas Agricultural Experiment Station, College Station, Texas

THE ACREAGE of cotton treated with chemical defoliants increased from a relatively few thousand acres in 1946 to more than 3½ million acres in 1951. Defoliation increases the speed, ease and completeness of hand picking, increases the efficiency of mechancial harvesting, and raises the grade of the cotton. It decreases and in some cases eliminates green leaf trash which cannot be dried sufficiently for removal in ginning.

Normal functioning of the leaves is interrupted and under good conditions the leaves are shed soon after chemical defoliants are applied. This results in a decrease in the manufacture and transport of leaf reserves to the young or immature bolls. The cotton fiber normally reaches its maximum length within 20 to 21 days, after which the fiber becomes thicker by laying down layers of cellulose within the outside, or primary, cell wall. Premature opening of the bolls, whether by chemical defoliants or other causes, checks growth of the fiber walls, resulting in thin-walled or immature fibers. Immature fibers retain trash more than mature fibers, increase manufacturing waste, produce neps in yarns, and cause uneven dyeing.

It is advisable to postpone the application of chemical defoliants which hasten the opening of the bolls until the fibers have fully developed. However, it is desirable to defoliate as early as possible for a number of reasons: to prevent rotting of the lower bolls, to hasten opening of the bolls by permitting sunlight to enter where dense foliage prevents penetration, to permit early plowing under of plants to control diseases and insects, to escape early frosts, to permit early harvesting, and to avoid unnecessary exposure of the fibers to weathering.

* Approved for publication by the Texas Agricultural Experiment Station as Technical Article No. 1601.

† Professor, Department of Rural Home Research, Texas Agricultural Experiment Station, Texas A & M College, College Station, Texas.

The problem, then, is to determine the earliest possible period when defoliants can be applied safely without decreasing the quality of the seed and fiber. This report deals with only one phase of the problem —the effect of time of application upon the quality of the fiber, particularly the maturity or development of the cell wall. It is a small part of a comprehensive study undertaken by ten states and the Bureau of Plant Industry, Soils, and Agricultural Engineering. Cotton from four states—Arkansas, Arizona, Missouri, and Mississippi—for 1948 are included in this study.

Plan of Study

The defoliant and rate of application used at each location were those which gave satisfactory defoliation under prevailing conditions. Therefore, applications differed between locations, and at some locations different procedures were used. However, there was an acceptable degree of defoliation at each location.

When it was estimated that the peak of bloom was just past, all open blooms were tagged. The defoliant was then applied at 17, 23, 29, 35, and 41 or 42 days after tagging. Plots were arranged for four randomized replicates of each treatment.

Series 1 included the cotton which had bloomed prior to the date of the tagged bolls; it was harvested when the bolls from the tagged blooms began to open. Series 2 (and series 3 at Arkansas) included the tagged bolls of known age when defoliated. Series 4 included the bolls that bloomed after the date of tagging; it was harvested after the cotton in series 1, 2, and 3 was removed.

The control and defoliated samples were sent to this laboratory, where the maturity of the fibers was determined by the polarized light method. By this method, fibers can be classed readily as mature (with thick walls), as immature (with thin walls), or as

partially mature if they fall between these two classes. Results are expressed as the percentage of fibers falling within each of the three classes.

Differences between replicates were sometimes great; therefore, analysis of variance was used to see if the differences in maturity at different dates of defoliation were significant. The maturity of the fibers for each series from each state and the significance of the differences in maturity within each series are given in Table I.

Discussion

Arkansas

The maturity of early bulk cotton, series 1, and cotton of known age, series 2 and 3, differed at the

TABLE I. PERCENTAGE OF FIBERS AT THREE STAGES OF MATURITY

Days after peak of bloom when defoliant was applied	Series 1			Series 2			Series 3			Series 4		
	Immature	Partially mature	Mature	Immature	Partially mature	Mature	Immature	Partially mature	Mature	Immature	Partially mature	Mature
Arkansas												
Control	14**	12	74**	16**	19	65*	21**	18	61**	24	18	58
17	21	15	64	33	25	42	35	16	49	28	20	52
23	17	15	68	24	20	56	30	14	56	23	19	58
29	19	15	66	22	17	61	33	15	52	27	18	55
35	16	13	71	17	24	59	26	16	58	23	19	58
42	14	12	74	17	21	62	22	14	64	21	18	61
Average	17	14	70	22	21	58	28	16	57	24	19	57
Missouri												
Control	26	13	61	30	12**	58				30	10	60
17	31	14	55	36	13	51				37	10	53
23	29	11	60	33	11	56				34	11	55
29	27	12	61	33	10	57				32	12	56
35	25	14	62	27	10	63				27	11	62
41	26	13	61	29	9	62				33	11	56
Average	27	13	60	31	11	58				32	11	57
Arizona												
Early Final Irrigation												
Control	15*	10**	75*							17	12	71
17	15	9	76							19	12	69
23	15	8	77							19	13	68
29	13	9	78							17	12	71
35	11	9	80							17	12	71
41	11	7	82							16	11	73
Average	13	9	78							18	12	70
Late Final Irrigation												
Control	11	7*	82**							19	12	69
17	12	7	81							22	11	67
23	13	6	81							23	12	65
29	11	6	83							24	14	62
35	8	5	87							28	11	61
41	12	5	83							24	12	64
Average	11	6	83							23	12	65
Mississippi												
Control	8	16	76									
20	12	18	70									
27	9	16	75									
34	8	16	76									
41	6	16	78									
Average	9	16	75									

* Significant variance among treatments within series, 5% level.
** Highly significant variance among treatments within series, 1% level.

1% level. There was no significant difference between the maturity of series 2 and 3, which was expected because they were replicates. Neither series 2 nor 3 differed significantly from series 4.

Series 1 contained some bolls that were older and series 4 contained some bolls that were younger than those in series 2 and 3. The average percentage of mature fibers in series 1 was 70%; in series 2, 58%; and in series 3 and 4, 57%.

Series 1, 2, and 3 each showed a significant difference within the series in the maturity of the fibers due to the date of defoliation. Differences due to date of treatment were significant at the 1% level for the immature and mature fibers in series 1 and 3 and for the immature fibers in series 2. The differences were significant at the 5% level for the mature fibers in series 2.

In each of the four series the highest maturity occurred in the cotton defoliated at the latest date, 42 days after peak of bloom. At this Arkansas location, cotton should not be defoliated before approximately the 42nd day after peak of bloom in order to obtain a high percentage of mature fibers.

Missouri

With the exception of series 1 and 4, where series 1 was significantly higher in maturity than series 4, there was no significant difference in maturity between any two series from Missouri.

Only in series 2, partially mature fibers, were there differences due to date of defoliation. Here the differences were significant at the 1% level, with fewer partially mature fibers at the later dates.

The highest percentages of mature fibers occurred in the cotton defoliated 35 days after tagging. Therefore, it is concluded that defoliants should not be applied earlier than 35 days after peak of bloom.

Arizona

Blooms were tagged at two different dates in Arizona, in both cases at the time of the last irrigation for those plots. Days after tagging thus refer also to days after the last irrigation.

The differences in maturity between the early and late irrigated cotton, series 1, were significant at the 1% level, the early irrigated cotton being less mature than the late irrigated cotton. In series 4, the difference between early and late irrigated cotton was significant at the 5% level, the early irrigated cotton having higher maturity than the late irrigated cotton. Both series 1 and 4 contained bolls of unknown age. Unfortunately, samples for series 2 containing bolls of known age were not available for study.

For early irrigated cotton, series 1, the differences in stage of maturity due to date of defoliation were significant at the 1% level for the partially mature fibers and at the 5% level for the mature and immature fibers. For late irrigated cotton, series 1, the differences were significant at the 5% level for the partially mature fibers and at the 1% level for the mature fibers.

There were no significant differences in the maturity of the fibers of either the early or the late irrigated cotton in series 4 which could be attributed to the time of defoliation. The cotton of series 4 probably contained more young bolls than that of series 1, which may account for its lower maturity.

For series 1 and 4 of the early irrigated cotton, the highest percentage of mature fibers occurred 41 days after peak of bloom. For series 1 of the late irrigated cotton, the highest maturity occurred 35 days after tagging. The late irrigated cotton of series 4 which had been defoliated 41 days after tagging apparently did not regain the maturity of the control.

Defoliants should not be applied in Arizona earlier than 35 days after peak of bloom, and preferably later, in order to obtain a high percentage of mature fibers.

Mississippi

Only series 1 samples of cotton were available from Mississippi. No significant differences in maturity were attributable to date of defoliation. However, the highest maturity occurred in the sample which had been defoliated 41 days after peak of bloom. The data support the same conclusion as for the other states—more mature fibers are obtained from cotton defoliated 41 days after peak of bloom.

Comparison of Two Methods for Determining Maturity

The results obtained by the polarized light method correspond closely with the results obtained by the differential dyeing method for the same cottons. All of the samples except those from Mississippi were analyzed by the dye method of determining maturity by Charles F. Goldthwait of the Southern Regional Research Laboratory. The correlation coefficient be-

tween the maturities obtained by the two methods is .84 ± .02. The average maturity for the 192 samples was 65% by the polarized light method and 67% by the dye method. This seems to be close agreement, because it is probable that duplicate tests by either method would not be in closer agreement than 2%.

Conclusion

For the four states included in this study of fiber maturity, the most mature fibers were obtained when defoliants were applied 35 and 41 days after peak of bloom. For eight of the twelve series from the four states, 41 days gave better results than earlier dates; for four series, 35 days gave an insignificantly higher percentage of mature fibers than 41 days.

From these results it is concluded that defoliants should not be applied earlier than 35 days, and preferably 41 days, after the peak of bloom in order to get the highest percentage of mature fibers.

Acknowledgment

Grateful acknowledgment is made to W. H. Tharp, W. E. Meek, W. R. Langford, and V. T. Walhood for the samples and information on the defoliation. Sincere thanks are given to Charles F. Goldthwait for the dye determinations of maturity.

(Manuscript received July 10, 1952.)

The following comments, which were submitted to the author, will be of interest to our readers.—Editor.

"I should like to say that additional data on defoliation in Missouri accumulated during the 1949 and 1950 seasons clearly support your conclusions as to the correct time to defoliate."

—W. R. Langford, *Assistant Agronomist*
West Florida Experiment Station, University of Florida, Jay, Fla.

"In support I would like to add that subsequent work along these lines corroborate your studies almost in detail. You are probably on the conservative side in concluding that [defoliation] 35 to 41 days after peak of bloom is required for maintaining highest fiber maturity. Specifically, we have found that bolls that are 37 days old and less when the plants are defoliated yield considerable and increasingly immature fiber. To maintain our fiber quality we must initiate a practise of a proper time to defoliate."

—V. T. Walhood, *Plant Physiologist*
Cotton Division, Bureau of Plant Industry,
United States Department of Agriculture, Shafter, Calif.

Mechanics of Elastic Performance of Textile Materials

Part IX: Factors Affecting the Translation of Certain Mechanical Properties of Cordage Fibers into Cordage Yarns*

M. M. Platt, W. G. Klein, and W. J. Hamburger

Fabric Research Laboratories, Inc., Boston, Massachusetts

Abstract

This report is concerned with the study of the mechanical properties of cordage yarns. The relationship between fiber properties and yarn performance is expressed mathematically by a method involving a generalized extension of the work of Hamburger [2] and Philipp [7]. The mathematical formulas representing the mechanical behavior of cordage yarns are shown to be useful by a comparison between theoretically calculated and experimentally obtained data. The validity and accuracy of the mathematical analysis is further tested by a detailed examination of the range of possible error due to unforeseen discrepancies between reality and the two assumptions: (*a*) a normal distribution of fiber properties, thus permitting the application of standard statistical treatment; and (*b*) no fiber slippage during the application to yarns of loads to rupture.

The results of the mathematical analysis are shown graphically over a range of fiber properties in excess of those evidenced by cordage fibers. Thus, if the assumptions made hold for all textile fibers, the behavior of other fibers than those normally used for cordage can be predicted for the case of yarns of cordage type.

Work is in progress covering further aspects of the research—namely, applying similar mathematical analysis to the translation of yarn properties into strand, plied yarn, and rope structures.

Introduction

This is the second Technical Report on the phase of this project concerned with determining the factors involved in the translation of the properties of cordage fibers into cordage structures.

Broadly, the approach being followed in the entire research can be divided into the following sections: (*a*) A fundamental study of the basic mechanical properties of the commonly used cordage fibers. (*b*) Comparison of these fiber properties with similar properties of cordage yarns. Yarns represent the next higher order of cordage structure after fibers. (*c*) A study of the translation of yarn properties into cordage strands. (*d*) A study of the translation of strand properties into ropes.

The present report covers the second phase (*b*) of the foregoing sections. Consistent with the philosophy of this research, not only are data on yarn properties given, but also generalizations of the factors which influence these yarn properties are made. Thus, quantitative theoretical analysis has been the objective of this work, and prediction of yarn properties the ultimate goal. This has been accomplished, and therefore the second phase of the research, aimed at the engineering design of cordage structures, has been completed.

Consistent with the objectives and findings, this report is logically divided into two sections, as follows: data on the properties of cordage yarns of varying geometry and made of different fibers; and the exploration of the factors which are responsible for the properties of the yarns in terms of fiber properties and yarn geometry.

Frequent reference will be made to two previous publications which bear pertinently on this work:

* The authors acknowledge the support of the United States Navy, Office of Naval Research, and the Bureau of Ships, in sponsoring the research, part of which is covered in this paper. The work on continuous-filament yarns, of which the research herein is an expansion, was sponsored by the Textile Section, Research and Development Branch, Office of The Quartermaster General.

Parts I and II of this series appeared in the February and December, 1948, issues, respectively; Part III in the January, 1950; Parts IV and V in the August, 1950; Part VI in the October, 1950; Part VII in the May, 1951; and Part VIII in the March, 1952, issues.

the first is "Mechanical Properties of Hard Fibers with Reference to Their Use in Cordage Structures," by E. R. Kaswell and M. M. Platt [4], Technical Report No. III on this project; the second is "Some Aspects of Stress Analysis of Textile Structures—Continuous-Filament Yarns," by M. M. Platt [8]. As will be shown, the analysis in the latter reference, while forming the framework of the study of cordage yarns, actually represents a special case of the more general relationships as developed in this work.

Section I—Properties of Cordage Yarns

The major study has been concerned with the characterization of the rupture properties of yarns. From a use point of view, the criterion of performance of cordage, whether in yarn form or in rope form, is adequate tensile strength and/or tensile energy absorption when impact loading is involved. This implies both adequate initial tensile strength and also maintenance of this tensile strength over a reasonable period of use while the product is subjected to the degrading influences of atmosphere, mechanical working, abrasion, flexing, etc. While a study of these degrading influences is important in evaluating the durability and serviceability of any cordage product, it is clear that research aimed at defining the factors responsible for initial tensile performance must be made before an intelligent approach to the study of durability can be made. Of great significance, in this regard, is the degree to which yarn properties depend upon fiber properties. Obviously, if the dependence is great, changes in fiber properties with use may critically alter yarn properties. As will be shown, the dependence *is* great.

The purpose of investigating yarns in this work was not to amass a large quantity of data listing the comparative properties of one yarn *versus* another, but, instead, to form a springboard from which an analysis of the dependence of yarn properties upon fiber properties would be forthcoming. Thus, the data on yarn properties are by no means sufficiently inclusive to form a handbook of yarn performance, but are given to represent the general qualitative relationship between yarns and fibers.

Four distinct groups of yarns were studied:

Blended abaca yarns.—These are yarns of varying twist made of Manila abaca and Costa Rican abaca fibers prepared by the Boston Navy Yard. These yarns have been and will be concerned only with the study of yarn performance.

Abaca strand yarns.—These are also yarns of varying twist made of Manila abaca fiber prepared by the Boston Navy Yard. However, they have been used not only for the study of yarn performance, but also for research on strand performance, the discussion of which is part of a future study.

Henequen yarns.—These are a series of yarns of varying twist made of henequen fiber prepared by the Columbian Rope Company. This fiber is of interest since it is classified as a hard fiber, and yet possesses basic stress-strain properties [4] considerably different from Manila abaca fiber. The extensibility of henequen fiber at all loads exceeds that of Manila abaca, and, in addition, the stress-strain curve of henequen fiber is concave down while that of Manila abaca is concave up. These differences are significant in affecting yarn properties.

TABLE I. PROPERTIES* OF BLENDED ABACA YARNS (YARN WEIGHT = 270 FT./LB., OR 50,000 DENIER (NOMINAL))

Yarn code No.	Yarn twist (turns/ ft.)	Yarn surface helix angle (degrees)	Yarn strength (lbs.)	Yarn tenacity (g./den.)	Yarn elongation (%)
2A	9.0	16.5	349 (18)†	2.95 (12)	2.66 (11)
2B	11.1	20.0	279 (12)	2.69 (13)	2.35 (7)
2C	13.9	24.5	243 (10)	2.28 (12)	3.01 (8)
2D	17.2	29.4	190 (11)	2.00 (8)	2.78 (9)

* Each value is the average of 10 tests.
† Figures in parentheses are coefficients of variation (%).

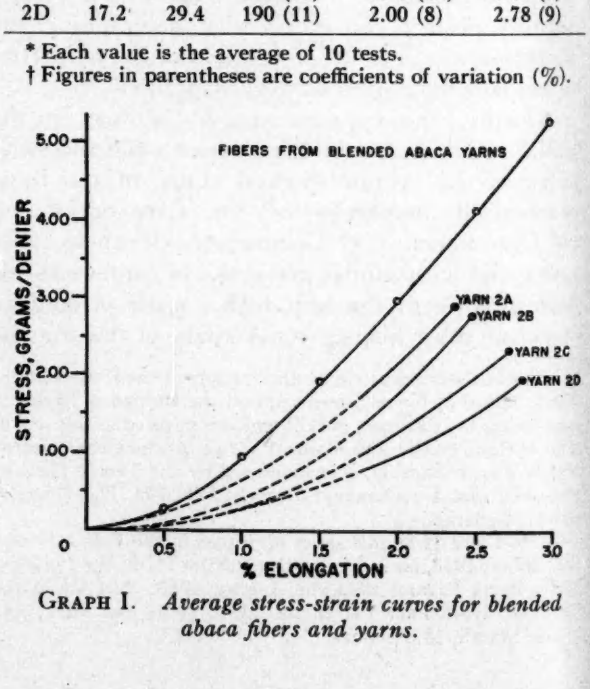

GRAPH I. *Average stress-strain curves for blended abaca fibers and yarns.*

Sansevieria yarn.—This is a single yarn (*i.e.*, not a series) prepared at the Boston Navy Yard, which forms part of a sequence of structures from fiber to rope.

A—Properties of Blended Abaca Yarns

These yarns were all spun from the same lot of fiber into yarns of nominally the same weight per unit length—*i.e.*, 50,000 denier, or 270 ft./lb. The only variation is in yarn twist. The pertinent yarn data are given in Table I.

Examination of the data in Table I indicates the following:

(*1*) The tenacity of the yarns decreases continually with increase in the yarn twist.

(*2*) There is no consistent trend in yarn extensibility to break, although it appears that the high-twist yarns have a somewhat higher rupture elongation than do the low-twist yarns. However, statistical analysis fails to indicate any one elongation as being significantly different from any other.

(*3*) Comparison of the data given in Table I with corresponding fiber data [4] shows that average fiber tenacity of about 5–6 g./den. is translated into yarns with an efficiency of the order of only 50%. Fiber elongation, on the other hand, is translated with close to full efficiency. The average fiber extension to break of 3.0% [4] is insignificantly different from any of the elongations given in Table I.

(*4*) With respect to their gross stress-strain characteristics, the yarns are compared with each other and with the fiber of which they are composed on Graph I. The yarn curves are typical ones, while the fiber curve is the average curve obtained by averaging arithmetically the loads at equal elongations of all fiber tests. The yarn curves are shown dotted over a large portion of their length. This is done because of the extreme difficulty of determining valid results at low elongations. The "effective gage length" technique [3] was used to determine yarn elongations, and, while accurate results are attainable by using this procedure in the region of stress close to yarn rupture, the use of capstan jaws (necessary to avoid consistent jaw breaks) for the compressible cordage yarns produces a high degree of yarn flattening. Thus, yarn elongations in the low (0%–2%) elongation range cannot justifiably be compared with the fiber elongations.

It is obvious from Graph I that the organization of the fibers into yarn form does not materially change the stress-strain curve shape. All the curves of Graph I are of the same character. At equal loads the elongation of the yarns increases with increasing twist. This difference is explained by the stress-distribution differences amongst the fibers as yarn twist increases [8]. Such stress distributions are discussed in section *II* of this report. The differences in ultimate load are apparent. The explanation of the causes of these differences in load is also given in detail in section *II*.

B—Properties of Abaca Strand Yarns

As part of the program concerned with the translation of yarn properties into strands, the Boston Navy Yard prepared a series of Manila

TABLE II. PROPERTIES* OF ABACA STRAND YARNS (YARN WEIGHT = 300 FT./LB. (NOMINAL))

Yarn code No.	Yarn twist (turns/ft.)	Yarn surface helix angle (degrees)	Yarn strength (lbs.)	Yarn tenacity (g./den.)
YS	6.0	14	360	3.45
YM	10.8	18	240	3.00
YH	14.4	24	262	2.68

* All results are averages of 10 tests.

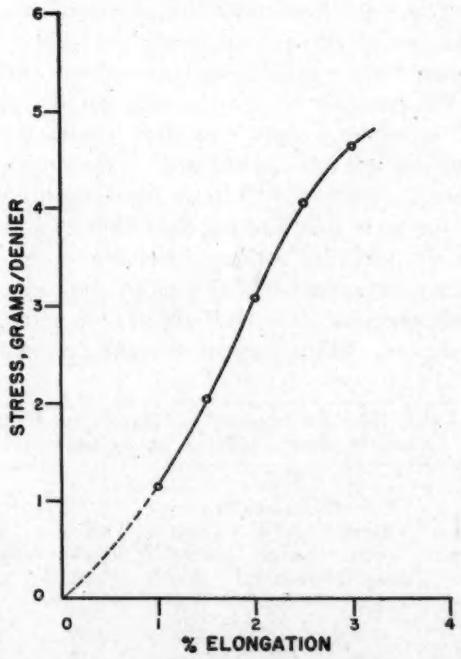

GRAPH II. *Average stress-strain curve for fibers from abaca strand yarns.*

abaca yarns of different twists to be made into strands with different twists. Data are given on these yarns not because they present any new features, but to further exemplify the general nature of the theoretical developments which have been produced in the course of this study. The pertinent yarn data are given in Table II.

The properties of single fibers removed from these yarns were determined. The average stress-strain curve of these fibers is given in Graph II. It is seen again that the average fiber tenacity of 5.4 g./den. is translated into yarns with an efficiency of the order of 50%. Again, with increase in yarn twist, yarn tenacity decreases.

No further discussion of the results of these particular yarn tests will be made since they supplement the data given for the abaca yarns in Table I.

C—Properties of Henequen Yarns

A series of henequen yarns of varying twist was studied since the henequen fiber differs considerably in its basic properties from the abaca fibers [4]. These yarns were produced by the Columbian Rope Company. The pertinent yarn data are given in Table III.

Typical stress-strain diagrams of these three yarns are given on Graph III. Here, again, it can be seen that the character of the shapes of the curves is alike, all of them duplicating the shape of the henequen fiber stress-strain curve given on Graph IV. With respect to the rupture points, as yarn twist increases, yarn tenacity decreases. The elongations are not significantly different amongst the yarns. With respect to the fiber rupture values, it can be seen that the average fiber extension to break of 5.0% is attained by the yarns. The difference between 5.0% elongation and any of the yarn elongations given in Table III is statistically insignificant. With respect to tenacity, the yarn tenacities given in Table III must be compared with an average fiber tenacity of 3.30 g./den. Thus, for the case of the henequen yarns, fiber tenacity is translated into yarns with an efficiency in the range of 40%–50%.

TABLE III. PROPERTIES* OF HENEQUEN YARNS (YARN WEIGHT = 220 FT./LB. (NOMINAL))

Yarn code No.	Yarn twist (turns/ft.)	Yarn surface helix angle (degrees)	Yarn strength (lbs.)	Yarn tenacity (g./den.)	Yarn elongation (%)
9T	9.0	22	251	1.82	5.60
15T	15.0	28	204	1.59	5.10
21T	21.0	35	131	1.10	5.70

* All results are averages of 15 tests.

D—Properties of Sansevieria Yarn

Only one Sansevieria yarn was studied. This was supplied by the Boston Navy Yard as part of a controlled sequence of construction from fiber to small-size Sansevieria ropes. This yarn weighed 380 ft./lb., and had 10.5 turns/ft. twist. The average yarn strength was 219 lbs., and the average yarn tenacity 2.82 g./den. Yarn breaking extension was 3.65%. These values should be compared to the average fiber tenacity of 5.84 g./den. and the fiber extension to rupture of 3.30%.

Once again, it is seen that fiber tenacity is translated into yarns with an efficiency of the order of 50%, while fiber extensibility to rupture is fully translated. The difference between 3.30% elonga-

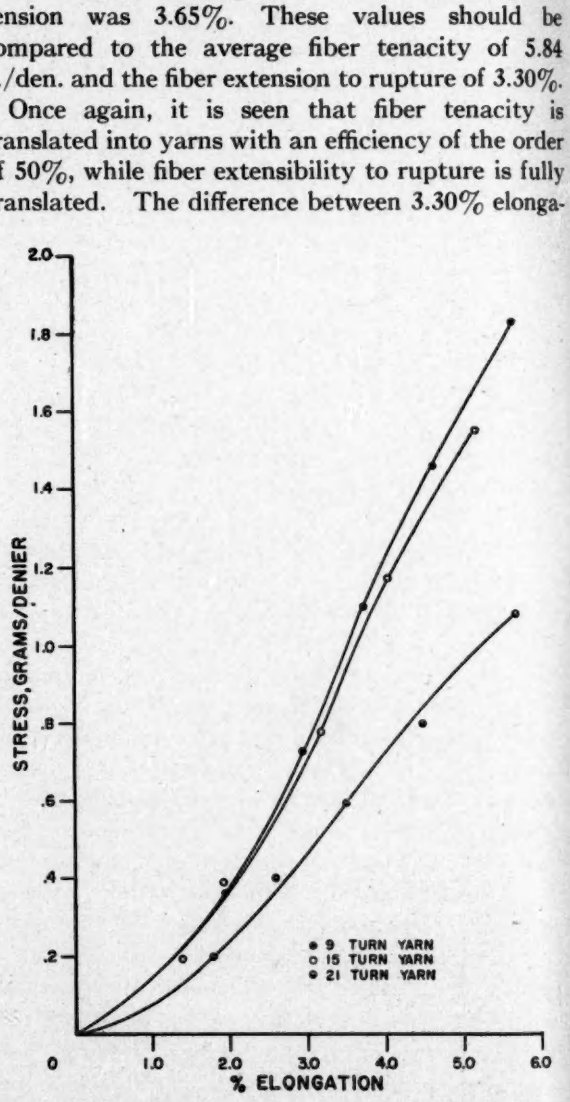

GRAPH III. *Typical stress-strain curves for henequen yarns of various twists.*

tion for the fibers and 3.65% for the yarns is statistically insignificant.

A typical yarn stress-strain curve is given on Graph V. Here, again, the low-strain region of the yarn curve has been dotted in because of the lack of precision of the data.

E—Summary of Yarn Data

The foregoing data have shown quite conclusively, for a wide range of the natural cordage fibers, that, essentially independently of the yarn structure, fiber tenacity is translated into yarns very inefficiently, with only 50%–60% of the fiber strength realizable in the yarn. There are, of course, differences in yarn tenacity produced by yarn twist, which differences are real, consistent, and of sufficient magnitude to alter the yarn strengths significantly. The effects of the yarn twist are quantitatively predictable, as is shown in the following section. However, the results of computations show that, at most, yarn twist can produce losses in translation of approximately 15%. It is clear that there must exist a general interaction amongst fibers when they are placed together in a twisted state, apart from the effect of twist itself, which produces a major loss in achievable yarn strength. As is shown in section *II*, this interaction arises from the fact that all of the hard cordage fibers possess high variability in their inherent properties [4].

Section II—Theoretical Analysis of the Factors Involved in Translation of Fiber Properties into Cordage Yarns

It was shown in a previous Technical Report [4] that the magnitude of any fiber damage resulting from processing the fiber into yarns was too small, if at all existent, to determine experimentally. Similarly, it was shown [4] that the twisted configuration of fibers did not in any way alter the fiber strength in a tensile test. Thus, it is clear that the fibers, as they lie in the yarn, possess strengths in the direction of their axes equal to their original strength. This section is concerned with developing a logical basis of explanation and prediction for the efficiency of a yarn in terms of its component fibers.

In order to avoid undue repetition, frequent reference will be made to a previous publication [8]. The information contained in this publication is an analysis of the stresses in yarns made of

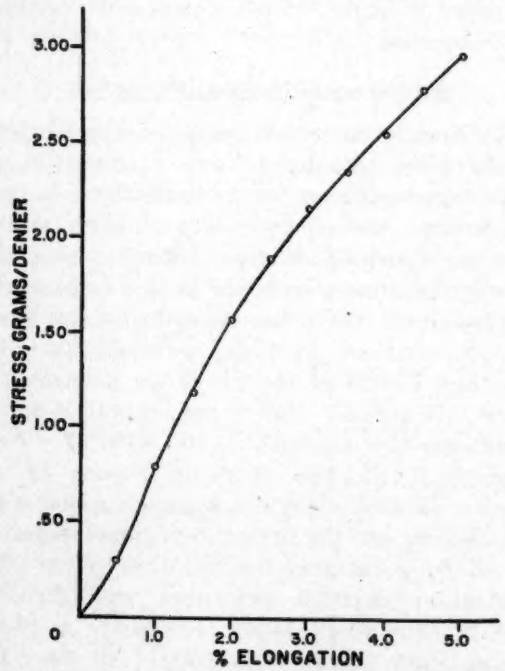

GRAPH IV. *Average stress-strain curve for fibers from henequen yarns.*

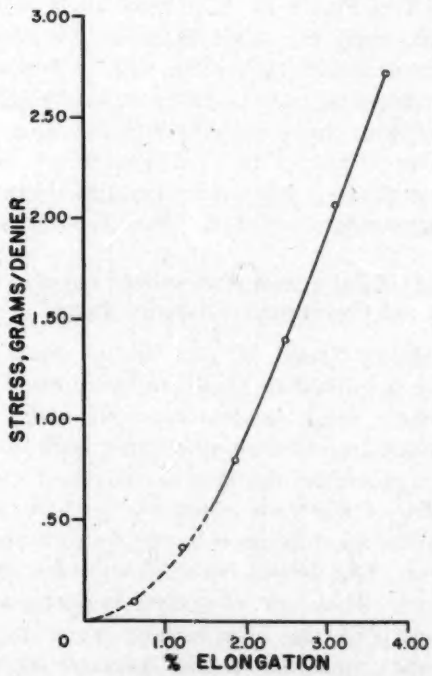

GRAPH V. *Typical stress-strain curve for Sansevieria yarn.*

continuous-filament fibers and the relationship between the yarn properties and those of the fibers. Yarn geometry was idealized in order to enable mathematical analysis to be made. Such an "idealized" geometry does not necessarily represent the geometry of an ideal (from the performance point of view) yarn, but merely a convenient simplification of the structural formation of a yarn. Since the extension of the work involved in the publication [8] to cordage yarn represents, when reduced to its simplest terms, the removal of the restriction of an assumption, the initial assumptions made for continuous-filament yarns are repeated:

(*1*) The yarn is uniform along its length, and its cross-sectional outline is circular.

(*2*) All fibers within a yarn possess the same properties.

(*3*) The center line of each fiber lies in a perfect helix, with the center of the helix located at the center of the yarn cross section.

(*4*) The fibers fall into a rotationally symmetric array in cross-sectional view.

(*5*) The diameter of the yarn is large compared with the fiber diameter.

These assumptions result in the yarn geometry illustrated in Figure 1. The helix angle, θ, shown in *A* represents the angle between the yarn and fiber axes of the outside fibers only. Assumption (*4*) describes this angle as being equal for all fibers which fall into the outer sheath of the yarn. Any other layer of fibers, such as those shown in *B* to lie at a distance r from the yarn axis, possesses a helix angle designated by θ_r, where $\theta_r < \theta$.

A—Limitations of Previous Theory of Continuous-Filament Yarns

The theory based on the above assumptions obviously is limited in applicability to those yarns which obey these assumptions. Broadly, these assumptions are of two major types, both of which refer to uniformity: the first is concerned with the uniformity of the yarn geometry; and the second involves the assumption of perfectly uniform fiber properties. Obviously, both assumptions may be questioned. However, of greater importance than the validity of the assumptions from the yarn performance viewpoint is the question as to the magnitude of the effects produced by any deviations.

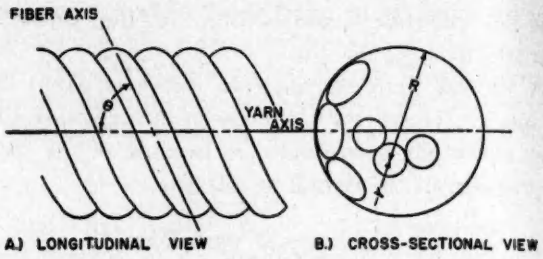

FIG. 1. *Idealized singles yarn geometry.*

When yarns made of the natural cordage fibers are considered, the obvious reaction to the assumptions is that the fibers are so variable [4] in their inherent properties that severe inaccuracies must exist in any analysis which does not take this variability into account.

The following will, then, be concerned with bringing the development closer to reality for cordage-fiber yarns by introducing into the analysis the variability of the fiber properties. All of the other assumptions concerned with yarn geometry are assumed to be valid here. In addition, it is presumed that sufficient twist has been imparted to the yarn so that fiber slippage does not have to be considered. As shown later, experimental results indicate that slippage may be neglected in the determination of cordage yarn properties for the range of yarn twists commercially produced for cordage use.

B—Variation in Fiber Properties

Variations in the tensile mechanical properties of the fibers are considered, since yarn tensile mechanical properties are under discussion. In order to introduce the concept of variability and to indicate its possible effects, the simple case of two fibers of the same population loaded in parallel is analyzed first. Let it be assumed that two sets of such combinations are under consideration. The load-strain curves of the fibers are illustrated in Figure 2 (*A* and *B*). In the case of both *A* and *B*, the average fiber strength is $(100 + 60)/2 = 80$ g. However, if the two fibers in Figure 2*A* are loaded in parallel, the fiber whose elongation is 4% will fail first, and the other fiber will contribute a load of 80 g. at this first rupture point. The combination strength per fiber will then be $(80 + 60)/2 = 70$ g., which represents a 12.5% decrease from the average load of 80 lbs. The case of Figure 2*B* represents two fibers which also differ in elongation by 2%, but whose magnitude

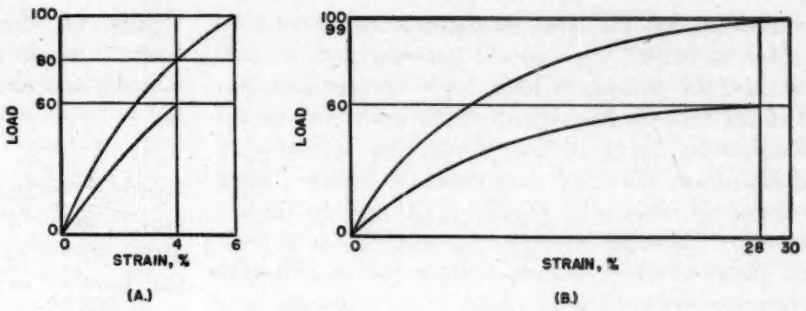

FIG. 2. *Two fibers loaded in parallel.*

of elongation is much greater than that of the fibers of A. In this case, the strength of the combination per fiber would be $(60 + 99)/2 = 79.5$ g. Thus, the second combination is shown to be more efficient than the first.

While the foregoing appears obvious and simple, it is essential that the elementary principles indicated be understood, since the application to both a large number of fibers in parallel and a yarn having twist become increasingly complex. As the succeeding developments show, the translation of the properties of fibers into yarns depends upon the following: average fiber stress-strain curve, found by averaging the loads at given elongations of a statistically adequate fiber sample; the mean elongation to rupture of the fibers; the coefficient of variation of elongation to rupture of the fibers; and the yarn surface helix angle.

C—Large Number of Fibers in Parallel

Let it be assumed that a bundle of parallel fibers is subjected to a tensile strain application ranging continuously from zero to complete rupture. As tensile strain is applied to such a combination, resistance to the extension is afforded by the fibers in accordance with their stress-strain characteristics. Consider, first, extensions less than that of the rupture elongation of any fiber in the group Let the magnitude of the extension be e. Then, the total load, P_B, supported by the bundle at this strain, e, is

$$P_B = P_1 + P_2 + P_3 + \cdots P_n, \qquad (1)$$

where P_n is the load supported at this strain, e, by any fiber. Now it is clear that P_B may also be written as

$$P_B = N_f \bar{P}, \qquad (2)$$

where N_f is the total number of fibers in the bundle, and $\bar{P}$ is the numerical average of the loads supported by each of the fibers at the strain e. This is so since by definition:

$$\bar{P} = \frac{P_1 + P_2 + \cdots P_n}{N_f}. \qquad (3)$$

Thus, it is clear that for bundle extensions less than that at which the lowest-elongation fiber breaks, the load-extension diagram of the bundle is the same as the average load-extension diagram of the fibers.

As the extension increases beyond the point where the fibers of lowest elongation rupture, progressive failure occurs, with the load increasing or decreasing in a manner defined by the nature of the fiber (stress-strain characteristics) and the

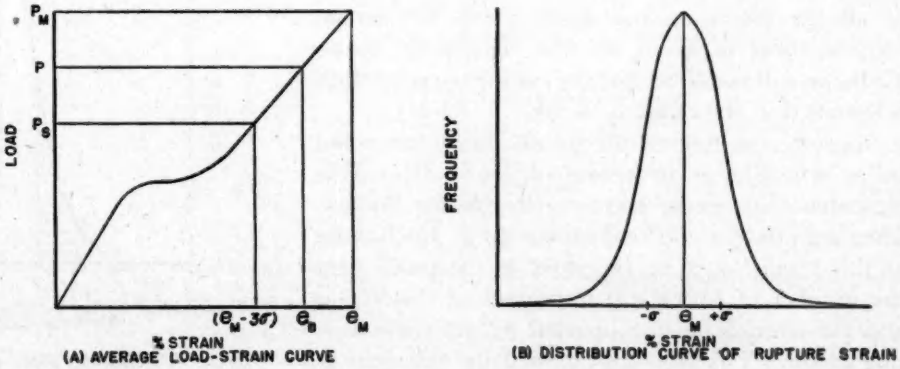

FIG. 3. *Hypothetical fiber stress-strain curve and rupture-elongation distribution curve.*

variability of the fiber elongation to break. In order to define this rupture process, and, in particular, the maximum load, let it be assumed that two curves have been constructed: one is an average load-strain curve of the fibers; the second is a distribution curve of extensions to break. Such curves are shown in Figure 3 (*A* and *B*, respectively). In order to make the analysis as general as possible, it is assumed that the distribution curve of elongations to break, *B*, is a normal one, so that the distribution equation is only a function of the standard deviation of the material and of the mean value of the elongation to rupture, e_m.

It is known from statistical theory that the distribution curve of Figure 3*B* may be standardized by converting the abscissa scale to number of standard deviations from the mean. Thus, the abscissa e_m, which represents the mean elongation to break, would be 0 standard deviations from the mean, while the points labelled $(e_m \pm \sigma)$ would be plus and minus 1 standard deviation from the mean, and similarly for the other abscissa points of *B*. Thus, Figure 3*B* may be converted to Figure 4, which is the standardized normal distribution curve.

The curve given in Figure 4 is the Gaussian curve. Of great significance in the utilization of this curve are the facts that: (*1*) the total area under this curve is numerically equal to 1; and (*2*) the percentage of fibers having elongations between any two abscissa values is merely the area subtended by the curve and bounded laterally by the ordinates corresponding to these abscissas. Thus, the percentage of fibers having elongations falling between -1 and -2 standard deviations from the mean elongation would be the shaded area shown in Figure 4, and similarly for other areas.

Actually, the curve of Figure 4 extends from $-\infty$ to $+\infty$, but since it is known from statistical theory that the mean value $\pm 3\sigma$ contains over 99% of all the fibers, in the work which follows no consideration is given to the remaining fibers. Thus, we will presume that the complete population is specified in the range $e_m \pm 3\sigma$.

Consider the case of the bundle being stretched to e_b, where e_b is in excess of $(e_m - 3\sigma)$. This indicates that some fibers have already broken. The magnitude of the load supported by the bundle at this strain, e_b, must be equal to the product of the number of fibers still unbroken at this strain and the average load supported by such fibers at this strain. This may be clarified by reference to Figure 3*A*, the average load-strain curve of the fibers. At the strain $e_m - 3\sigma$ no fibers have been broken, and the load supported by the fiber bundle is

$$P = N_f P_s, \tag{4}$$

where N_f is the total number of fibers in the group, and P_s is the average load supported by the fibers at the strain $(e_m - 3\sigma)$. As further load is applied, the number of fibers capable of supporting load decreases, but the load carried by each still unbroken fiber increases. Thus, at the bundle strain e_b, the load carried per fiber is P, where P exceeds P_s, but the number of fibers is less than N_f since some have already broken. Therefore, in general, the load supported by the bundle may be written as

$$P_B = (N_f)_u(P), \tag{5}$$

where $(N_f)_u$ is the number of fibers unbroken at the strain e_b, and P is the average load supported by the fibers at the strain e_b. It is clear that the value of P may be taken directly from the average load-strain curve. The magnitude of $(N_f)_u$ may be determined from the standardized normal distribution curve as follows: Consider first the percentage of unbroken fibers at $(e_m - 3\sigma)$. This percentage we have assumed to be 100% since all fibers have elongations falling within the limits $e_m \pm 3\sigma$. Now, if the fiber bundle is strained to $e_m - 2\sigma$, all fibers having elongations between $(e_m - 3\sigma)$ and $(e_m - 2\sigma)$ will be broken. The % of the total number of fibers in the bundle having elongations between these two limits will be equal to the area *a-b-c-d* in Figure 4. Thus, the % of unbroken fibers at a bundle strain of $e_m - 2\sigma$ would be (100) [1-area (*a-b-c-d*)]. Similarly, the % of fibers unbroken at any bundle strain e_b

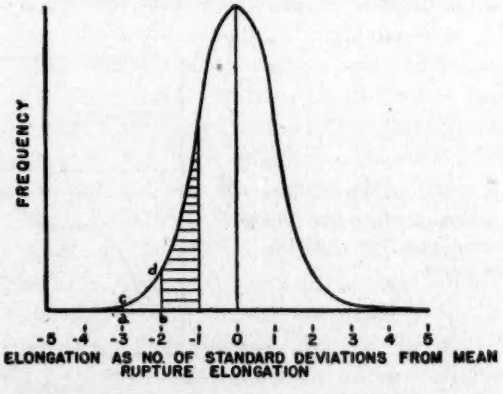

FIG. 4. *Standardized normal distribution curve.*

would be equal to 100 [1-(area to the left of this strain and bounded by the curve of Figure 4)]. Thus, a general curve of % of unbroken fibers can be drawn corresponding to the normal distribution curve. This curve is shown in Figure 5. The exact equation for the curve of Figure 5 is complex and cumbersome to use in what follows. As an approximation to the exact equation, the following power series, sufficiently accurate for the computations which will be made, has been derived:

$$n_u = 100(0.496 - 0.442t - 0.0979t^2), \quad (6)$$

where t is the number of standard deviations from the mean. Obviously, then, $(N_f)_u$ would be equal to $n_u N_f/100$. To convert the value of e_b to the t of equation (6), it is clear that

$$t = \frac{e_b - e_m}{\sigma}. \quad (7)$$

Since $(\sigma/e_m) \times 100$ is the coefficient of variation of the population, v, equation (7) may be rewritten as

$$t = \frac{100}{v}\left(\frac{e_b}{e_m} - 1\right). \quad (8)$$

Therefore, the % of unbroken fibers, n_u, given in equation (6) may be rewritten directly in terms of the mean fiber elongation, e_m, the bundle strain, e_b, and the coefficient of variation of elongation of the fibers, v, as

$$n_u = 100\left[0.496 + \frac{44.2}{v} - \frac{979}{v^2} + \frac{e_b}{e_m}\left(\frac{1958}{v^2} - \frac{44.2}{v}\right) - \frac{979}{v^2}\left(\frac{e_b}{e_m}\right)^2\right]. \quad (9)$$

Referring now to equation (5), it is clear that if P, the average load supported by the fibers at the strain e_b, is expressed analytically in terms of e_b, the total load supported by the bundle at any elongation can be determined. The maximum load can then be found by determining at which value of e_b the derivative of equation (5) is zero, followed by substitution of this particular value of e_b back into equation (5). Thus, it is first necessary to determine the analytic equation of the average load-strain curve of the fibers. As already stated, this average load-strain curve is that found by numerically averaging the loads supported by the fibers at given elongations. It is assumed in the subsequent analysis that the fibers which comprise the bundle exhibit a random distribution of breaking loads and breaking elongations, so that, consequently, the loads supported by the various fibers at given elongations are also randomly distributed about the mean value of the load. As shown later, such curves are essentially linear for most natural fibers, such as cotton, linen, Manila abaca, sisal, etc., in the region of 0.5 e_m to e_m. While similar analyses may be made for any shape load-strain curve, for the sake of simplicity the analysis is here confined to linear curves only. For convenience, Figure 3*A*, with slight modification, is reproduced as Figure 6. If a and b represent the load intercept and slope, respectively, of the linear portion of the average load-elongation curve, then it is clear that

$$P = b\left(\frac{a}{b} + e_b\right). \quad (10)$$

Thus, it is possible to rewrite equation (5) for the load on the bundle in terms of the following variables: v, the coefficient of variation of extension

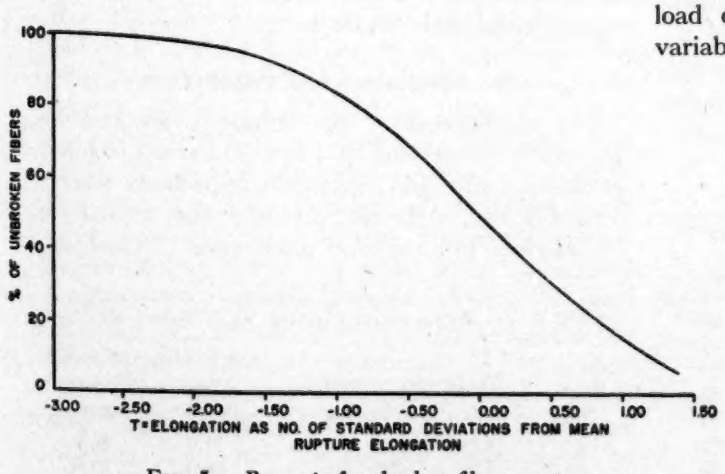

FIG. 5. *Percent of unbroken fibers* vs. t.

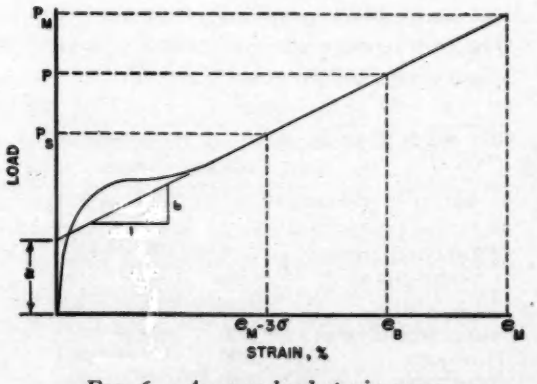

FIG. 6. *Average load-strain curve.*

to break of the fibers; e_m, the mean elongation to break of the fibers; a/b, an inherent property of the fiber found from the load-strain curve; and e_b, the strain on the bundle.

In summary, the procedure is as follows: substitute equations (9) and (10) into equation (5); differentiate with respect to e_b, equate the derivative to 0; and substitute the resulting value of e_b back into equation (5). Thus, the maximum value of P_B can be found for any e_m, v, and a/b. Since the work is purely arithmetical, no further explanation is given. Instead, the results of such computations are given in the theoretical curves plotted in Graph VI. Here, the results are expressed in terms of efficiency. The efficiency is the ratio of maximum bundle load divided by the value obtained by multiplying the average breaking load of the fibers by the total number of fibers in the bundle, and thus represents the degree to which average fiber strength has been translated into the bundle.

Examination of Graph VI shows that synthetic fibers, having high uniformity (low v) translate well into bundles. For zero v (no variability in fiber extension to break), bundle tenacity should be the same as fiber tenacity. As variability increases, efficiency decreases. For a given variability, as the fiber extension increases, the efficiency will increase or decrease depending upon whether a/b is negative or positive, respectively. For a given mean fiber rupture elongation and variability of rupture elongation, the smaller the values of a/b, the less the bundle efficiency. Natural cordage fibers have low elongations to break and high variability of rupture elongation [4]. In addition, the stress-strain curve shapes are extremely steep, indicating low values of a/b. Thus, it would be anticipated that bundle efficiencies would be low for all of the cordage fibers which were made into the yarns whose properties were described in section *I* of this report. Bundle efficiencies calculated for these fibers are given in Table IV.

TABLE IV. THEORETICAL BUNDLE EFFICIENCIES FOR CORDAGE FIBERS

Fibers from yarns designated as:	Fiber properties e_m	a/b	v	Theoretical bundle efficiency (%)
Blended abaca	3.00%	−0.73	28%	58
Abaca strand yarns	3.00	+2.10	24	71
Henequen	5.00	+2.10	20	74
Sansevieria	3.30	0	30	60

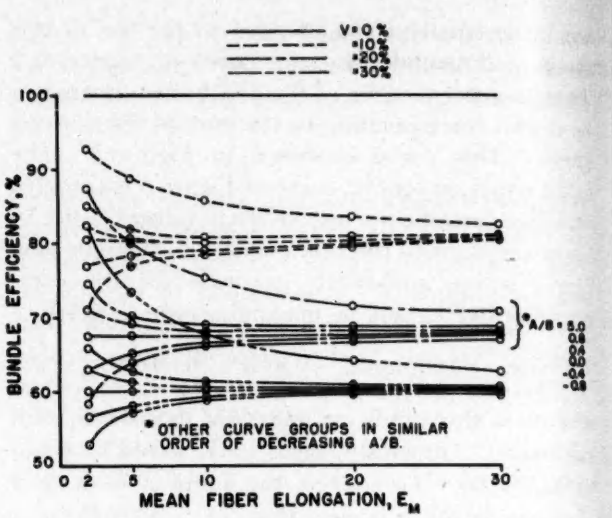

GRAPH VI. *Bundle efficiency* vs. *fiber elongation.*

From Table IV it can be seen that severe losses in translation of fiber tenacity can occur in a bundle break. As shown later, additional losses occur in twisted yarns, but it is emphasized that even in a bundle break of the variable hard fibers, where all of the fibers would be throughgoing from pulling jaw to fixed jaw, losses in translation of a considerable magnitude would occur.

To illustrate the degree of precision of the theoretical analysis of bundles, some data have been obtained on the so-called "skein breaks" of cotton yarns. These data are given in Table V.

For the skein-break analysis, the single ends correspond to the fibers considered in the theoretical development, while the skein corresponds to the fiber bundles. It is apparent that the results of the analysis of the bundles compare favorably with experimental skein-break data.

D—Application to Twisted Yarn

The application of the foregoing sections on variability to the case of a twisted yarn is complex mathematically, but physically represents merely a combination of the effects of both fiber inclination as described in a previous publication [8] and also

TABLE V. RESULTS OF COTTON YARN SKEIN BREAKS

Skein No.	Single-end properties e_m	a/b	v	Skein efficiencies (%) Theoretical	Experimental
a	9.2%	−1.5	9.8%	77.0	80.0
b	9.9	−2.0	7.1	80.0	79.5

variability of fiber elongations and progressive failure resulting therefrom.

Elsewhere [8] it was shown that for the case of no slippage and with no variability of the fiber extension, maximum yarn load is attained when the center fiber group is strained to its rupture value. At this point, the load on the remaining fibers in the yarn is specified by the fact that their strains, e_θ, must be related to the yarn strain by

$$e_\theta = e_y \cos^2 \theta, \tag{11}$$

where e_θ is the strain in the fibers inclined at the angle θ to the yarn axis, and e_y is the yarn strain. Having fixed the fiber strains, the corresponding fiber stresses are found from the stress-strain diagram of the fiber. The final determination of yarn load is made by integrating all of the components of these fiber stresses parallel to the yarn axis.

For the case of yarns composed of variable fibers, the same geometric dependency of fiber stresses and strains upon helix angle exists. The only ramification is that since variability in extension to break exists, maximum yarn load will not necessarily and rarely does occur when the yarn is stressed to the average fiber rupture elongation.

It has been shown [8] that for the case of a twisted structure the total axial load on the yarn may be written as

$$P_y = 2\pi \int_0^R f(\theta) \cos^2 \theta r dr, \tag{12}$$

where $f(\theta)$ represents the stress intensity in the yarn in the fiber direction where the fiber is inclined θ degrees to the yarn axis. Equation (12) assumes that all fibers in the yarn are bearing load, and therefore is valid only for yarn elongations less than those necessary to cause the lowest-elongation fiber to rupture. For these low elongations, yarn characteristics such as modulus, extension, and energy absorption are independent of variability. For such low yarn elongations, increasing yarn twist produces the following changes: modulus decreases [8], total elongation at a given load increases [8], energy absorbed at a given load increases [8], permanent set increases [8], and the "elastic performance coefficient" [1] decreases [8]. However, above that yarn elongation where some fibers break, obviously not all fibers are carrying load, and the problem must again be approached statistically.

Only the case where the fiber rupture elongations are normally distributed is considered here in detail. It is presumed that an average stress-strain curve for the fibers has been obtained. Thus, Figures 5 and 6 can be used for purposes of discussion.

It is now assumed that the normal distribution curve of elongation to break of the fibers applies to each layer of fibers which comprise the yarn [8]. Since the number of fibers in a layer increases as the distance of the ring from the yarn center increases, the absolute number of fibers remaining unbroken at any yarn elongation, e_y, increases as the distance increases. However, it follows from the previous assumption that the % of unbroken fibers in any layer is dependent upon its elongation only. Hence, Figure 5 applies to each layer, and thus also does equation (9).

However, equation (9) must be modified in accordance with the helix-angle effect on fiber strains—*i.e.*, e_b in equation (9) must be replaced by the axial strain on the fibers, e_θ, in any particular layer. This strain is known from equation (11). Thus, for the case of the twisted yarn:

$$n_u = 100 \left[0.496 + \frac{44.2}{v} - \frac{979}{v^2} + \frac{e_y \cos^2 \theta}{e_m} \left(\frac{1958}{v^2} - \frac{44.2}{v} \right) - \frac{979}{v^2} \left(\frac{e_y \cos^2 \theta}{e_m} \right)^2 \right]. \tag{13}$$

In equation (13) n_u is the % of fibers unbroken at a yarn strain e_y, when the coefficient of variation of fiber rupture elongation is v, with a mean fiber elongation to rupture of e_m, for the layer within which fiber inclination is θ. Thus, layer position does influence the % of the fibers unbroken, but only by virtue of the fact that at a given yarn strain the fiber strain in those layers which are furthest from the yarn center is least and, hence, the fewer the number of fibers which have exceeded the rupture point. It is emphasized that size of the layer is assumed to have no effect on the distribution.

Thus, equation (12) must be modified by the % of unbroken fibers, as given by equation (13). Also, f, the fiber stress, must be expressed in terms of θ. Again assuming a linear stress-strain curve in the rupture region, the stress may be written

$$f_\theta = b \left(\frac{a}{b} + e_\theta \right), \tag{14}$$

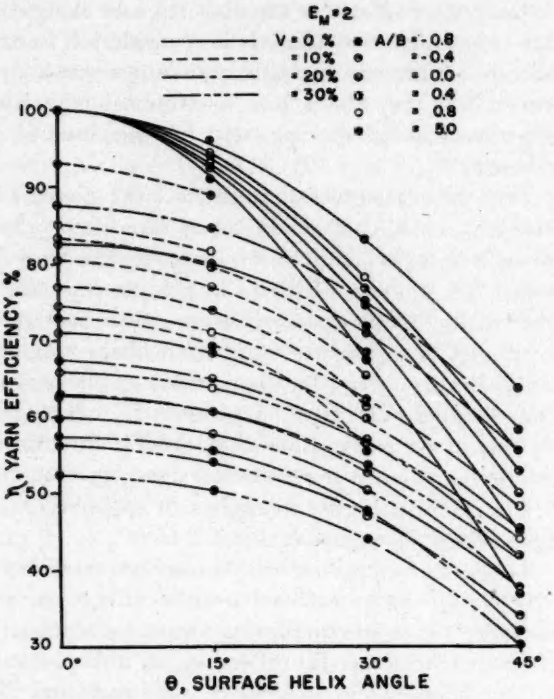

GRAPH VII. *Yarn efficiency* vs. *helix angle.*

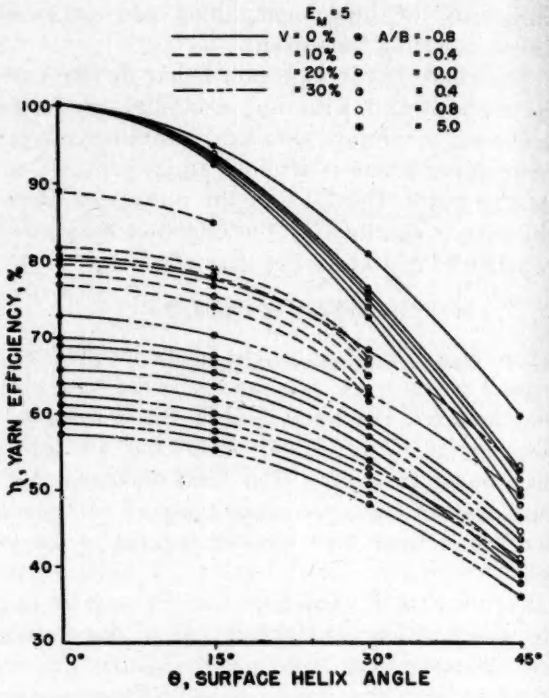

GRAPH VIII. *Yarn efficiency* vs. *helix angle.*

where f_θ is the stress in fibers inclined at the angle θ to the yarn axis, e_θ is the strain for these inclined fibers, and a and b are as previously defined. Combining equations (11), (12), (13), and (14), there results

$$P_y = 2\pi \int_0^R b \left(\frac{a}{b} + e_y \cos^2 \theta \right) \cos^2 \theta \, \frac{n_u}{100} \, r dr, \quad (15)$$

where P_y is the yarn load, and n_u is defined by equation (13). All that remains is to express θ in terms of r. This is done simply by

$$\cos^2 \theta = \frac{1}{1 + 4\pi^2 N^2 r^2}. \quad (16)$$

From this point on, the analysis involves the integration of equation (15) to obtain a general equation for P_y, followed by determination of specific maximum values of P_y for different a/b values, v's, and θ's.

The results of such laborious computations are given as Graphs VII–XI. It is clear that the case of the bundle of fibers previously discussed is merely a special case of the solution of equation (15) when $\theta = 0°$. Thus, Graphs VII–XI contain results which are applicable to the bundle.

It is emphasized again that slippage has been assumed not to occur in this analysis. In this sense, the numerical data given in Graphs VII–XI only apply to the range of twists within which slippage does not exist. Hence, if experimental results check the theoretical results to a reasonable degree of precision, slippage may be assumed to be unimportant as concerns yarn strength. As shown later, sufficient experimental determinations of fiber friction in cordage yarns have been made to ensure that slippage considerations are insignificant here.

E—Application of Theoretical Results to Cordage Yarns

The application of the theoretical Graphs VII–XI to the cordage yarns described in section *I* is relatively simple. All that is necessary is to determine the pertinent fiber data, pick points off the curves, and compare the theoretical efficiencies with the experimental results. Certain corrections, however, must be made to either the experimental or theoretical efficiencies as follows:

1—Correction for Oil Pickup

In all cases, experimental yarn efficiencies are determined as the ratio of yarn tenacity to fiber tenacity. The yarn tenacity is, of course, the

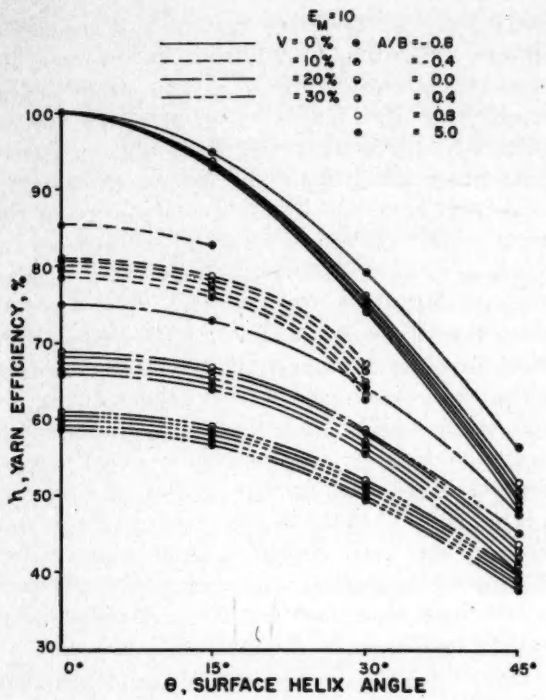

GRAPH IX. *Yarn efficiency* vs. *helix angle.*

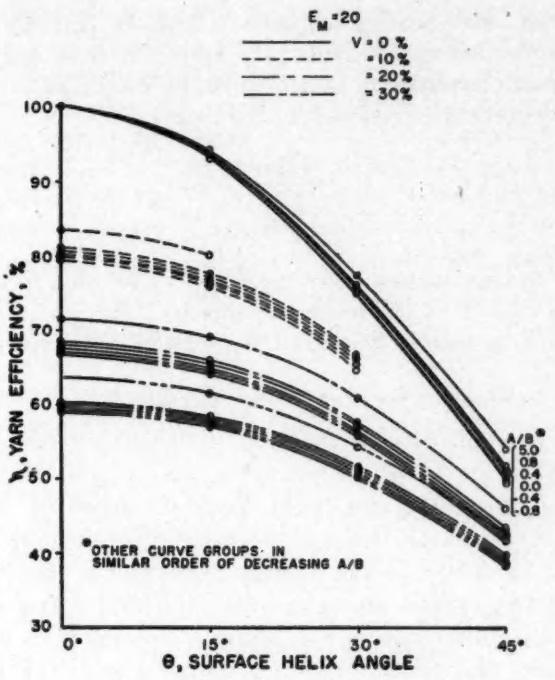

GRAPH X. *Yarn efficiency* vs. *helix angle.*

yarn strength per unit weight—*i.e.*, grams per denier. Since, in most cordage yarn processing, oil is added to the fiber before spinning to the extent of 10%–20% by weight, appreciable losses would appear to exist if yarn efficiency were calculated on the basis of unoiled fiber tenacity. As has been shown [4], the oil adds weight, but not strength, to the fibers. Thus, in order to represent experimental yarn efficiencies on a comparable basis, since different oil pickups may be involved for different yarns, all experimental yarn efficiencies are computed using oiled-yarn tenacity in conjunction with oiled-fiber tenacity, or unoiled-yarn tenacity in conjunction with unoiled-fiber tenacity. Either procedure will give the same result. The precaution to be observed is not to compute experimental yarn efficiencies using oiled-yarn tenacities in conjunction with unoiled-fiber tenacities.

2—Correction for Twist Take-up in Yarns

Where high yarn twists are encountered, correction of the theoretical efficiencies is necessary to account for the extra fiber length resulting from the longer helical paths of the inclined fibers. The effect here is to reduce the theoretical efficiency,

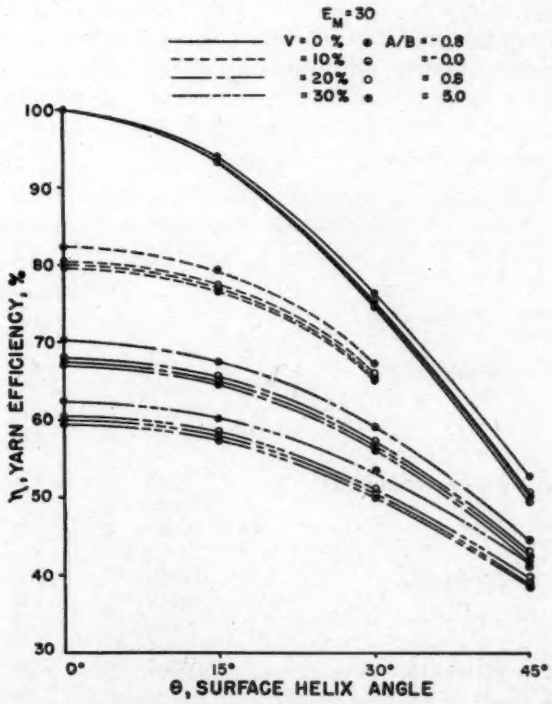

GRAPH XI. *Yarn efficiency* vs. *helix angle.*

since the longer helical path lengths of fibers add yarn weight, with no concomitant increase in

yarn load-bearing capacity. This is actually a correction for the twist take-up of the yarn, and is most conveniently taken care of by multiplying the theoretical efficiencies by the factor

$$\frac{\frac{3}{2}\tan^2\theta}{\left(\frac{1}{\cos^3\theta}-1\right)}.$$

For yarn surface helix angles up to 15° this factor is close to 1.00, while for angles of 20°, 25°, and 30°, the factors are 0.97, 0.96, and 0.93, respectively.

3—Correction for Mean Fiber Strength

The theoretical efficiency, as developed analytically in the preceding subsections **C** and **D** for bundles and yarns, respectively, is based on the fiber stress (g./den.) at the mean fiber elongation, e_m, as found on the average stress-strain diagram of the fibers. In many cases the fiber stress at mean fiber rupture elongation is not equal to the mean fiber tenacity, the former being less than the latter. Thus, the theoretical efficiency computed using the fiber stress at mean fiber rupture elongation would be too great. To compensate for this difference, theoretical efficiencies as read from the graphs must be multiplied by the correction factor

$$\frac{f(e_m)}{\bar{f}},$$

where $f(e_m)$ is the stress (g./den.) at mean fiber rupture elongation found from the average fiber stress-strain curve, and $\bar{f}$ is the mean rupture tenacity of the fibers. The necessity for this correction arises from the fact that, in general, those fibers which have the highest elongation to break also have the lowest average slope of their stress-strain curves. Thus, when stresses are averaged to form the average stress-strain diagram, a shape distortion may occur. This distortion, when it occurs, is in the direction for cordage fibers, which involves a lowering of the stress coordinate of the stress-strain curves. At present, there is no analytic method of predicting the magnitude of the correction factor. The procedure given above is considered the most logical method of correction. It is emphasized that this correction factor is not an arbitrary one, but, instead, it is necessary in order to compare theoretical and experimental efficiencies on the same basis, and this basis, in order to be a realistic one, must be the mean fiber tenacity.

Table VI compares theoretical and experimental efficiencies of the cordage yarns whose properties were given in section *I*. In all cases, corrections were made in accordance with *1*, *2*, and *3* (above).

Examination of the theoretical and experimental yarn efficiencies given in Table VI shows that it is theoretically possible to predict the extent to which fiber strength is translated into yarns with a high

TABLE VI. COMPARISON OF THEORETICAL AND EXPERIMENTAL YARN EFFICIENCIES

Yarn type	Pertinent fiber properties e_m	a/b	v	θ	Yarn efficiencies Theoretical (%)	Experimental (%)
Blended abaca	3.00%	−0.73	22%†	16.5°	54.0	56±3*
	3.00	−0.73	24	20.0	50.0	50±3
	3.00	−0.73	31	24.5	47.0	43±3
	3.00	−0.73	32	29.4	42.0	38±3
Abaca strand yarns	3.00	+2.10‡	24	14.0	62.0	64±1
	3.00	+1.51	24	18.0	58.5	56±2
	3.00	+0.91	24	24.0	52.5	50±2
Henequen	5.00	+2.10	20	22.0	59.0	63±1
	5.00	+2.10	20	28.0	54.0	56±2
	5.00	+2.10	20	35.0	45.0	39±3
Sansevieria	3.30	0.00	30	17.0	55.5	56

* ± Values are 2 standard errors computed from variance of yarn tenacity.

† Data on fibers removed from yarns showed a consistent increase in variability with increase in yarn twist only in the case of the blended abaca yarns. (See [4], Table XVII.)

‡ For the abaca strand yarns the average fiber stress-strain curve is not linear. Varying a/b values were computed from the best straight line through the points on the stress-strain curve at e_m and $e_m \cos^2\theta$. All other average stress-strain curves were linear over a wide range near rupture.

degree of precision. In most cases the agreement is well within the statistical variation of yarn tenacity, and it appears probable that if variation in fiber tenacity were considered in assessing the range of experimental yarn efficiencies, still closer agreement than that shown in Table VI would result.

F—Investigation of Assumptions Made in Analysis

It has been shown that the analysis yields reliable results for cordage yarns. Two assumptions were made, the validity of which will now be explored, namely: (*1*) the population of rupture elongations may be represented by the classical Gaussian normal distribution; and (*2*) at loads equal to or less than the maximum load exhibited by the cordage yarns, fiber slippage does not occur.

1—Effects of Shape of Rupture-Elongation Distribution Curve

In order to solve the problem of the translation of fiber strength to bundle or yarn strength explicitly, it is necessary to assign a shape to the curve of distribution of rupture elongations. For the sake of generality, it has been assumed in the analysis that the curve is normal, and therefore mathematically represented by the standard equations of such normal curves. However, as indicated in the analysis, approximations to the exact equation of the normal curve are necessary in order to obtain numerical results, since the exact equation is nonintegrable. The curve which is approximated is that given in Figure 5, which plots % of unbroken fibers *versus* elongation, expressed as the number of standard deviations from the mean. The form of the approximate distribution curve is given by equation (6). The degree to which the approximate expression checks the exact one is shown in Figure 7. The fit is extremely close for elongations equal to or less than the mean, but somewhat poorer at higher elongations. Since the computations show that maximum yarn load is attained in the lower elongation range, it is clear that the use of the approximation is valid.

In order to determine the extent to which the rupture elongations of the cordage fibers approximate normality, fibers removed from the abaca strand yarns were studied. The distribution was tested by comparison of the calculated n_u for these fibers with the theoretical n_u determined from the normal distribution curve. As shown on Graph XII, the agreement is very close.

However, of greater general significance than the degree to which the rupture elongations of any single group of fibers departs from normal is the more general comparison of results which would be obtained for different types of distributions with those obtained for normal distributions. For example, if a standard deviation of rupture elongations for any type of fiber were calculated by well-known statistical formulas, with no check to ascertain whether or not the population is a normal one, it would be important to know if the theoretical efficiencies plotted on Graphs VII–XI would be markedly in error if used for prediction. Reference

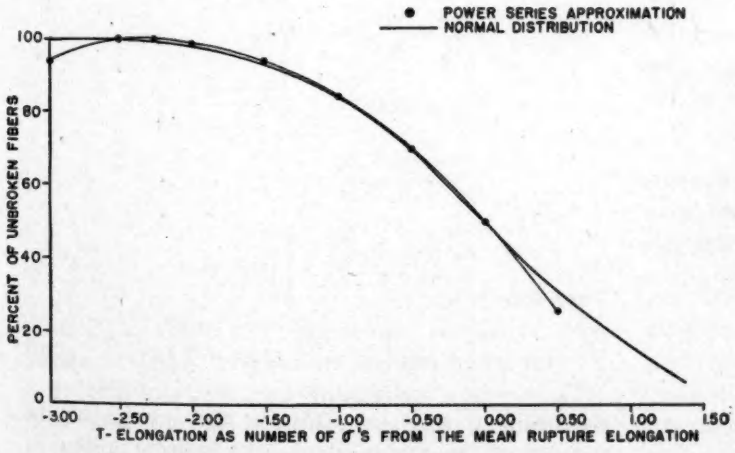

FIG. 7. *Percent of unbroken fibers* vs. t.

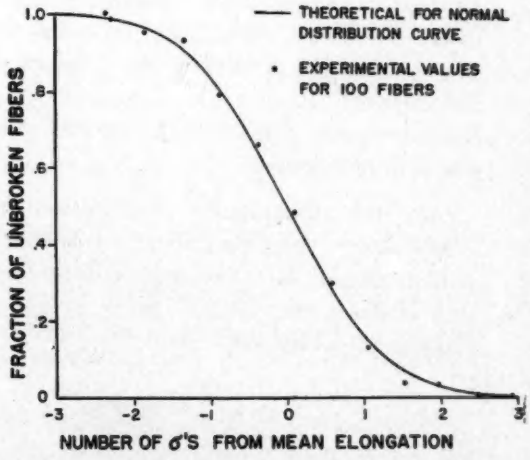

GRAPH XII. *Statistical distribution of fiber elongations for fibers from abaca strand yarns.*

to the analysis will show that the only errors arising from differences in type of distribution are those which affect Figure 5, which plots % of unbroken fibers *versus* elongation, expressed as the number of standard deviations from the mean. Thus, from continuous distribution curves of rupture elongations designed to illustrate particular abnormal shapes, it is possible to indicate the magnitude of error of predicted results arising from extreme departures from normality. In order to analyze such abnormal shape curves, it is necessary to generalize both the computation of the standard deviation and also the meaning of the area under the distribution curve as follows:

(*a*) In general, the calculation of standard deviations by the formula

$$\sigma = \sqrt{\frac{\sum(x - \bar{x})^2}{n - 1}} \qquad (17)$$

is equivalent, in the continuous case, to

$$\sigma = \sqrt{\frac{I}{A}}, \qquad (18)$$

where A is the area under the distribution curve, and I is the moment of inertia of this area about an axis through its center of gravity—*i.e.*, about the ordinate passing through the mean elongation. Thus, equation (18) permits computation of the standard deviations for distribution curves of any shape.

(*b*) The area under the distribution curve bounded by the ordinates erected at any two elongation values, when divided by the total area under the curve, equals the fractional part of the total population of fibers whose rupture elongation lies between these two elongation values. This equality holds independently of the shape of the distribution curve.

Case (a)—Rectangular Distribution of Rupture Elongations.—Assume that the distribution curve of fiber elongation to rupture is a rectangular one with defined end-values. Such a distribution is illustrated in Figure 8. For this case,

$$\sigma = \sqrt{\frac{I}{A}} = 0.288a,$$

and

$$n_u = 100\left[1 - \frac{(e - c)}{a}\right].$$

TABLE VII. PERCENT OF UNBROKEN FIBERS FOR RECTANGULAR DISTRIBUTION CURVE

t = elongation as no. of σ's from mean	Percent of unbroken fibers (equation (19))	Percent of unbroken fibers (normal distribution)
0	50.0	50.0
−0.25	57.2	60.0
−0.5	64.4	69.2
−1.0	78.8	84.1
−1.5	93.2	93.3
−1.74	100	95.9

But e, the fiber elongation, is expressible in terms of the number of standard deviations from the mean, t, as

$$t = \frac{e - e_m}{0.288a},$$

where

$$e_m = c + a/2.$$

Therefore,

$$\begin{aligned} n_u &= 100[1 - (0.288t + 0.5)] \\ &= 100(0.50 - 0.288t). \end{aligned} \qquad (19)$$

Thus, for this type of distribution curve, a table of comparison may be made (see Table VII).

The maximum error in the case of the rectangular distribution would be 7% if maximum load on a bundle occurred at an elongation equal to − 0.5 standard deviations from the mean. In the case of twisted yarns, the error would be even less, since the fibers would not be supporting equal strains.

Case (b)—Triangular Distributions.—The case of *extreme negative skew* will be analyzed first. Such a distribution is illustrated in Figure 9. For the case of Figure 9,

$$\sigma = \sqrt{\frac{I}{A}} = 0.237a$$

$$n_u = 100\left[1 - \left(\frac{e - c}{a}\right)^2\right]$$

$$t = \frac{e - e_m}{0.237a}$$

$$e_m = c + \frac{2a}{3}.$$

Therefore,

$$n_u = 100\left[1 - \left(0.237t + \frac{2}{3}\right)^2\right]. \qquad (20)$$

By utilizing equation (20) for the calculation of the % of unbroken fibers, the results given in Table VIII are obtained.

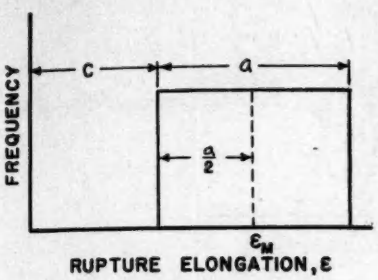

FIG. 8. *Rectangular distribution of rupture elongation.*

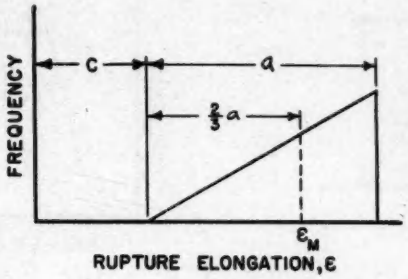

FIG. 9. *Triangular distribution, with extreme negative skew.*

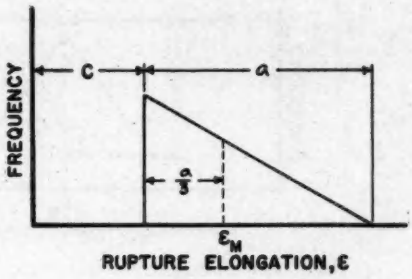

FIG. 10. *Triangular distribution, with extreme positive skew.*

TABLE VIII. PERCENT OF UNBROKEN FIBERS FOR TRIANGULAR DISTRIBUTION WITH EXTREME NEGATIVE SKEW

t = elongation as no. of σ's from mean	Percent of unbroken fibers (equation (20))	Percent of unbroken fibers (normal distribution)
0	55.5	50.0
−0.1	58.7	54.0
−0.2	61.6	57.9
−0.5	70.0	69.2
−1.00	81.4	84.1
−1.50	90.2	93.3
−2.00	96.3	97.7
−2.50	99.4	99.4
−2.81	100	99.8

For the above case, the maximum error would be 11% if maximum load on a bundle occurred at the mean fiber elongation. Again, in the case of yarns the maximum error would be less than 11%.

The case of *extreme positive skew* is illustrated in Figure 10. For this case,

$$\sigma = \sqrt{\frac{I}{A}} = 0.237a$$

$$n_u = 100\left[1 - \frac{(e-c)}{a}\right]^2$$

$$t = \frac{e - e_m}{0.237a}$$

$$e_m = c + a/3.$$

Therefore,

$$n_u = 100\left[\frac{2}{3} - 0.237t\right]^2. \qquad (21)$$

The % of unbroken fibers was calculated from equation (21). The results are given in Table IX.

In this case, the maximum error would be 12%, and would occur if maximum bundle load were exhibited at an elongation of − 0.2 standard deviation from the mean.

TABLE IX. PERCENT OF UNBROKEN FIBERS FOR TRIANGULAR DISTRIBUTION WITH EXTREME POSITIVE SKEW

t = elongation as no. of σ's from mean	Percent of unbroken fibers (equation (21))	Percent of unbroken fibers (normal distribution)
0	44.4	50.0
−0.1	47.8	54.0
−0.2	51.0	57.9
−0.5	62.0	69.2
−1.0	81.6	84.1
−1.41	100	92.5

As the final example of triangular distributions, the *symmetrical* case will be considered. The distribution is defined in Figure 11.

$$\sigma = \sqrt{\frac{I}{A}} = 0.408a$$

$$n_u = 100\left[1 - \frac{1}{2}\left(\frac{e-c}{a}\right)^2\right]$$

$$t = \frac{e - e_m}{0.408a}$$

$$e_m = c + a.$$

Therefore,

$$n_u = 100\left[1 - \frac{1}{2}(1 + 0.408t)^2\right]. \qquad (22)$$

The values for % of unbroken fibers calculated from equation (22) are given in Table X.

As would be expected, the symmetrical triangular distribution gives results which are very close to the normal curve. The maximum error, in this case, is only 2%.

Case (c)—Double-Peaked Distribution.—Only one example will be given—that of two normal distribution curves—each duplicating the other in all respects except for the mean value of rupture

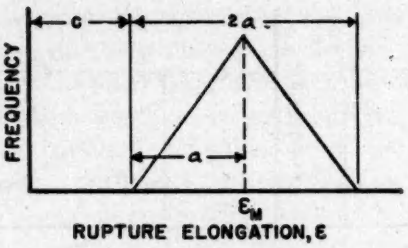

FIG. 11. *Symmetrical triangular distribution.*

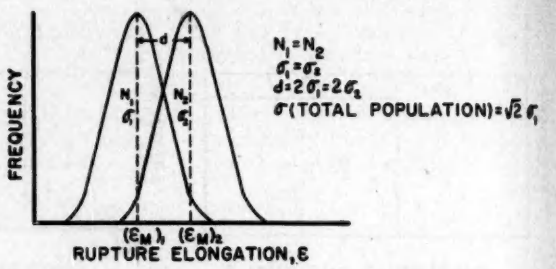

FIG. 12. *Double-peaked distribution.*

TABLE X. PERCENT OF UNBROKEN FIBERS FOR SYMMETRICAL TRIANGULAR DISTRIBUTION

t = elongation as no. of σ's from mean	Percent of unbroken fibers (equation (22))	Percent of unbroken fibers (normal distribution)
0	50.0	50.0
−0.5	68.2	69.2
−1.0	82.5	84.1
−1.5	92.5	93.3
−2.0	98.3	97.7
−2.45	100	99.4

TABLE XI. PERCENT OF UNBROKEN FIBERS FOR DOUBLE-PEAKED DISTRIBUTION

t^* = elongation as no. of σ's from mean	Percent of unbroken fibers (double-peaked distribution)	Percent of unbroken fibers (normal distribution)
0	50.0	50.0
−0.5	67.0	69.2
−1.0	82.1	84.1
−1.5	92.9	93.3
−2.0	99.0	97.7
−2.5	99.9	99.4

* σ, in this case, is the standard deviation of the total population.

elongations, which are assumed to be separated by twice the standard deviation of either population (see Figure 12). For this case, the results were determined graphically, and are given in Table XI. The agreement here is very close, the maximum error being 3% at $t = -0.5$.

The results of the foregoing analyses on the effects of shape of distribution curves of fiber rupture elongation are indicated more critically by Graphs XIII–XIV. Graph XIII compares the number of unbroken fibers for normal distribution curves with those of each of the distribution curves considered. As seen, the degree of fit is extremely close, even though the shapes of the curves differ. Since maximum load is functional with the ordinates of the curves given in Graph XIII, the shape difference is of no great concern. Graph XIV plots the % deviation of the ordinates of the curves of Graph XIII from the ordinates corresponding to the normal curve. Thus, Graph XIV is a plot of % error in number of unbroken fibers for each of the assumed distributions. It is easily seen from this graph that the maximum error (± 12%) occurs for the two skewed triangular distributions at the point where approximately half the fibers are unbroken—*i.e.*, near where $t = 0.0$. For the case of cordage fibers, where bundle efficiencies of the order of 50%–70% are encountered, the maximum error in bundle efficiencies would be 6%–8½% corresponding to the error of 12%. Since, in practical cases, no such extreme departure from a normal curve as that exhibited by the triangular distributions would ever be encountered, maximum errors would probably be less than 6%–8½%. For twisted yarns the error is even less.

In summary, then:

(*1*) It has been shown by analysis of curves of distribution of fiber rupture elongation exhibiting extreme departures from normality that deviations in number of unbroken fibers with increase in strain are small.

(*2*) Thus, the theoretical analysis based on normal distributions is sufficiently accurate to enable quantitative prediction of bundle and yarn strengths, without the necessity of correction for the shape of the particular distribution curve which may exist.*

2—Fiber Slippage Considerations

Throughout the analysis developed herein, frequent references have been made to the fact that fiber slippage has been assumed not to occur when

* The strength of blends may not, in general, be predicted by the theoretical curves in Graphs VII–XI. However, similar types of analysis may be employed.

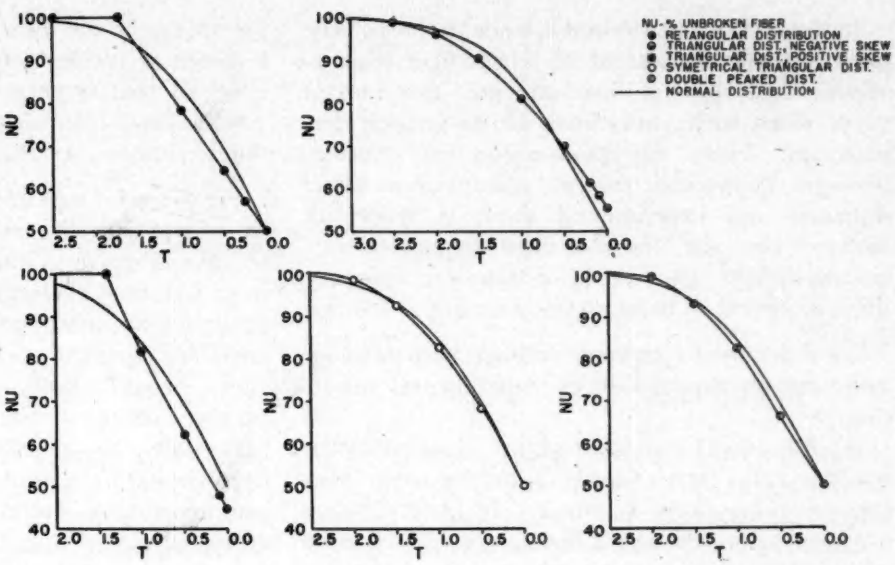

GRAPH XIII. *Comparison of special and normal distributions.*

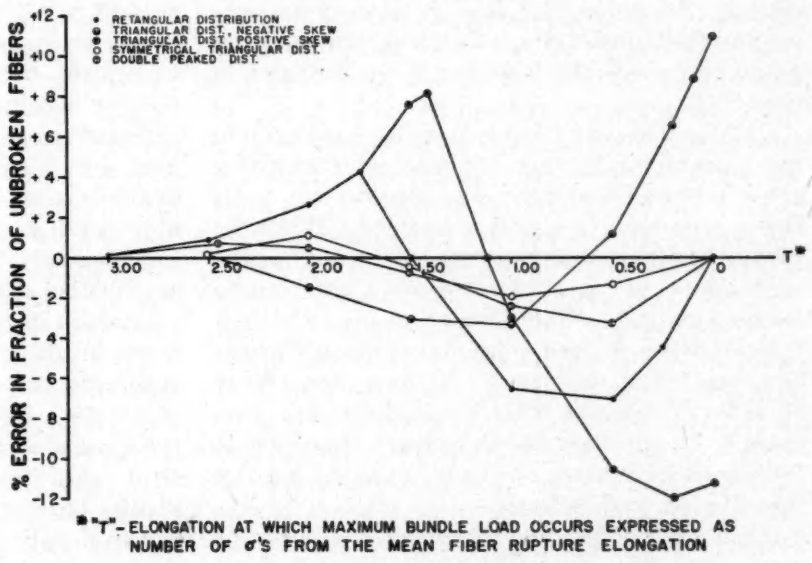
RETANGULAR DISTRIBUTION
TRIANGULAR DIST., NEGATIVE SKEW
TRIANGULAR DIST., POSITIVE SKEW
SYMMETRICAL TRIANGULAR DIST.
DOUBLE PEAKED DIST.
% ERROR IN FRACTION OF UNBROKEN FIBERS
T*
* "T" - ELONGATION AT WHICH MAXIMUM BUNDLE LOAD OCCURS EXPRESSED AS NUMBER OF σ'S FROM THE MEAN FIBER RUPTURE ELONGATION

GRAPH XIV. *Error in fraction of unbroken fibers* vs. *elongation at which maximum bundle load occurs.*

the yarn is loaded. As a result both of this assumption and also idealization of the geometry of cordage yarns, it became possible to handle the cordage yarns, analytically, as though they were comprised of continuous-filament fibers exhibiting a large variance in ultimate elongation. However, it must be recognized that the strength of any yarn which is composed of fibers whose lengths are not infinite may be limited by frictional considerations. Obviously, if insufficient friction is developed along the sides of a fiber when a twisted yarn is loaded, the possibility exists for fibers to slip rather than support their ultimate tensile strength. If such slippage occurs for a large percentage of the fibers in a given length of yarn, and if the maximum load capable of being transmitted by friction is a small fraction of the fiber strength, then poor translation of such fiber strength is the inevitable result. Conversely, if fiber slippage is absent, yarn elongations produce load-bearing fiber strain, and the translation of fiber strength is limited by the factors already described in the analysis. While it is apparent that fiber slippage occurs for staple yarns in the twist range below optimum, the situation is unclear in the twist range higher than optimum.

In this section, an attempt is made to characterize quantitatively the extent to which fiber slippage affects translation of fiber strength into cordage yarns when such yarns have twists greater than optimum. From the good agreement obtained between theoretical results, assuming no fiber slippage, and experimental data, it might be assumed that the effects of fiber slippage, if any, are negligible. Qualitative reasons for assuming slippage effects to be negligible here are as follows:

(*a*) Calculated results of cordage yarn tenacity assuming no slippage check experimental results closely.

(*b*) The experimental rupture elongations of cordage yarns agree closely with the mean fiber rupture elongations to break. If fiber slippage occurred before the fibers broke, it would be quite improbable for fiber and yarn elongation to agree closely. Assuming fiber slippage to occur throughout the load application, yarn elongation to break would be considerably less than fiber elongation to break.

(*c*) Visual examination of breaking yarns and of the autographically recorded load-elongation diagram indicated that fiber slippage does not occur before maximum yarn load is attained. While the yarn is breaking, it is apparent from simultaneous observation of the load-extension curve being recorded on the Instron Tester and the yarn itself that decreases in load coincide exactly with fiber breaking. Not only does the load drop when fibers break, but, also, when the load does not drop, there is no apparent fiber rupture. Detection of cordage-fiber rupture is quite evident from a characteristic audible snap.

(*d*) If the pulling jaw movement is stopped as soon as possible after the maximum yarn load has been attained, visual examination of the yarn in the region of rupture indicates that approximately half of the fibers are non-throughgoing in this region. This region is of the order of 2 in. in length. The only means other than fiber rupture for ends to appear would be slippage. For fibers of length 30–60 in. only 3%–7% of the fibers would appear to be non-throughgoing if only slippage occurred. The analysis already described demands approximately 50% of the fibers to be non-throughgoing in the rupture region if the fibers broke rather than slipped. Of course, it is possible, once maximum yarn load has been reached, for gross disruption of the yarn geometry to produce fiber slippage as further yarn extension occurs. However, all that is necessary for the analysis to be valid is that fiber slippage does not occur before the maximum yarn load is attained.

While the information given in *a–d* above appears to substantiate the validity of the assumption of no fiber slippage in cordage yarns for loads equal to or less than the maximum, it is obvious that a quantitative knowledge of the degree to which fibers are bound to each other, as they exist in the yarns, would clarify more rigorously the part friction plays in determining yarn strength. Specifically, the possibility of coincidental agreement between the results of the theoretical analysis and experiment would be very small if a direct measurement of the friction per unit length of fiber capable of being developed as tension is applied to a twisted yarn indicates that the fiber breaks at loads less than those at which it slips. Coincident with "slip" or "break" results, important information on the length of embedment necessary to develop the breaking strength of the fiber by friction would be forthcoming. The significance of uniquely determining the effect of fiber length as a geometric modifier is obvious.

Accordingly, a technique has been developed for determining the resistance to slippage afforded by a single-cordage fiber when all of the remaining fibers in the yarn are loaded in tension. The apparatus for performing the tests is illustrated in Figure 13. Before insertion of the yarn into the jaws, a single fiber is partially pulled by hand out of the yarn from its lower end. The yarn is then slightly untwisted at its lower end for a length of approximately 1 in. so that all of the fibers except the one previously pulled out may be spread over a circular area and clamped between two plates. The assembly is then mounted, as shown in Figure 13, with the upper end of the yarn clamped in the upper jaw of the Instron, and the free end of the partially pulled fiber clamped in the lower jaw. Tensile load is then applied to the yarn by means of the lever which rests on the upper plate. The magnitude of this tension is controlled by reading the Instron chart and varying the magnitude and position of the dead load, w. Load is then applied to the individual fiber by means of downward travel, at constant rate, of the lower jaw. A complete record of the load on the fiber is auto-

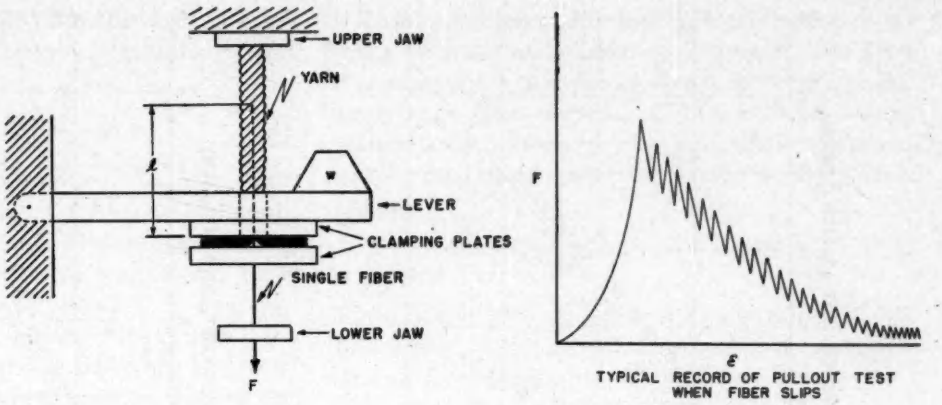

FIG. 13. *Schematic diagram of fiber pull-out test.*

graphically produced on the Instron chart. By observation of the fiber being pulled, it is, of course, possible to determine whether the fiber slips or ruptures. For those tests where slippage occurs, the length of embedment of the fiber in the yarn at any load can be calculated from the total length of the fiber and the distance the fiber has been pulled out, as given by the Instron chart.

A typical record of a test is illustrated in Figure 13, which plots F, the load on the fiber which is slipping, *versus* ϵ, the lower jaw movement. Initial application of load produces fiber stretch. When the load reaches the maximum which the fiber can transmit by friction, the fiber slips. This slippage produces a load drop, since dynamic friction is less than static friction. This load drop causes the slippage to cease, and a further increase in load takes place until slippage again occurs. Thus, following the initial load build-up, the autographic record consists of a series of peaks, the envelopes of which continuously decrease to zero load. The envelope of the upper peaks represents the resistance to slippage produced by static friction, while the lower envelope reflects the resistance produced by dynamic friction. Both envelopes, of course, approach the zero-load axis, since as the length of fiber embedment decreases, both total static and dynamic frictional forces must decrease.

By using the technique described, it is possible to determine the frictional force capable of being transmitted by a fiber, using the upper envelope of curves of the type shown in Figure 13. Corresponding to each frictional force there is an associated length of fiber embedment. Division of the frictional force by the length of embedment gives a value of the friction force per unit length of fiber. Data of this type have been determined for a variety of loads, w, and for a variety of yarn twists. Since friction is produced by normal pressure, it would be anticipated that frictional resistance would increase with increase in both total load, w, and yarn twist. In the calculations, a conservative value of frictional resistance was determined by using the mean value of the upper and lower envelopes of the pull-out tests for force rather than the upper value. It is emphasized that the results of these tests give the value of frictional resistance of the fibers for the geometric state in which the fibers actually exist in the cordage yarns.

The results of the tests are given on Graph XV for the abaca strand yarns and the Sansevieria yarn, and on Graph XVI for the low- and high-twist henequen yarns. These results apply only to the cases where fibers slipped rather than broke. It is to be noted that it was necessary to impose extreme conditions of test in order to produce fiber slippage rather than fiber rupture. Thus, for example, at yarn loads above 20 lbs. for the 11 and 15 turns/ft. abaca strand yarns, it was very difficult to produce a test in which the fiber slipped.

To indicate the degree to which the fibers are bound, consider the results given on Graph XV for the 6.6 turns/ft. abaca strand yarn. The mean breaking strength of this yarn is 360 lbs. Extrapolating the abscissa of Graph XVI to 360 lbs. gives a value of friction of 4.5 lbs./in. Since the average strength of abaca fibers is of the order of 6 lbs. [4], it is clear that at the maximum yarn load of 360 lbs., a minimum length of fiber of the order of 1.5 in. for the test is necessary to prevent slippage. In the case of a long length of yarn loaded as it would be in service, approximately 3 in. of fiber would be necessary, 1.5 in. to receive and 1.5 in. to transmit the load. For any fiber length

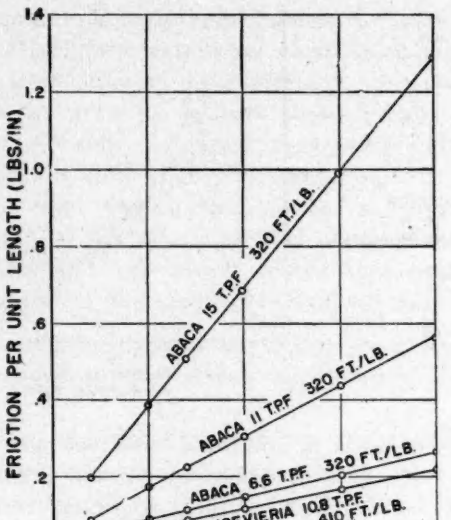
FRICTION PER UNIT LENGTH (LBS/IN)
EFFECTIVE YARN LOAD, LBS.
ABACA 15 T.P.F. 320 FT./LB.
ABACA 11 T.P.F. 320 FT./LB.
ABACA 6.6 T.P.F. 320 FT./LB.
SANSEVIERIA 10.8 T.P.F. 410 FT./LB.

GRAPH XV. *Fiber friction* vs. *yarn load.*

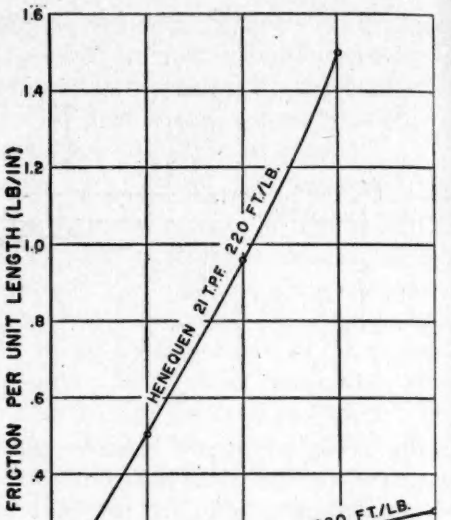

GRAPH XVI. *Fiber friction* vs. *yarn load.*

greater than the value of 3 in., it is clear that fiber slippage will not occur prior to fiber rupture. Since the lengths of the cordage fibers investigated in this work varies from approximately 2 ft. for the Sansevieria to 5 ft. for the abaca, the possibility of slippage appears extremely remote.

Calculations similar to those described above when made for the other yarns given on Graphs XV and XVI will indicate that the ability of the cordage fibers to develop their full tensile strength by friction far exceeds the possibility of their slipping. This can be shown to be the case for all of the yarn tensions considered. This, of course, does not mean that if a yarn were processed from fiber whose length satisfied minimum frictional requirements that the full strength of the fibers would be realized. Obviously, the frictional resistance of fibers, as they lie in a yarn, is functional with their orientation, and it is doubtful if fiber as short as 2 in., or even 7 in., would be sufficiently flexible to achieve optimum orientation. Nevertheless, the data given in Graphs XV and XVI indicate quite clearly that for the orientation of the long fibers which exist in the yarns tested, the available length far exceeds the minimum required for no slippage. It remains for future work to determine at which minimum length optimum orientation occurs.

The abscissa values given on Graphs XV and XVI have been termed "effective yarn loads." In the case of the low-twist yarns, and for large values of the dead load where the pull-out force is usually low, the effective yarn load is substantially the same as the dead load. However, a correction must be made when the pull-out force, F, approaches the dead load, w. It is clear, since the tension in the fiber which is being pulled out must decrease to zero along its length, that the total tension in the yarn exceeds that of the dead load alone. Thus, the normal pressure, which is functionally related to the yarn tension, is not constant along the length of embedment of the fiber in the yarn. The normal pressure is a minimum at the point along the fiber where it just encounters the rest of the yarn, and at maximum, when slippage is occurring, at the upper end of the fiber. The difference between the two extremes in yarn tension is the pull-out force itself. When the pull-out force is of the same order of magnitude as the dead load, it is obvious that a greater normal pressure than that arising from the dead load alone will act to produce the frictional resistance. Therefore, in order to present the results as rationally as possible, a fraction of the pull-out force has been added to the dead tension, and the resultant sum, against which the friction per unit length has been plotted, has been termed "effective yarn load."

Analytically, the raw test data have been converted to satisfy the unknown constants in the following equation:

$$F = k(w + cF)(l - q), \tag{23}$$

where F = recorded pull-out force (lbs.), w = dead load on yarn (lbs.), l = length of fiber embedment, as shown on Figure 13 (in.), k = proportionality factor between friction per unit length and yarn tension, c = fractional part of F which is effective in increasing the normal pressure, averaged over the length of the fiber, and q = unknown length of poor contact between the fiber and the rest of the yarn in the region of the clamping plate. Rough measurements indicate the length q to be no greater than 0.3 in., and more probably closer to 0.15 in. Since the major part of the data given on Graphs XV and XVI was determined for lengths of fiber embedment of the order of 4–6 in., with the lowest values accepted for calculation being 1.0–1.5 in., the correction, q, has a small effect on the plotted values.

The quantity c given in equation (23) demands further consideration. As has already been explained, the frictional resistance of a fiber is functional with the normal pressure exerted by the remainder of the yarn on that fiber. This normal pressure varies with the yarn tension. The yarn tension equals the dead load on the yarn, w, plus a portion of the pull-out force, F. The following analysis indicates the magnitude of the portion of F which is effective in increasing the tension in the yarn.

Let dT equal the incremental change (decrease) in fiber tension occurring for a length of embedment dx. Then:

$$\begin{aligned} dT &= -f dx \\ &= -k(w + F - T)dx, \end{aligned} \tag{24}$$

where all terms are as previously defined, and, in addition, T is the tension in the fiber being pulled at a point x inches from the end being pulled, and f is the friction per unit length of fiber embedment. Solving the differential equation (24), there results:

$$\ln\left(1 + \frac{F}{w}\right) = kl. \tag{25}$$

Equation (25) may be converted to the more usable form of equation (26):

$$F = w(e^{kl} - 1). \tag{26}$$

In both equations (25) and (26), l is the total length of fiber embedded in the yarn. As seen from equation (26), the pull-out force, F, is not linear with fiber length, l, but instead varies exponentially. However, by expanding the logarithmic expression given in equation (25), there results:

$$\frac{F}{w} - \frac{1}{2}\left(\frac{F}{w}\right)^2 + \cdots = kl. \tag{27}$$

If in equation (27) all terms in F/w of power higher than 2 are neglected, then, following a rearrangement of terms, equation (28) results:

$$F = kl\left(w + \frac{1}{2}F\right). \tag{28}$$

Thus, theoretically, when F/w is less than 1, equation (28) indicates that approximately $\frac{1}{2}$ of the value of F is effective in increasing w.

From another point of view, the problem may be solved as follows. Knowing that equation (26) gives the theoretical relationship between pull-out force, F, dead tension, w, and length of embedment, l, is it possible to find c in the expression

$$F = kl(w + cF) \tag{29}$$

such that the results of equations (26) and (29) check? Equation (29) may be rewritten as

$$c = \frac{F - wkl}{Fkl}. \tag{30}$$

By assuming various values of F/w in equation (26) and calculating corresponding values of kl, the value of c given by equation (30) may be determined. The results are shown in Table XII. Since, in the experimental data, values of F/w greater than 0.50 were not found, it is clear that using $c = 0.50$ in determining the "effective yarn load" is justified.

It has been stated previously that the linearly extrapolated values of F/l given on Graphs XV

TABLE XII. VALUES OF c DETERMINED FROM EQUATIONS (26) AND (30)

Assumed value of F/w	Value of kl from equation (26)	Value of c from equation (30)
0.05	0.048	0.495
0.10	0.0953	0.492
0.50	0.4055	0.466
1.00	0.6932	0.443
2.00	1.0986	0.410

TABLE XIII. LENGTH OF FIBERS NECESSARY TO DEVELOP STRENGTH BY FRICTION

Yarn	Average fiber breaking strength [4] (lbs.)	Extrapolated F/l at yarn rupture (lbs./in.)	x = Length to develop fiber strength (in.)	$\frac{x}{\text{Fiber length}}$
Abaca				
6.0 turns/ft.	6	4.5	1.3	0.03
10.8 turns/ft.	6	6.7	0.9	0.02
14.4 turns/ft.	6	16.0	0.4	0.008
Sansevieria				
10.5 turns/ft.	1	2.3	0.4	0.02
Henequen				
9 turns/ft.	3	3.8	0.8	0.03
21 turns/ft.	3	13.5	0.2	0.007

and XVI indicate that the fibers break rather than slip. Table XIII indicates, for all of the yarns, the fractional part of the fiber length necessary to develop the breaking strength of the fibers, calculated by such extrapolation. As seen from Table XIII, the extrapolated values F/l clearly indicate that the chances of slippage are extremely remote. However, it is possible to question the validity of linear extrapolation of the data given on Graphs XV and XVI. It is evident that the F/l values given on the graphs for 20 lbs. effective yarn load are less than those which occur at the breaking load of the yarn. However, let it be momentarily assumed that there is no increase in F/l from a 20-lb. yarn load to the yarn breaking load. Under these conditions, the values given in Table XIV would apply. Table XIV indicates, by an extremely conservative calculation, that the fibers do not slip. It is probable, however, that considerably lower values of x/fiber length than those shown in Table XIV actually exist in these yarns. Lack of ability to load the untwisted end of the yarn uniformly in the pull-out test prevented the use of higher yarn loads than 20 lbs. for the entire range of yarn twists given on Graphs XV and XVI. However, for some of the lower yarn twists, additional data to those given in the graphs may be found in Table XV. The values of x/fiber length given in Table XV were calculated assuming that no increase in F/l would occur for further increase in yarn load beyond 40 lbs. Comparison of the F/l data at 40 lbs. with that at 20 lbs. indicates F/l still to be increasing linearly with yarn load. Thus, it is altogether reasonable to assume that the

TABLE XIV. LENGTH OF FIBERS NECESSARY TO DEVELOP STRENGTH BY FRICTION

Yarn	F/l at 20-lb. yarn load (lbs./in.)	x = Length to develop fiber strength (in.)	$\frac{x}{\text{Fiber length}}$
Abaca			
6.0 turns/ft.	0.25	24.0	0.48
10.8 turns/ft.	0.56	10.7	0.21
14.4 turns/ft.	1.30	4.6	0.09
Sansevieria			
10.5 turns/ft.	0.22	4.6	0.18
Henequen			
9 turns/ft.	0.30	10.0	0.36
21 turns/ft.	1.60	1.9	0.07

TABLE XV. LENGTH OF FIBERS NECESSARY TO DEVELOP STRENGTH BY FRICTION

Yarn	F/l at 40-lb. yarn load (lbs./in.)	$\frac{x}{\text{Fiber length}}$
Abaca		
6.0 turns/ft.	0.513	0.23
10.8 turns/ft.	1.45	0 08
Henequen		
9 turns/ft.	0.545	0.20

results given in Table XIII actually apply at the yarn rupture load. Basically, the values of F/l depend upon fiber to fiber coefficient of friction and normal pressure. The normal pressure would be proportional to the yarn load if the density of fiber packing remained constant over the entire range of yarn loads. It would be anticipated that major effects resulting from yarn compaction occur in the low load range, and this is borne out by the fact that most of the lines on Graphs XV and XVI appear to have zero-load intercepts. Other investigators [5, 6] have shown hyperbolic shapes for curves of coefficient of friction *versus* normal pressure. As normal pressure increases, the coefficient decreases, but stabilizes at a constant level once a relatively small normal load has been applied. It is entirely probable that the coefficient remains constant for the data given in Graphs XV and XVI when loads of, say, 2 lbs. have been exceeded, and that, as a consequence, the slope of the F/l *versus* yarn load curves is constant over the range of yarn loads from 2 lbs. to yarn rupture. Under these conditions, it is valid to conclude, by way of summary, that:

(*1*) Fiber slippage does not occur before the maximum yarn load is attained.

(*2*) Only a very small portion of the length of the cordage fibers is necessary to develop the breaking strength of the fiber by friction. The exact portion is difficult to ascertain because of testing difficulties. There are indications, however, that probably no more than 5%–10% of this fiber length is necessary for frictional purposes.

3—Effect of Fiber Ends

Having determined the approximate value of the length of fiber embedment necessary to develop the strength of the fiber by friction, it is now possible to indicate the magnitude of the effect of fiber ends on the strength of a long length of yarn. To simplify the analysis, a graphical representation of the distribution of fibers is given in Figure 14. Here, the organization of the yarn structure is simplified by assuming the yarn to be twistless, and statistically varying the placement of fiber ends to give a uniform geometry to the resultant idealized form.

Consider the yarn to rupture along the section *a-a*. We concern ourselves with the distribution of fiber ends over a yarn length x inches to either side of this rupture section. Again, x is the length of fiber necessary to develop the fiber strength by friction. If T represents the fractional number of total fibers in any cross section which are throughgoing in the length $2x$, then

$$T = \frac{L - 2x}{L}, \tag{31}$$

where L is the staple length of the fibers, which is assumed to be constant as it is for the cordage fibers which are cut to a given length. Thus, the fraction of ending fiber, E, is

$$E = \frac{2x}{L}, \tag{32}$$

where E would be the same for fibers approaching the length interval $2x$ from either side of the yarn. The throughgoing fibers contribute their full load-carrying capacity at the rupture section *a-a*. The ending fibers contribute load, at the section *a-a*, only to the extent that they cross the section *a-a*. Thus, of the fibers which approach *a-a* from the right and which are not throughgoing, 50% will cross the section *a-a*. The average length of protrusion of this number of ending fibers to the left of *a-a* will be equal to $x/2$. Thus, assuming the length of protrusion to be proportional to the total load developed by friction for these ending fibers, the load supported by the ending fibers which approach section *a-a* from the right will be

$$\begin{aligned} P_{\text{ending}} &= (\text{T.S.})\left(\frac{1}{2}\right)\left(\frac{2x}{L}\right)\left(\frac{x}{2}\right)\left(\frac{1}{x}\right) \\ &= \text{T.S.}\left(\frac{x}{2L}\right), \end{aligned} \tag{33}$$

where T.S. is the breaking strength of the fibers. The load contributed by those ending fibers which approach section *a-a* from the left will be the same as those which approach from the right. Thus, the total strength of the yarn at the rupture section will be

$$\begin{aligned} P_T &= \text{T.S.}\left(\frac{L - 2x}{L}\right) + \text{T.S.}\left(\frac{2x}{2L}\right) \\ &= \text{T.S.}\left(1 - \frac{x}{L}\right). \end{aligned} \tag{34}$$

Thus, the efficiencies given on the theoretical Graphs VII–XI will be too high, and should be corrected by multiplying by the factor $(1 - x/L)$. However, if the quantity x/L is very small compared with unity, then the correction is negligible. Thus, if the extrapolated values of x/L given in Table XIII are correct, errors in efficiency less than 3% exist—that is, if the graphs call for an efficiency of, say, 50%, the correction would yield an efficiency of $0.97 \times 50\% = 48.5\%$. The efficiency for any twisted yarn, however, would be greater than 48.5%, since, because of helix angle effects, not

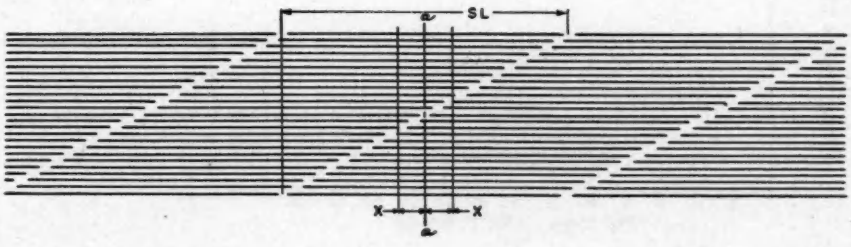

FIG. 14. *Idealized fiber placement.*

all of the fibers would be supporting the breaking load, and would thus require a shorter length than the length x to develop the loads that they *are* supporting. Thus, as a practical matter, the effect of fiber ends is negligible on yarn breaking strength. However, if fiber length were greatly reduced, the factor $(1 - x/L)$ could become significant.

It should be pointed out that the values of F/l used to calculate the length x should theoretically depend upon the location of the fiber in the yarn—*i.e.*, whether the fiber is at the outside or the inside of the yarn cross section. Thus, the normal pressure is greatest at the center of the yarn, and least at the outside. Experimentally, it has been found impossible to distinguish, for the lengths of embedment used in the pull-out tests, between F/l values for outside *versus* inside fibers. This is probably the result of fiber darting—*i.e.*, fibers not remaining a constant distance from the yarn center over a long length of yarn. Because of such darting, it is reasonable to utilize in the calculation F/l values averaged for all fibers, independent of location in the yarn cross section. This averaging increases the variability of F/l values. The variation, however, is of the same magnitude as that of other fiber properties, such as tenacity and elongation [4]. At any rate, the length of fiber necessary to develop the strength of the fiber by friction is such a small percentage of the fiber length that were the value of F/l in error by as much as 100% for the outside fibers, the conclusions regarding slippage and fiber-end effects would still apply.

It is obvious from the foregoing analysis of the effect of fiber ends that the fibers, as they lie in twisted yarns, are called upon to resist rupture over the length $2x$. This length is small compared to the gage length of fibers which have been tested and previously reported [4]. This would present a problem if it could be shown that the strength, elongation, and variability of the cordage fibers were significantly affected by gage length for gage lengths of the order $2x$. Structurally, it would be anticipated that significant changes in fiber properties with gage length would occur for gage lengths sufficiently low to enable a large number of the true cell fibers [9] to be throughgoing. Since, for the cordage fibers studied herein, true cell-fiber length is of the order of 0.10–0.20 in. [9], with approximately 50–300 cells in the cross section of a commercial fiber, gage lengths considerably less than these would be necessary to indicate significant strength changes. The lengths, $2x$, given in Table XIII are all in excess of the average ultimate cell length. Thus, it is reasonable to assume that the use of fiber strength determined from a 10-in. gage length is valid for the calculations previously described in this report. A small number of tests on Manila abaca fiber performed at gage lengths of 0.50 in. did not indicate any change in fiber strength.

In order to indicate the effect of weak "spots" in yarns, a series of tests were performed on yarns of different gage lengths ranging from $2\frac{1}{4}$ in. to 25 in. The results are shown on Graph XVII. Each value represents the mean of 40 individual breaks. The variation in means is indicated by the limit

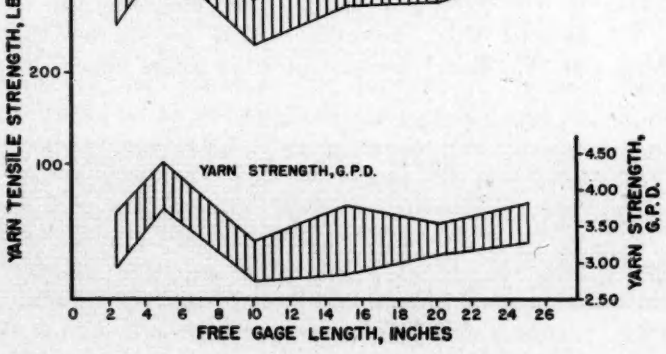

GRAPH XVII. *Yarn strength* vs. *free gage length for Manila abaca yarn (12 turns/ft.; 320 ft./lbs.).*

lines, which are ± 2 standard errors of the mean strength found at each gage length. It can be seen that it has not been found possible, within the range of gage lengths tested, to ascribe any consistent decrease in strength with gage length. Thus, it might be concluded that the weak "spots" in yarns are closer than the minimum gage length of 2¼ in. However, this is extremely unlikely, considering the fact that the lengths of the cordage fibers are of the order of 2 ft. to 5 ft. It is more likely that:

(*1*) If weak "spots" of a definable repetitive nature exist in the cordage yarns studied, they are not sufficiently weaker than normal "spots" to be significant in affecting average yarn strength.

(*2*) Rather than weak "spots," cordage yarns possess weak regions of short length separated by long lengths of "normal" properties. Thus, until very long gage lengths are reached, the number of extremely low breaks would be a small fraction of the total number of breaks. Thus, the mean strength would not be affected significantly, although a somewhat skewed distribution of strengths would occur. Variation of strength at any of the gage lengths studied would then be the result of random variations produced by variance in fiber strength, mean fiber elongation, coefficient of variation of fiber elongation, and yarn twist. It would then be expected that ruptures of very long yarns—*i.e.*, two or more staple lengths of the fiber in length—might be significantly weaker than the average yarn strengths reported herein.

Work is in progress covering further aspects of the research—namely, applying similar mathematical analysis to the translation of yarn properties into strand, plied yarn, and rope structures.

Acknowledgment

The assistance of Mr. David Himmelfarb, of the Boston Navy Yard, and Mr. Raymond T. Starr, of the Columbian Rope Company, both in supplying samples and for many stimulating discussions of the work, is gratefully acknowledged. Acknowledgment is also made to Mrs. M. Landing, Miss J. Rea, and Mrs. L. Saslaw for their painstaking efforts in the experimental work and in making the numerous calculations.

Literature Cited

1. Hamburger, W. J., Mechanics of Elastic Performance of Textile Materials: Part I: Development of an Elastic Performance Coefficient in Tension, TEXTILE RESEARCH JOURNAL **18**, 102 (Feb. 1948).
2. Hamburger, W. J., The Industrial Application of the Stress-Strain Relationship, *J. Textile Inst.* **40**, 700 (July 1949).
3. Hamburger, W. J., and Kaswell, E. R., Use of Effective Gage Length in Elongation Measurement, *Rayon Textile Monthly* **24**, 579 (Nov. 1943).
4. Kaswell, E. R., and Platt, M. M., Mechanics of Elastic Performance of Textile Materials: Part VII: Mechanical Properties of Hard Fibers with Reference to Their Use in Cordage Structures, TEXTILE RESEARCH JOURNAL **21**, 263 (May 1951).
5. Lindberg, J., and Gralén, N., Measurement of Friction Between Single Fibers: Part II: The Frictional Properties of Wool Fibers Measured by the Fiber-Twist Method, TEXTILE RESEARCH JOURNAL **18**, 287 (May 1948).
6. Mercer, E. H., and Makinson, K. R., The Frictional Properties of Wool and Other Textile Fibers, *J. Textile Inst.* **38**, T227 (1947).
7. Philipp, H. J., Effect of Tire Cord Uniformity on the Strength of Tire Fabrics, TEXTILE RESEARCH JOURNAL **15**, 397 (Nov. 1945).
8. Platt, M. M., Mechanics of Elastic Performance of Textile Materials: Part III: Some Aspects of Stress Analysis of Textile Structures—Continous-Filament Yarns, TEXTILE RESEARCH JOURNAL **20**, 1 (Jan. 1950).
9. Weindling, L., "Long Vegetable Fibers," New York, Columbia University Press, 1947.

(*Manuscript received July 15, 1952.*)

The Mechanics of Bent Yarns*

Stanley Backer†

Abstract

This paper analyzes the idealized geometry of a bent yarn. Expressions are derived for the calculation of local fiber tensile strain, average strain in the helix half loop, motion of the fibers during bending of the yarn, changes in local helix angles, and fiber curvatures at the bend. The relationships between the geometric quantities of a bent yarn are presented graphically in dimensionless parameters, and conversions to the usual textile terms are provided. Attention is given to the practical applications of this analytical approach to textile problems.

Introduction

The influence of yarn geometry on the translation of fiber properties has received increasing attention during recent years. Early studies emphasized the relationship between the structure and the mechanical properties of singles yarns whose axes lie on a straight line [4, 5, 6, 9]. Later studies [3, 7] stressed the importance of bending in yarn geometry and in the mechanical properties of the end textile structure. This development was in recognition of the fact that the yarns we use are rarely straight; they are usually bent into torus shapes during the weaving process or into helical forms when twisted into plied structures. Yarn bending is inherent in woven and knitted structures, in sewing threads, tire cords, twines, and ropes. Moreover, yarns are subjected to bending during use of the end textile structure in flexing, draping, or creasing of an apparel fabric; in the waving of a flag; the billowing of a tent; the packing of a sleeping bag; the knotting of a rope; the forming of a stitch in the sewing process; the flexing of a rope over a pulley; and the washing of a blanket.

The mechanical properties of the original textile structure and its behavior under service conditions will depend to a great extent upon the strain to which its individual fibers are subject. The level of fiber strain will, in turn, depend upon the configuration which the fiber is forced to assume, and therefore upon the structure of the bent yarn. It follows that study of bent-yarn geometry is essential to the full understanding of strain and, therefore, of stress distributions in the textile structure. Only through such understanding can we hope to predict the integrated mechanical behavior of twisted, woven, or knitted textile products.

This paper attempts to outline the development of an idealized geometry of bent yarns. It is realized that actual yarn structure will at times depart to a significant degree from the mathematical forms proposed herein. However, even in such cases, the geometric forms will be useful as a common basis for structural comparisons; and considerable insight into the behavior mechanisms in bending of a given material will follow from study of the causes of its deviation from the ideal geometry. The implications of such insight have direct bearing on long-standing problems in many areas of textile research. We refer to such subjects as knot efficiencies, seam efficiencies, sewability (from the standpoint of loop formation), cord and power transmission, rope wear, flex-resistance and internal abrasion of fabrics, crease- and muss-resistance, and abrasion-resistance.

It should not be supposed that the following material is solely the work of the author. A major portion of the analysis here proposed is based on the work of others, notably Schwarz [7] and Chow [1]. The *modus operandi* of this study involves (*1*) the selection of special cases from the more general studies of twist in plied structures,

* This paper, issued as Quartermaster Textile Series Report No. 74, was presented in part at a meeting of The Fiber Society at Swampscott, Mass., Sept. 13, 1951. It forms a portion of the doctoral thesis of the author written at the Massachusetts Institute of Technology.

† Consultant, Textile Section, Office of The Quartermaster General, and Assistant Professor of Mechanical Engineering, Massachusetts Institute of Technology, Cambridge, Mass.

and (*2*) the extension of these special cases as they relate to the geometry of bent singles yarns. Specifically, the report deals with: the local strain caused in fibers at various yarn locations when they are bent; the average strain taking place in fibers forced to follow the idealized geometric path in bending without the benefit of freedom of relative motion within the yarn; the relative motion between fibers due to shifting from the bottom to the top part of the loop; the relative motion between fiber surfaces due solely to changes in local helix angles; the changes in local helix angles which occur in yarn bending; and the curvatures of fibers at all locations in a bent yarn.

In order to achieve maximum generality in the analytical development, it has been found expedient to use dimensionless parameters wherever possible. This feature does have the disadvantage of introducing additional computations when the data used are given in textile terms, rather than in the geometric parameters used throughout this paper. This difficulty has been alleviated by the provision of graphical conversions for use of the practical designer. Further ease in computation is made possible through provision of the graphical form of the analytical relationships, plotted over practical ranges of the geometric parameters. The analysis follows.

Local Strain

A singles yarn is taken as the major element of structure. The yarn is made of continuous filaments which are considered to lie on right cylindrical surfaces along circular-helical paths. The cylindrical surfaces are concentric and are spaced one fiber diameter apart. All fibers on all surfaces are subject to the same number of turns about the yarn axis per unit length along that same yarn axis. It follows that helix angles formed by the fibers at each concentric surface will vary, with the maximum helix angle occurring at the outermost fiber, and zero helix angle at the yarn axis. It is assumed that differences in path length of filaments at different concentric surfaces occur in the spinning or twisting operation, without the presence of fiber tension or compression. The local helix angle for a given surface is constant for all fibers on that surface, and

$$\tan Q_v = 2\pi v T, \tag{1}$$

where Q_v is the fiber helix angle on the cylindrical surface of radius v, and T is the twist per inch of the yarn. In particular, the outer fibers of the yarn form the helix angle Q with the yarn axis, and, if d is the yarn diameter,

$$\tan Q = \pi d T. \tag{2}$$

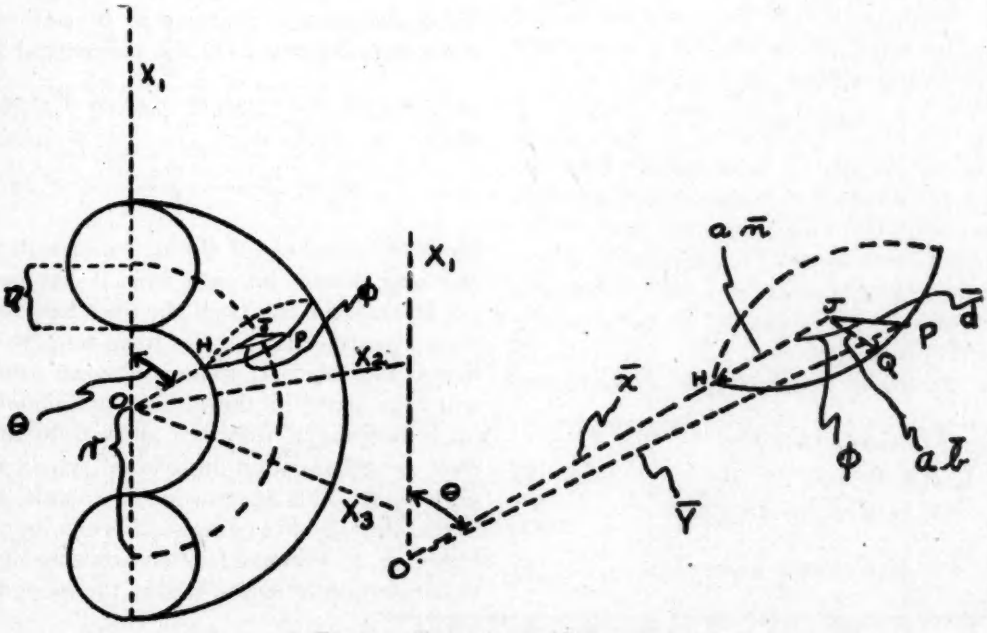

FIG. 1. *Torus form of bent yarns.*

The single yarn described above (taken to be a warp yarn for convenience in nomenclature) is assumed to form a torus when bent around a filling yarn, as illustrated in Figure 1. The radius of the bent warp yarn is designated as a, and the radius of the torus as r. The torus radius, r, equals the sum of the radii of the warp (crown) yarn and the filling (inner) yarn.

Let O be the torus center, and let P be a point on a fiber as it twists around the warp yarn. Let X_1, X_2, and X_3 be mutually orthogonal axes forming the Cartesian coordinate system. Let X_3 be the axis of the torus—*i.e.*, the axis of the filling cross yarn. The circular path of the warp yarn lies in the X_3 plane. The intersection of a plane through X_3, making an angle θ with X_1, is indicated in Figure 1 as passing through point P. The circular intersection of the torus and the indicated plane is enlarged on the right side of Figure 1. Let J be the yarn axis at the circular section. Let OJ intersect the circle at H. Draw JQ in the plane of the section, perpendicular to JH.

Designate the vector OJ as $\bar{X}$, OP as $\bar{Y}$, HJ as $a\bar{n}$, JQ as $a\bar{b}$, and JP as $\bar{d}$. The vector $\bar{n}$ is a unit vector coinciding with, but in opposite direction to, vector $\bar{X}$. Vector $\bar{n}$ is the principal normal to the space path of the warp yarn axis. The vector $\bar{b}$ is also a unit vector, is perpendicular to $\bar{n}$, and is called the binormal of the warp axis space path. Angle θ lies between the X_1 coordinate and the vector $\bar{X}$. Angle ϕ lies between vector $\bar{X}$ and vector $\bar{d}$. The ratio between θ and ϕ is assumed to be constant, and is designated as λ—*i.e.*,

$$\phi = \lambda\theta. \tag{3}$$

This simply means that in proceeding along the warp yarn axis (in the torus configuration) through an angle θ about the torus axis, the fiber twists around its yarn axis through a corresponding angle, ϕ. For each revolution around the torus axis ($\theta = 2\pi$), there are λ revolutions or turns of the fiber about the warp yarn axis.

Consider the components of the above-named vectors:

$$\begin{aligned} &\bar{X}[r\cos\theta,\ r\sin\theta] \\ &\bar{b}[0,\ 0,\ 1] \\ &\bar{n}[-\cos\theta,\ -\sin\theta,\ 0]. \end{aligned} \tag{4}$$

Now

$$\bar{d} = a(\cos\phi)\bar{n} + a(\sin\phi)\bar{b}; \tag{5}$$

therefore,

$$\bar{Y} = \bar{X} + \bar{d} = \bar{X} + a\cos\phi\bar{n} + a\sin\phi\bar{b}, \tag{6}$$

or $\bar{Y}[Y_1, Y_2, Y_3]$ can be written as:

$$\begin{aligned} Y_1 &= r\cos\theta + a\cos\phi(-\cos\theta) \\ Y_2 &= r\sin\theta + a\cos\phi(-\sin\theta) \\ Y_3 &= a\sin\phi. \end{aligned}$$

By substituting from equation (3):

$$\begin{aligned} Y_1 &= r\cos\theta - a\cos\lambda\theta\cos\theta \\ Y_2 &= r\sin\theta - a\cos\lambda\theta\sin\theta \\ Y_3 &= a\sin\lambda\theta. \end{aligned} \tag{7}$$

If dS is taken as a differential element of arc length along the fiber passing through point P, it follows from differential geometry that

$$\frac{dS}{d\theta} = \sqrt{\Sigma \frac{dY_i}{d\theta}\frac{dY_i}{d\theta}}. \tag{8}$$

Following Chow's analysis [1], an expression is now derived for the element of arc length, dS, in terms of the torus geometry. Note that this is but a special case of Schwarz's consideration [7] of the twist structure of plied yarns. For first derivatives:

$$\begin{aligned} \frac{dY_1}{d\theta} &= -r\sin\theta + a\sin\theta\cos\lambda\theta + a\lambda\sin\lambda\theta\cos\theta \\ \frac{dY_2}{d\theta} &= r\cos\theta - a\cos\lambda\theta\cos\theta + a\lambda\sin\lambda\theta\sin\theta \\ \frac{dY_3}{d\theta} &= a\lambda\cos\lambda\theta. \end{aligned} \tag{9}$$

By squaring each equation in (9) and adding, we have from equation (8) the differential arc length

$$dS = \sqrt{(a\cos\lambda\theta - r)^2 + a^2\lambda^2}\, d\theta, \tag{10}$$

or

$$dS = \sqrt{\frac{(r - a\cos\phi)^2}{\lambda^2} + a^2}\, d\phi.$$

By integration of dS through a complete turn of the fiber about the yarn axis, it has been shown [1, 7] that the length of the fiber loop in the bent yarn equals* that of the fiber loop in the yarn before bending. It follows that no tensile strain will take place in the individual fibers of a yarn upon bending if they are allowed to redistribute their lengths within individual loops about the yarn axis. This assumption was made by Czitary in his analysis of bending strains of wire cables [2]. However, if excessive friction prevents the slightest redistribution of length within the loop, differences

* Within well-defined limits.

in local fiber path lengths must result in local tensile and compressive fiber strains.

Axial fiber strain, E, is defined, in the case of yarn bending, as

$$\mathrm{E} = \frac{dS - dS_o}{dS_o}, \tag{11}$$

where dS is the fiber path length in the angular increment $d\phi$ when the yarn is bent, and dS_o is the corresponding arc length in the same $d\phi$ for the straight yarn. It is here assumed that during the bending process no new fiber material is introduced into the angular increment $d\phi$ because of the restriction on fiber movement. The arc length dS_o is determined from

$$\frac{ad\phi}{dS_o} = \sin Q, \tag{12}$$

and λ from

$$\lambda = 2\pi rT = 2\pi r\left(\frac{\tan Q}{2\pi a}\right) = \frac{r \tan Q}{a}. \tag{13}$$

Substituting equations (12) and (13) into equations (10) and (11):

$$\mathrm{E} = \frac{\sqrt{\dfrac{(r - a\cos\phi)^2 + a^2}{(r^2 \tan^2 Q)/a^2}}\, d\phi}{\dfrac{ad\phi}{\sin Q}} - 1$$

$$\mathrm{E} = \sqrt{\frac{\left(\dfrac{r}{a} - \cos\phi\right)^2 + \lambda^2}{\left(\dfrac{r}{a}\right)^2 + \lambda^2}} - 1. \tag{14}$$

Values of E are plotted against ϕ in Figure 2 as ϕ varies from 0 to 180°. Symmetry conditions apply in the range ϕ equals 180° to 360°. The parameter r/a varies from 1.5 to 2.5, the normal range of diameter variation encountered in practical fabrics. Parameter λ is varied from .5 to 1.25. If F is defined as the twist multiplier,

$$T = F\sqrt{N}, \tag{15}$$

where T is the twist in turns per inch, and N is the yarn count. If the specific volume of the yarn is taken to be 1.1, so that

$$d = 2a = \frac{1}{K\sqrt{N}}, \tag{16}$$

where K depends upon the yarn system used (K = 28 for cotton, 15.4 for woolen cut, 22.8 for worsted), then

$$\lambda = \left(\frac{r}{a}\right)\frac{\pi F}{K}. \tag{17}$$

For r/a equal to 2—*i.e.*, where warp and filling yarns are of equal diameter—the range "λ equals .5 to 1.25" represents a range in twist multiplier from "F equals 2.23 to 5.58" in the cotton system, "1.23 to 3.07" for woolen cut, and "1.38 to 4.54" in the worsted system. It is evident in Figure 2 that E is 0 at $\phi = \pi/2$ and reaches a maximum in tension (positive strain) at ϕ = 180° and a maximum in compression (negative strain) at ϕ = 0°. As the relative twist, represented by λ, is increased, E is decreased. As the ratio r/a increases, E decreases.

Average Strain

In an actual yarn it is probable that local slippage and length redistribution take place before strains of the magnitude plotted in Figure 2 are reached.

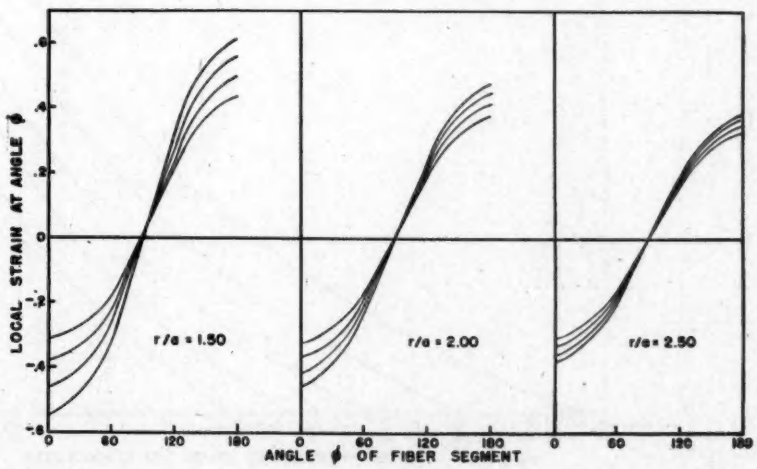

FIG. 2. *Local fiber strain caused by yarn bending, assuming no freedom of motion between fibers. In each of the three diagrams of Figure 2, the range of curve slopes from maximum to minimum correspond to* λ = .5, .75, 1.00, *and* 1.25, *respectively.*

A parameter of a more practical nature is the average strain which takes place in tension or that which takes place in compression. It is evident from Figure 2 that the fiber path between $\phi = \pi/2$ and π is in tension in the bent yarn, while between $\phi = 0$ and $\pi/2$ it is in compression. It remains to determine the path lengths along the outer segment of the path and along the inner segment, and to compare these lengths with the helical fiber path of the unbent yarn. As has been indicated [1, 7], the length of the fiber loop in the bent yarn equals that of the fiber loop in the yarn before bending. It follows that the over-all extension of the outer path must equal the over-all extension of the inner path, since both have the same length in the unbent yarn—*i.e.*, half a helical loop. Let ΔS be the difference in path length in the outer and inner parts of the bent yarn fiber loop. By symmetry, we can deal with

$$\frac{\Delta S}{2} = \int_{\phi=\pi/2}^{\phi=\pi} dS - \int_{\phi=0}^{\phi=\pi/2} dS. \tag{18}$$

The incremental distance can be expressed as

$$dS = \sqrt{(r - a\cos\lambda\theta)^2 + a^2\lambda^2}\, d\theta =$$

$$a\lambda\sqrt{\left[\left(\frac{r}{a\lambda}\right) - \frac{\cos\lambda\theta}{\lambda}\right]^2 + 1}\, d\theta. \tag{19}$$

Upon integration of equation (18),

$$\frac{\Delta S}{2} = \frac{2ar}{\lambda\sqrt{a^2\lambda^2 + r^2}} - \frac{2a^5r\lambda}{3(\sqrt{a^2\lambda^2 + r^2})^5}. \tag{20}$$

The average tensile strain in the top loop is

$$\overline{E_T} = \frac{\frac{\Delta S}{2}}{\int_0^{\pi} dS}. \tag{21}$$

From the geometry of the straight yarn,

$$\int_0^{\pi} dS = \frac{\pi\sqrt{a^2\lambda^2 + r^2}}{\lambda}, \tag{22}$$

which agrees with Chow's derivation [1] of the length of λ loops:

$$S = 2\pi(a^2\lambda^2 + r^2)^{\frac{1}{2}}. \tag{23}$$

Therefore,

$$\overline{E_T} = \frac{\frac{2ar}{\lambda\sqrt{a^2\lambda^2 + r^2}} - \frac{2a^5r\lambda}{3(\sqrt{a^2\lambda^2 + r^2})^5}}{\frac{\pi}{\lambda}(a^2\lambda^2 + r^2)^{\frac{1}{2}}} \tag{24}$$

$$\overline{E_T} = \frac{2ar}{\pi(a^2\lambda^2 + r^2)} - \frac{2a^5r\lambda^2}{3\pi(a^2\lambda^2 + r^2)^3}. \tag{25}$$

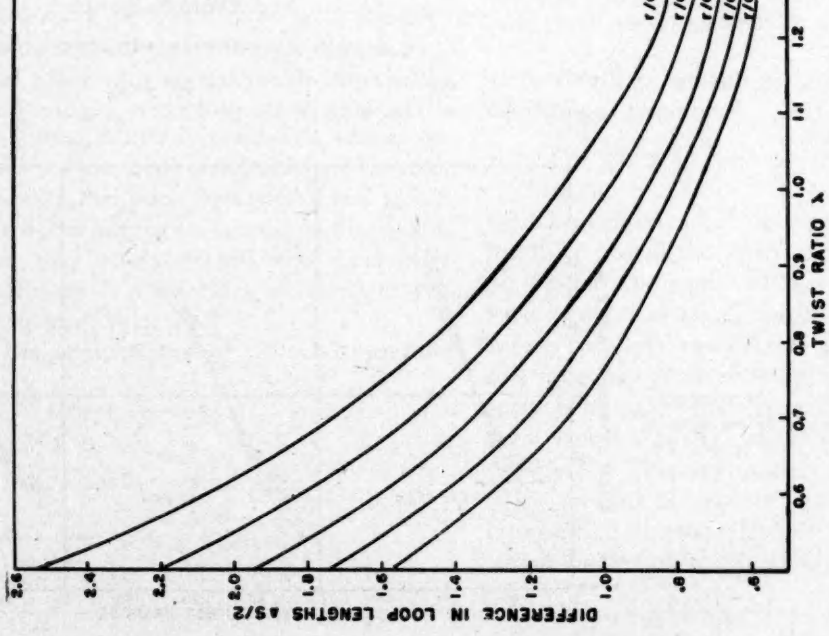

FIG. 3. *Difference in path length of upper and lower parts of the fiber loop indicated as a function of* r/a *and* λ. *Here* r *is taken as the unit of length, and* ΔS/2 *is expressed in terms of this unit.*

In Figure 3 the relationship between $\Delta S/2$ and λ is presented graphically for various r/a ratios. For the purpose of this computation, $\Delta S/2$ has been set equal to the first term in equation (20), or

$$\frac{\Delta S}{2} \cong \frac{2r}{\lambda\sqrt{\lambda^2 + (r/a)^2}}. \tag{26}$$

It is seen in Figure 3 that ΔS decreases with increases in λ or in r/a. Omission of the second term of equation (20) causes less than 1% error for the case where $r/a = 2$ and $\lambda = 1$. In Figure 4, $\bar{E}$ is plotted against λ for various r/a ratios. For the purpose of this computation, $\bar{E}$ is set equal to the first term of equation (25), or

$$\bar{E} \cong \frac{2r/a}{\pi\left[\lambda^2 + \left(\frac{r}{a}\right)^2\right]}. \tag{27}$$

Again, an error of less than 1% is introduced by this approximation for the case $r/a = 2$ and $\lambda = 1$.

The practical utility of the quantities $\bar{E}$ and $\Delta S/2$ must, of necessity, be limited by the degree to which actual yarns follow the geometric assumptions of the derivation. In a general sense, however, $\bar{E}$ gives a comparative value which may find use in the design of more durable twisted structures in which fiber or strand movement is restricted. In structures which allow complete freedom of movement, the quantity $\Delta S/4$ *represents the length of fiber which passes the point* $\phi = \pi/2$ *in the redistribution of material from lower to upper parts of the helix loop.*

Local Helix Angle

It has been indicated in equations (1) and (2) that the helix angle Q_v of a straight singles yarn is dependent [1, 7] upon the local radius, v, of the yarn and upon its twist. This angle Q_v is therefore constant for a given v and T at every point along the yarn. However, when the yarn assumes the bent form of Figure 1, the local helix angle is no longer a function of v and T alone, as has been indicated by Chow [1] for the general case of the singles yarn as it lies in the ply. By following the method used for the ply yarn, we derive the relationship between the local helix angle and the parameters λ, r/a, and ϕ for the special case of the bent singles.

In Figure 1, $\bar{X}$ represents the vector connecting the origin and a point on the path of the yarn axis,

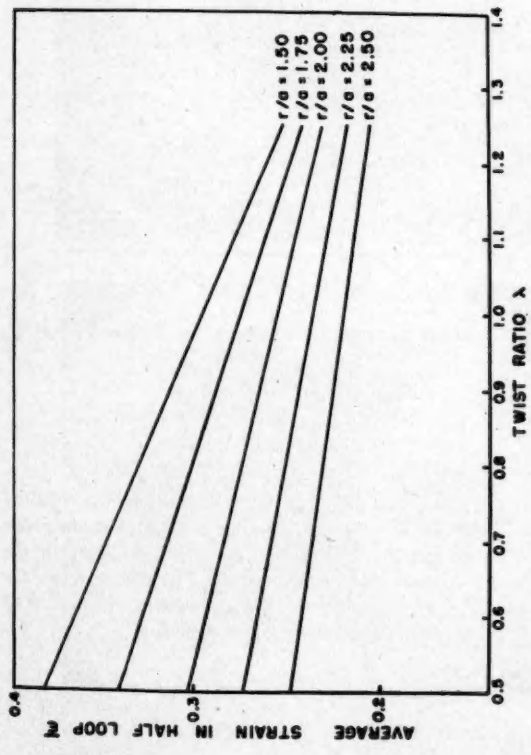

FIG. 4. *Average strain in half loop due to difference in path length for varying* λ *and* r/a.

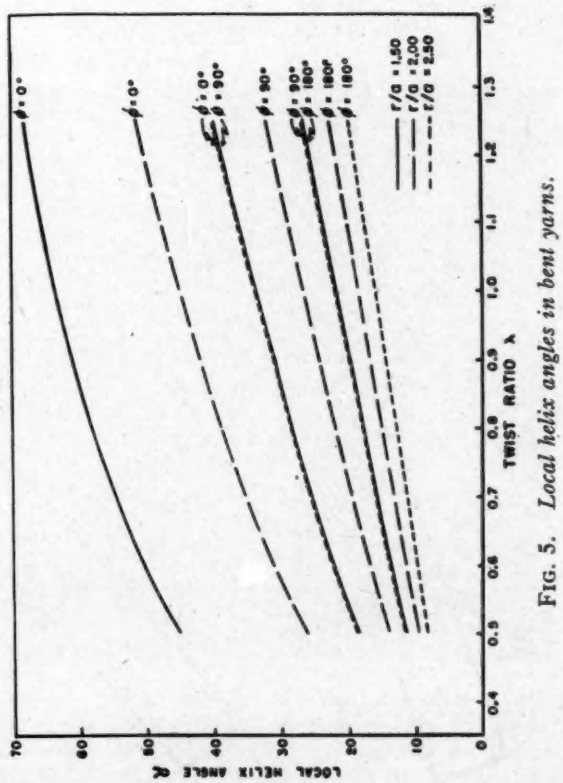

FIG. 5. *Local helix angles in bent yarns.*

while $\bar{Y}$ is the fiber path vector. In order to determine the local helix angle, we first derive expressions for $\bar{t}$, the unit tangent vector to the path of the yarn axis at point J, indicated in Figure 1, and $\bar{T}$, the unit tangent vector to the path of the fiber at point P. It follows from

$$\bar{t} \cdot \bar{T} = |\bar{t}||\bar{T}| \cos \alpha, \tag{28}$$

that

$$\cos \alpha = \bar{t} \cdot \bar{T}, \tag{29}$$

where α is the local helix angle. From Frenet:

$$\frac{d\bar{X}}{ds} = \bar{t}; \qquad \frac{d\bar{Y}}{dS} = \bar{T}, \tag{30}$$

where s is the distance along the yarn axis, and S is the distance along the fiber as it lies in the bent yarn.

For $\bar{t}$:

$$\begin{aligned} \bar{t} &= [t_1, t_2, t_3] = \frac{d\bar{X}}{ds} = \frac{d\bar{X}}{rd\theta} \\ &= \left[\frac{d(r\cos\theta)}{rd\theta}, \frac{d(r\sin\theta)}{rd\theta}, 0\right] \\ &= [-\sin\theta, \cos\theta, 0]. \end{aligned} \tag{31a}$$

From equations (30), (10), and (8):

$$\bar{T} = \frac{d\bar{Y}}{dS} = \frac{d\bar{Y}}{d\theta}\frac{d\theta}{dS} = \frac{d\bar{Y}}{d\theta}\frac{1}{\sqrt{\sum \frac{dY_i}{d\theta}\frac{dY_i}{d\theta}}}. \tag{31b}$$

Now,

$$\begin{aligned} \bar{t} \cdot \bar{T} &= \frac{(r - a\cos\lambda\theta)}{\sqrt{(r - a\cos\lambda\theta)^2 + a^2\lambda^2}} \\ &= \frac{1}{\sqrt{1 + \dfrac{a^2\lambda^2}{(r - a\cos\lambda\theta)^2}}} = \cos\alpha, \end{aligned} \tag{32}$$

or

$$\tan\alpha = \frac{a\lambda}{(r - a\cos\lambda\theta)} = \frac{a\lambda}{(r - a\cos\phi)}. \tag{33}$$

In Figure 5 a graphical relationship between α and λ is presented for the inner, outer, and center points of the bent yarn ($\phi = 0$, π, and $\pi/2$) and for various r/a ratios. Clearly, α is larger at $\phi = 0$ than at any other angle, and is a minimum at $\phi = \pi$. At $\phi = \pi/2$,

$$\tan\alpha = \frac{a\lambda}{r} = \frac{a2\pi rT}{r} = 2\pi aT, \tag{34}$$

which is the value of $\tan Q$ in the unbent yarn. No helix-angle change will take place along the "neutral axis" of a yarn during bending, whereas maximum changes will be effected at $\phi = 0$ and π.

A change in the local helix angle will cause some relative movement between the surfaces of adjacent fibers—a factor of importance in studies of the internal wear and friction or felting of yarns and fabrics. The extent of this movement may be demonstrated easily with the aid of Figures 6 and 7. Figure 6 demonstrates the appearance of fibers in the singles yarn before bending (*a*) and after

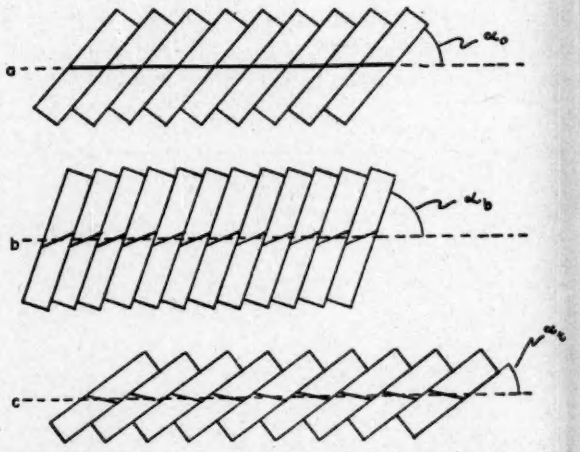

FIG. 6. *Change in local helix angle due to yarn bending.*

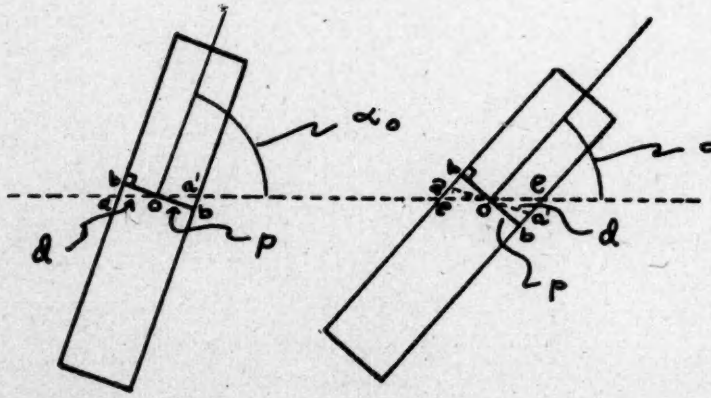

FIG. 7. *Relative movement between fibers due to yarn bending. The diagram on the left shows the fiber as it lies in the yarn before bending. The diagram on the right shows the fiber as it lies on the top of the yarn crown after bending.*

bending, when viewed from the bottom (b) and top (c) of the yarn crown. The dark horizontal line drawn across the fibers in (a) is rotated counterclockwise in segments in (b) and clockwise in (c). These segments are indicated as $\overline{aa}'$ in Figure 7, while $\overline{bb}$ represents the fiber diameter, and $\overline{Ob}$ or ρ is the fiber radius. The relative movement between two points originally in contact on adjacent fibers will therefore be $2\overline{ae}$, where

$$2\overline{ae} = 2\rho(\cot\alpha - \cot\alpha_o) \qquad (35)$$

$$2\overline{ae} = \frac{-2\rho\cos\phi}{\lambda}.$$

In order to demonstrate effectively the change of helix angle at the inner and outer points of a yarn bend, Figures 8 and 9 have been included [6, 8]. These illustrate the more general singles yarn bend as it exists in the ply of a wire rope and of a 3-ply nylon yarn. Ellipticity of the filament or strand section reflects the relative helix angles. Practical considerations of the local helix angle will be discussed in a subsequent paper.

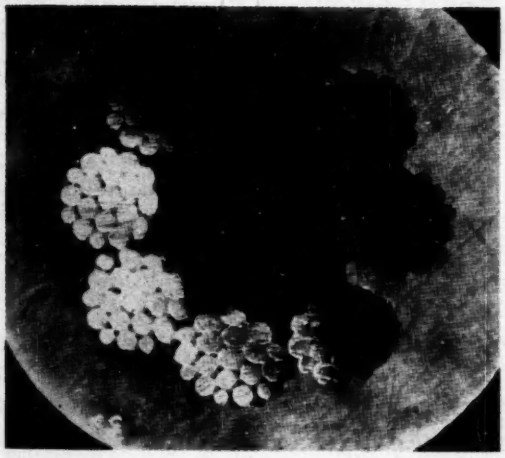

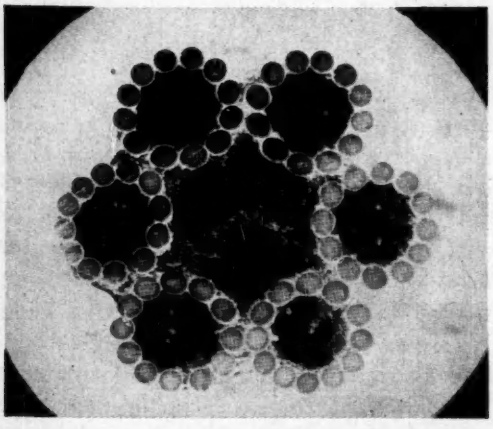

FIG. 8. *Cross sections of wire ropes corresponding to plied yarns.* (Courtesy of E. R. Schwarz [6].)

Local Curvature

For the case where complete freedom of fiber or strand movement exists, local strains occurring in the bending process will depend solely upon the local fiber or strand curvature. Computation of these local strains has been reported by several workers in the field of civil engineering [2], but their work has been confined, for the most part, to low helix angles typical of wire-cable construction. Here, we are dealing with much higher helix angles than were employed in the previous work, and must therefore derive more exact expressions for local curvatures.

From Frenet:

$$\frac{d\bar{T}}{dS} = k\bar{m}, \qquad (36)$$

where $\bar{T}$ is the unit tangent to the fiber at point P in Figure 1, dS is the increment of fiber length, $\bar{m}$ is the principal normal to the fiber path at P, and k is the local curvature of the fiber at P. Let

$$u = (a\cos\lambda\theta - r)^2 + a^2\lambda^2; \qquad (37)$$

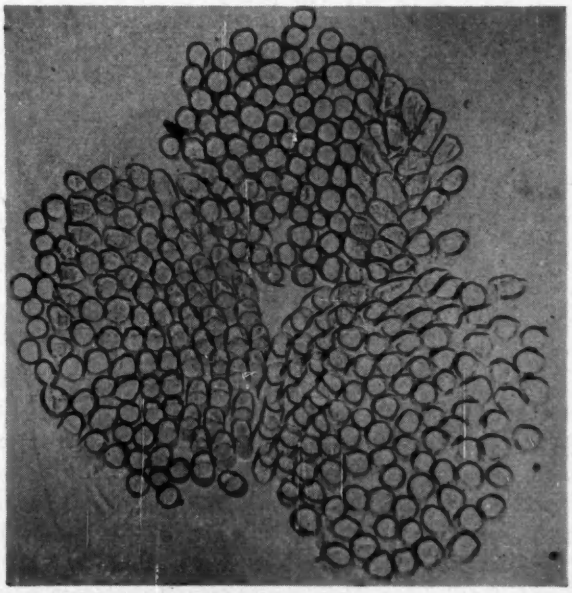

FIG. 9. *Cross section of 3-ply, 102-filament nylon yarn. Note that fibers at the center of the ply lie at a steep angle with the ply axis, as evidenced by their elliptical appearance.* (Courtesy of E. R. Schwarz [8].)

then, from equations (19) and (31*b*):

$$\bar{T} = \frac{d\bar{Y}}{dS} = \frac{d\bar{Y}}{d\theta}\frac{d\theta}{dS} = \frac{d\bar{Y}}{d\theta}\frac{1}{\sqrt{u}}. \tag{38}$$

Now

$$\frac{d\sqrt{u}}{d\theta} = \frac{1}{2}u^{-\frac{1}{2}}\frac{du}{d\theta} = \frac{1}{2}u^{-\frac{1}{2}}2(a\cos\lambda\theta - r)(-a\lambda\sin\lambda\theta)$$

$$= \frac{-(a\cos\lambda\theta - r)\,a\lambda\sin\lambda\theta}{\sqrt{(a\cos\lambda\theta - r)^2 + a^2\lambda^2}}, \tag{39}$$

and

$$k\bar{m} = \frac{d\bar{T}}{d\theta}\frac{d\theta}{dS} = \frac{d}{d\theta}\left[\frac{d\bar{Y}}{d\theta}\frac{1}{\sqrt{u}}\right]\frac{d\theta}{dS} \tag{40}$$

$$k\bar{m} = \frac{\sqrt{u}\dfrac{d^2\bar{Y}}{d\theta^2} - \dfrac{d\bar{Y}}{d\theta}\dfrac{d\sqrt{u}}{d\theta}}{u}\frac{1}{\sqrt{u}}$$

$$= \frac{u\dfrac{d^2\bar{Y}}{d\theta^2} + \dfrac{d\bar{Y}}{d\theta}(a\cos\lambda\theta - r)(a\lambda\sin\lambda\theta)}{u^2}. \tag{41}$$

By taking the product $k\bar{m}\cdot k\bar{m}$, we obtain (taking $g = r/a$)

$$k = \frac{\sqrt{(\cos\lambda\theta - g)^2 + \lambda^4 + 2\lambda^2\cos\theta(\cos\lambda\theta - g) + 4\lambda^2\sin^2\theta - \dfrac{\lambda^2\sin^2\lambda\theta(\cos\theta - g)^2}{(\cos\lambda\theta - g)^2 + \lambda^2}}}{a[(\cos\lambda\theta - g)^2 + \lambda^2]}. \tag{42}$$

This expression is greatly simplified for the case where $\phi = 0$ and $\cos\phi = \cos\lambda\theta = +1$ and $\sin\lambda\theta = 0$, so that

$$k = \frac{\sqrt{(1-g)^2 + \lambda^4 + 2\lambda^2(1-g)}}{a[(1-g)^2 + \lambda^2]}$$

$$= \frac{[(1-g) + \lambda^2]}{a[(1-g)^2 + \lambda^2]}. \tag{43}$$

At $\phi = \pi$, $\cos\lambda\theta = -1$, and $\sin\lambda\theta = 0$,

$$k = \frac{\sqrt{(1+g)^2 + \lambda^4 + 2\lambda^2(1+g)}}{a[(1+g)^2 + \lambda^2]}$$

$$= \frac{[(1+g) + \lambda^2]}{a[(1+g)^2 + \lambda^2]}; \tag{44}$$

and at $\phi = \pi/2$, $\cos\lambda\theta = 0$, and $\sin\lambda\theta = 1$,

$$k = \sqrt{\frac{g^2 + \lambda^4 + 4\lambda^2 - \dfrac{g^2\lambda^2}{g^2+\lambda^2}}{a(g^2+\lambda^2)}}$$

$$= \frac{\sqrt{\dfrac{g^4}{g^2+\lambda^2} + \lambda^4 + 4\lambda^2}}{a(g^2+\lambda^2)}. \tag{45}$$

In Figure 10 the dependance of k upon λ for several values of g or r/a is illustrated for the points $\phi = 0, \pi/2$, and π. It should be emphasized that in dealing with cabled structures, the reciprocal of k computed for the major element of the basic structure becomes the bending radius, r, in computations of strains set up in the subelement. For example, in a plied structure whose single twist is hard but whose ply twist is soft, bending will impose little tensile strain on the singles since they are relatively free to move about. However, the change in curvature of the singles yarn axes, brought about by the bending, will impose tensile strains in individual fibers since they are restricted from moving freely within the singles yarn. In this latter calculation of yarn geometry, r is taken as $1/k$ of the previous calculation.

The Geometric Parameters in Textile Terms

Textile designers seldom work with data relating to twist ratios or radius ratios. The dimensionless parameters used throughout this report can be computed readily from practical yarn data. Equations (15), (16), and (17) illustrate the simplicity of the conversions. In order to facilitate computations, however, it was deemed advisable to reduce equation (17) to graphical form and designate the radius ratios in terms of yarn-number ratios according to the relationship:

$$\frac{r}{a} = \sqrt{\frac{N_1}{N_2}} + 1, \tag{46}$$

where the warp yarn of count N_1 is considered to be bent around the filling yarn of count N_2. This has been done in Figures 11 and 12, which may be used in connection with Figures 3, 4, 5, and 10 to determine differences in path length, average strains, local helix angles, and fiber curvatures in terms of yarn counts and twist multiples.

It should be emphasized that this geometric analysis does not allow for flattening of one yarn as it is bent about the other. Flattening alters the geometry of the yarn being bent, but the greatest effect, as Platt pointed out, is due to an increase in the radius of curvature of the warp and filling yarns at their point of contact. It can be

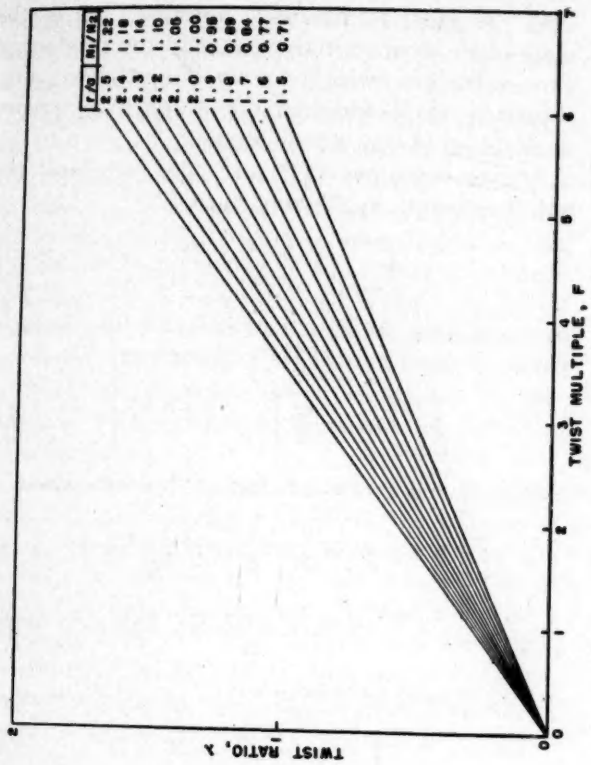

FIG. 11. *Twist ratio, λ, in terms of yarn-number ratios and twist multiples.*

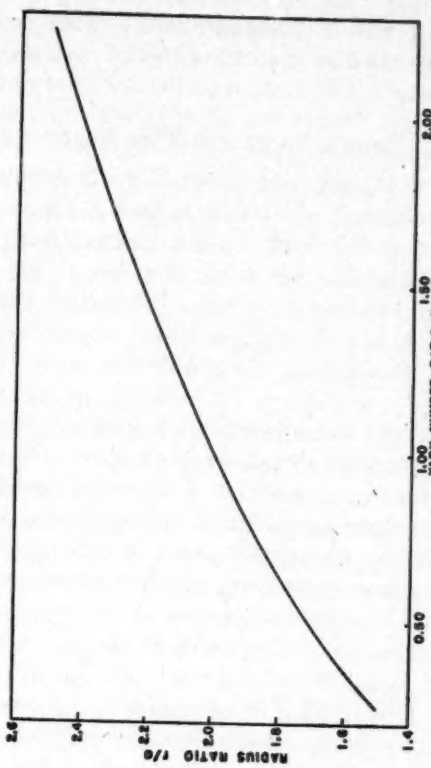

FIG. 12. *Radius ratios in terms of yarn-number ratios.*

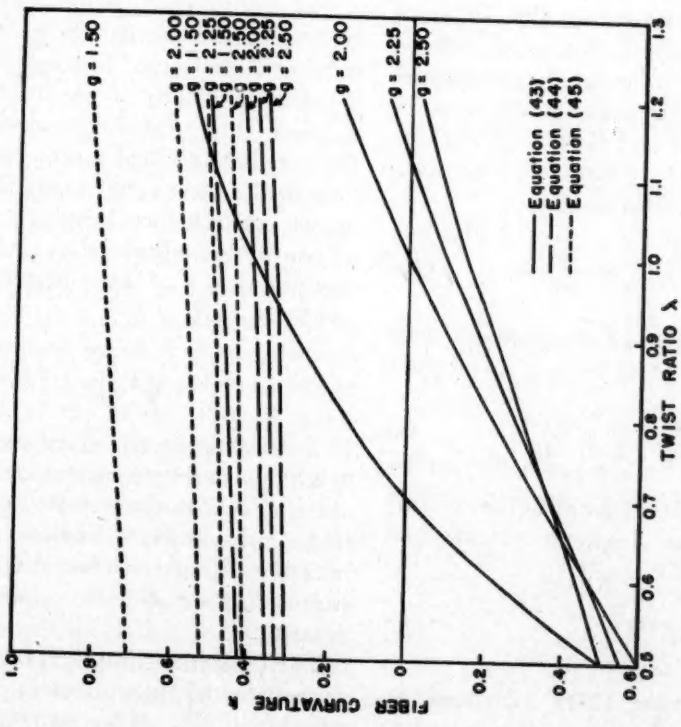

FIG. 10. *Fiber curvature* vs. *the variables of yarn geometry.*

shown that this new radius (corresponding to $r - a$ in Figure 1) is equal to the original radius of curvature divided by the cube of the flattening coefficient.

Textile Yarns and Wire Ropes

Civil engineers have studied the distribution of bending stresses in wire ropes used for heavy-duty hauling. Since 1912 several analytical solutions of the geometric structure of twisted cables subjected to bending have been proposed. One such solution based on the kinematic method was first used by Woernle in 1912, and was more recently amplified by Czitary [2]. It is of interest to compare the assumptions and results of Czitary's study with the analyses of this paper.

The kinematic method is based on assumptions which are similar to those of the above analysis. In kinematic terms, the cable is considered to form a torus whose cross sections are circular and plane. The ratio of ϕ to θ is considered to be constant, as in equation (3). The method pictures a particle moving along the wire strand as it lies in the bent cable. The motion of the particle consists of: (*1*) constant velocity about the periphery of a circle comprising the plane section of the torus (around circle *HQP* of Figure 1); and (*2*) constant angular velocity of this plane section about the center of curvature of the cable axis—*i.e.*, the torus center.

Czitary derived an expression for the differential arc length along the particle path (strand axis) in terms of the radii of cable and torus, the angle θ, and the twist ratio λ. Integrating and discarding terms of lesser magnitude, he obtained

$$\int_{\phi=\pi/2}^{\phi=\pi} dS = \frac{r\pi}{2\lambda} + \frac{a}{\lambda} + \frac{\lambda a^2 \pi}{4r}, \tag{47}$$

representing the arc length of the outside quarter loop; and for the inside quarter loop,

$$\int_{\phi=0}^{\phi=\pi/2} dS = \frac{r\pi}{2\lambda} - \frac{a}{\lambda} + \frac{\lambda a^2 \pi}{4r}. \tag{48}$$

By subtracting equation (48) from equation (47) he showed the difference between outside and inside quarter loops to be

$$\frac{\Delta S}{2} = \frac{2a}{\lambda}, \tag{49}$$

as contrasted to equation (26). If, however, $r \gg a$ and $aT \ll 1$, λ^2 will be small compared to $(r/a)^2$, and equation (26) will reduce to equation (49). In most textile uses, however, r is of the same order of magnitude as a, and the product of yarn radius and twist is not small relative to unity. Equation (26) should therefore be used in preference to equation (49) in textile studies.

Adding equations (47) and (48), we have the half-loop length in the bent yarn:

$$\int_{\phi=0}^{\phi=\pi} dS = \frac{r\pi}{\lambda} + \frac{\lambda a^2 \pi}{2r}, \tag{50}$$

corresponding to equation (22) for the straight yarn. If equation (22) is expressed as

$$\int_{\phi=0}^{\phi=\pi} dS = \frac{\pi r}{\lambda}\left[1 + \left(\frac{a\lambda}{r}\right)^2\right]^{\frac{1}{2}}, \tag{51}$$

and use is made of the binomial theorem, where

$$\sqrt{1+x} = 1 + \frac{x}{2} - \frac{1}{8}x^2 + \frac{1}{16}x^3 + \cdots,$$

taking $x = \left(\frac{a\lambda}{r}\right)^2 \ll 1$, then the half-loop length in the straight yarn becomes

$$\int_{\phi=0}^{\phi=\pi} dS = \frac{\pi r}{\lambda} + \frac{\lambda a^2 \pi}{2r}, \tag{52}$$

corresponding to equation (50) for the bent yarn. Czitary concluded that the increase in length of the outside of the helix turn is taken care of by the decrease in length of the inside helix turn. This agrees with the previously stated conclusion [1, 7] that, within specified limits, the length of the fiber loop in the bent yarn equals that of the fiber loop in the yarn before bending. Chow's limitations [1] on this equality are specific, for he showed that the invariance of loop length depends upon the condition that

$$\frac{r}{a} - \sqrt{2\left(\frac{r}{a}\right)^2 + \lambda^2} < -1. \tag{53}$$

If λ is of negligible magnitude, r/a must exceed 2.42 in order to satisfy condition (53); or, conversely, when $r/a = 1.50$, λ must exceed 1.32; when $r/a = 1.75$, λ must exceed 1.19; when $r/a = 2.00$, λ must exceed 1.00; when $r/a = 2.25$, λ must exceed .40; and when $r/a = 2.50$, λ must exceed .00.

The limitations imposed by condition (53) apply as well to the integration of equation (18) to give equation (20). The concept of average strain

introduced in equations (20) and (21) is likewise limited by condition (53). Nevertheless, it was considered advisable to plot the entire practical (in textile terms) range of values for $\Delta S/2$ and $\bar{E}$ in Figures 3 and 4 for the purpose of achieving continuity and in order to permit estimation of orders of magnitude. If high accuracy is desired for values of average strain, one may integrate graphically the local strain plotted against ϕ and divide by the total change in ϕ in Figure 2. Where condition (53) is not met, the E *versus* ϕ curve between $\phi = 0°$ and 45° will not equal the curve between $\phi = 45°$ and 90°, as is evident in Figure 2. As would be expected from condition (53), the curves of Figure 2 show increased symmetry as r/a is increased.

The kinematic method has been used to determine local helix angles. In effect, the velocity of the particle at a given moment is the vector sum of its velocity components in the circle *HQP* of Figure 1 and around the torus due to movement of the plane section. The tangent of the angle between this velocity vector and the cable axis is simply the ratio of the two velocities, and can be shown to equal

$$\tan \alpha = \tan Q \frac{r}{r - a \cos \phi}. \tag{54}$$

From equation (13),

$$\tan Q = \frac{a\lambda}{r},$$

whence agreement with equation (33) is reached. Carrying the kinematic approach further, it has been shown that increased lateral-strand space is not needed for low-twist cables because of change in local helix angles during bending. This follows from the fact that changes in the major axes of the elliptical sections of the inclined strands in the outside loop are equal and opposite to the changes in the inner half of the loop. It follows that in low-twist structures there is no lateral stress developed around the small circle perimeter. This point bears further consideration in the study of densely packed high-twist structures.

In order to determine local curvatures, Czitary determined (*1*) the normal acceleration of the particle due to rotation in the circle *HQP* (Figure 1); (*2*) the normal acceleration due to rotation of the circle *HQP* about the axis *O*; and (*3*) the Coriolis acceleration parallel to the axis of the cable due to the angular velocity of the circular section *HQP* about the axis *O* and the component of relative velocity perpendicular to axis *O*. Czitary then determined the projections of these accelerations onto two mutually perpendicular planes, both containing the tangent to the strand, or particle path at *P*. One plane is the osculating plane of the strand path, while the other contains the binormal of the path. In each plane the components of acceleration perpendicular to the path tangent at *P* are used to obtain the curvature of the path projection, according to the relationship

$$\dot{v}_r = \frac{v^2}{\rho},$$

where $\dot{v}_r$ is the radial component of acceleration in each plane, ρ is the radius of curvature, and v is the particle velocity. The curvatures in the two perpendicular planes are combined to furnish the local curvature of the strand. The change in curvature due to bending was determined to be

$$\Delta k = \frac{\cos \alpha}{a(r - a \cos \phi)} [(a \cos \phi)^2 \cos^2 \alpha + a^2(1 - \cos^2 \phi)(1 + \sin^2 \alpha)^2]^{\frac{1}{2}}. \tag{55}$$

Equation (55) is based on the relationship between curvature and bending-moment components in a wire cross section, on the assumption that each component acts independently and that vectorial combination of the moments provides the resultant curvature changes.

At $\phi = 0$, equation (55) reduces to

$$\Delta k = \frac{(g - 1)}{a[\lambda^2 + (g - 1)^2]}, \tag{56}$$

and at $\phi = \pi$ to

$$\Delta k = \frac{(g + 1)}{a[\lambda^2 + (g + 1)^2]}. \tag{57}$$

The curvature of the strand of the unbent cable or yarn is

$$k = \frac{\lambda^2}{a(g^2 + \lambda^2)}, \tag{58}$$

which, when subtracted from equations (43) and (44), provides for $\phi = 0$ and π, respectively,

$$\Delta k = \frac{[(1 - g) + \lambda^2]}{a[(1 - g)^2 + \lambda^2]} - \frac{\lambda^2}{a(g^2 + \lambda^2)} \tag{59}$$

$$\Delta k = \frac{[(1 + g) + \lambda^2]}{a[(1 - g)^2 + \lambda^2]} - \frac{\lambda^2}{a(g^2 + \lambda^2)}. \tag{60}$$

If the ratio g or $r/a \gg 1$, as in the case of the bent cable, the denominators of the second terms in

equations (59) and (60) very nearly equal those in the first terms, and equations (59) and (60) reduce to equations (56) and (57). The change in curvature at $\phi = \pi/2$ is small, and the subtraction of equation (58) from equation (45) does not reduce so readily to equation (55), but, rather, to

$$\Delta k = \frac{\sqrt{(g^2 + 2\lambda^2)^2 + \lambda^4(g^2 + \lambda^2)}}{a(g^2 + \lambda^2)^{\frac{1}{2}}} - \frac{\sqrt{\lambda^4(g^2 + \lambda^2)}}{a(g^2 + \lambda^2)^{\frac{1}{2}}}, \quad (61)$$

while equation (56) becomes

$$\Delta k = \frac{(g^2 + 2\lambda^2)}{a(g^2 + \lambda^2)^{\frac{1}{2}}}. \quad (62)$$

However, if $r \gg a$ and $aT \ll 1$, equation (61) will approach equation (62), showing the general agreement of the two expressions for the special case of extremely low-twist structures bent into large radii of curvatures. For the average textile case equation (45) remains the more accurate expression for the determination of bending curvature in individual fibers.

The final subject of Czitary's paper has to do with the torsion of wire in bent cables. He assumed the wires to be free of torsion during the manufacturing process, while the difference in torsional strain between straight and bent forms is accounted for in a manner similar to length changes in the upper and lower loops. In other words, the torsional strains required in one half of the loop is provided by the other half, and there is no net twisting as a result. This is evidenced by observations of the rotation of a wire in a cable subjected to bending. To what extent this required rotation is hindered in densely packed highly twisted textile structures is not known, but it is safe to say that its effects are small compared to the tensile strains which occur due to restrictions on the longitudinal shifting of lengths from lower to upper loops during bending.

Summary and Conclusions

This paper has outlined the results of a geometric analysis of the idealized structure of a bent yarn. The importance of such knowledge in problems dealing with the mechanical properties of twisted woven and knitted textile structures has been stressed. Specific attention has been given to computations of local and average fiber strains which occur in highly twisted dense structures that are subjected to bending. The relative motion between fibers in both loose and tightly packed yarns has been considered, and, finally, the effect of bending on local fiber curvatures has been studied.

It is clear that the analysis has taken into account only the extreme cases of complete freedom or lack of freedom of motion between fibers during bending of the yarn. In practice, the packing density of the yarn and the frictional behavior of the fibers determine the relative length transfers between upper and lower loop halves. The length transfers influence the resultant local strains and, therefore, the fiber tensile stresses in the upper half loop. These stresses, in turn, develop lateral yarn pressure components which determine the frictional resistance to further length transfers.

For maximum bending fatigue-resistance and wrinkle-resistance, minimum friction between fibers and an open yarn structure appears desirable. In this way, tensile strains resulting from the bending of twisted structures may be kept to a minimum. If more elastic fibers are used in a fabric structure, closer packing of the yarn structure is possible without exceeding the yield level of the fiber in yarn bending. Clearly, some degree of interfiber friction and yarn density is desirable if sufficient fiber strain, and therefore permanent set, are to be achieved when inserting a crease during the pressing operation. This is believed to be the reason why tightly twisted worsted suitings can be given such durable creases, as contrasted to loosely twisted woolens. It has been said that the observed differences in crease acceptance of worsted and woolens are due to the relative radii of curvature reached at the fold. This factor is undoubtedly significant, but the analysis presented here demonstrates that freedom of fiber movement can very nearly eliminate strain over a wide range of curvatures. Considerably more emphasis must therefore be given to the packing and frictional behavior of fibers within the yarns.

Reasoning along the lines indicated above may be extended to studies of internal friction in yarn, cord, and rope structures. Where it can be shown experimentally that the cause of material failure is internal abrasion, the textile structure involved may be redesigned with the aid of the $\Delta S/2$ graphs developed here, and dislocations of its adjacent elements during bending may be drastically

reduced. In like manner, local rubbing due to changes in local helix angles may be controlled.

Cords and ropes are multiple textile structures for which bending generally does not induce tensile strains in the major structural components because of the relative freedom of movement between these major components. However, freedom of movement between the subcomponents within the major components is often restricted. In such cases, computations of the curvatures of the major components due to total bending of the structure is facilitated by the graphs presented in this paper. These curvatures can be used in subsequent computations of the local tensile strains in fibers or yarns of the subcomponents.

It is clear that much empirical work is necessary to demonstrate the applicability of these analyses. Such experimentation will throw light on the important factors of yarn flattening during bending and of yarn consolidation under tension. Without doubt, there will be cases where deviations from the idealized geometry of this paper will dominate the textile structure. It is our belief, however, that the cases for which the idealized geometry will be of use are numerous. For such cases this study provides much-needed quantitative relationships.

Acknowledgment

The author acknowledges with appreciation the sponsorship of this work by the Textile Branch, Research and Development Division, Office of The Quartermaster General. Thanks are due Dr. S. J. Kennedy, Director of Research of the Textile Branch, Office of The Quartermaster General, and Mr. L. I. Weiner, Head of the Textile Materials Engineering Laboratory, for their encouragement and support in this work. The problem of the geometry of the bent yarn was suggested by Dr. W. J. Hamburger and Dr. M. M. Platt in connection with their Quartermaster Corps sponsored research on the creasing behavior of textile fabrics. Grateful acknowledgment is made to Prof. E. E. Schwarz for his guidance and encouragement in this study. The assistance of Mr. W. J. Hynek in computing requisite tables and in the preparation of the graphs is noted with thanks.

Literature Cited

1. Chow, T., "Some Aspects of the Geometry of Yarn Structures," unpublished Master's thesis, Massachusetts Institute of Technology, Textile Division, Cambridge, Mass., June 1948.
2. Czitary, E., On the Bending Strains of Wire Cables, *Osterreichische Ingenieur-Archit* **1**, 342–50 (July 1947).
3. Gagliardi, D. D., and Grunfest, I. J., Creasing and Creaseproofing of Textiles, Textile Research Journal **20**, 180–8 (1950).
4. Platt, M. M., Mechanics of Elastic Performance of Textile Materials: Part III: Some Aspects of Stress Analysis of Textile Structures—Continuous-Filament Yarns, Textile Research Journal **20**, 1–15 (1950).
5. Platt, M. M., Mechanics of Elastic Performance of Textile Materials: Part IV: Some Aspects of Stress Analysis of Textile Structures—Staple-Fiber Yarns, Textile Research Journal **20**, 519–38 (1950).
6. Schwarz, E. R., "Textiles and the Microscope," New York and London, McGraw-Hill, 1934.
7. Schwarz, E. R., Twist Structure of Plied Yarns, Textile Research Journal **20**, 175–9 (1950).
8. Schwarz, E. R., Certain Aspects of Yarn Structure, Textile Research Journal **21**, 125–36 (1951).
9. Woods, H. J., The Kinematics of Twist, *J. Textile Inst.* **24**, T317–32 (1933).

(*Manuscript received August 15, 1952.*)

Effects of Mechanical Processing of Cotton on the Physical Properties of Fibers

James N. Grant, Ora W. Morlier,* and John M. Scott†

Southern Regional Research Laboratory,‡ New Orleans, Louisiana

Abstract

Fibers from ginned cotton and from 16/2s yarn of seven cottons of different physical properties were tested as a bundle and as individual fibers in order to determine what changes in properties, if any, could be attributed to the mechanical processing. Determinations of tenacity, length array distribution, and crystal alignment revealed no consistent differences between the cottons before and after processing. The maturity of carded cottons was slightly lower. The weight fineness and breaking load of individual fibers were unchanged with processing, but elongation at break was decreased. A higher modulus in tension was obtained from load-elongation curves of processed fibers, with the greatest difference found for loads below 2 g.

ANY DAMAGE that occurs to cotton fibers during mechanical processing will be carried over into the textile products and might reduce their usefulness.

Several studies of the possible damage or the extent of any changes in the properties of cotton fibers as they are processed from raw stock into yarn have been reported. Clegg [2], in a discussion of the Congo red method for determining damage to fibers by microscopical examination, found that in one study the number of bruised or torn fibers increased from 5% in the boll to 59% in the twisted yarn, while in another the proportion of bruised fibers increased from 20% in the bale to 36% in the processed yarn. This worker noted a marked drop in the mean breaking load of the fibers in the yarn relative to those in the bale. Recently, Krieble and Whitwell [9] reported a decrease in degree of polymerization of the cellulose as a result of mechanical processing, and concluded that processing alters the chain length, particularly during the picker operation. In other studies by the U. S. Department of Agriculture [17, 18] routine tests indicated very small changes in the average physical properties of fibers due to processing from ginned cotton into second-drawing sliver.

None of the studies mentioned above included an evaluation of the changes occurring in the strictly mechanical properties of cotton fibers due to processing. The present work includes determinations of the mechanical properties of individual fibers, as well as standard determinations of physical properties of fibers in bundles before and after processing. American-grown cottons in commercial production were used. The results show that the elongation properties are affected by processing between the ginned stage and the yarn stage; and indicate that the performance of textile products may have better correlation with the properties of the processed than with those of the unprocessed fibers.

Experimental

Samples

Seven varieties of American-grown commercial cottons, representing a range of fiber properties, were used: S×P, Hopi Acala 50, Acala 1517, Deltapine 14, Stoneville 2B, Coker 100 Wilt, and Rowden 41B. Since all samples were taken from a single bale of the variety, the physical properties of the fibers observed may vary slightly from an average of that variety.

Fibers for the tests of the unprocessed cotton were taken by standard sampling procedures from ginned cotton for all varieties except Hopi Acala 50, the samples of which were taken from picker lap. Fibers for the tests of processed cotton were taken from 16/2s yarns by untwisting a sufficient length of plied yarn, then untwisting the single yarn, and carefully withdrawing the fibers. These low-twist yarns had been spun at the Southern Regional Research Laboratory according to conventional methods, which in-

* Present address: 1361 E. 50 St., Chicago, Ill.

† On military leave.

‡ One of the laboratories of the Bureau of Agricultural and Industrial Chemistry, Agricultural Research Administration, U. S. Department of Agriculture.

cluded carding fibers of the upland cottons and combing those of the one long-fibered variety, S×P.

Testing Methods

After several weeks, during which the samples were permitted to relax from previous handling, the physical properties of bundles and of individual fibers were measured under standard atmospheric conditions (70°F, 65% R.H.).

Length by array, tenacity, and maturity of bundles of fibers were determined by A.S.T.M. procedures [1]. Crystallite orientation was determined by measuring half the angle between points of half-maximum intensity in an azimuthal scan of the diffraction from the 002 plane as recorded by the Geiger counter x-ray spectrometer [14].

Fineness, breaking load, and elongation at break of individual fibers were determined by procedures developed at this Laboratory, which have been described elsewhere [8, 11]; briefly, these procedures were as follows: 100 fibers were taken from each of three length groups which constituted the greater percentage of fiber by weight in the length-array distributions. Breaking load and elongation values were obtained at a constant rate of load of 0.9 g./sec. on a fiber segment averaging 0.71 cm. Load-elongation curves were made on 40 additional fibers with a similar instrument so modified to give the curve from 0.2 g. to rupture [4]. A small load, 0.2 g., was placed on all fibers to remove most of the natural kinks and to improve the reproducibility of curves in the initial section. Fineness (weight per unit length) was an average for 400–500 fibers, and was determined on a center section of fibers held in a clamp and cut to a length of 1.27 cm. (½ in.). The average fineness in grex (μg./cm.) was obtained by weighing together and counting the cut fibers.

Results and Discussion

In Table I are given the values for the properties determined on bundles of fibers, and in Tables II and III those for the individual fibers, before and after processing.

Fiber Bundles

The values in the bundle test for length, tenacity, and crystallite orientation for processed and unprocessed fibers are not significantly different. These differences are either within the limits of experimental error or not detectable by the test methods used. Although the differences between length of unprocessed and processed Rowden are greater than can be accounted for by experimental error, they are within the range of error often found in sampling bulk cotton. The unchanged length distribution indicates that there were counterbalancing effects from stretching, the removal of short fibers as waste, and fiber breakage which occurs during processing. While fiber lengths are essentially the same in the unprocessed and processed samples of these studies, it must be recognized that the mechanical condition of processing equipment, the machine setting, or the properties of other cottons may influence the effects of processing on the fiber length distribution. It is interesting that Williams [19] also found an equivalent numerical average length of fiber in the distribution after processing.

The slightly lower percentage of mature fibers in the six carded cottons after processing is at variance with the general concept that maturity is unchanged or that even a larger proportion of immature than mature fibers are removed during processing. The trend in the present work towards the lower maturity, although slight, is marked enough to indicate an effect of processing. When the percentages of immature fibers in corresponding length groups of unprocessed and processed fibers were compared, the percentage of immature fibers was greater among fibers of the shorter lengths but was less among the longer fibers of the length distribution. A selective removal of mature fibers is reasonable if an assumption is made that the larger, well-developed fibers, if broken during processing, are more easily separated, while the immature fibers have a greater tendency to become entangled, and so remain in the silver as they travel through the equipment. In processing the fibers, the percentage decrease of maturity was greater in cotton of the greater percentage of immature fibers, except for the Acala 1517, which originally had a high percentage of immature fibers. Evidence of this lower maturity was also found by Hasling [7] in work in which a special dye test indicated that a lower percentage of mature fibers was present in card sliver than in the unprocessed sample.

Individual Fibers

The results of determinations of individual fiber properties (Table II) show that breaking load and weight-fineness of the fibers were essentially the

TABLE I. PHYSICAL CHARACTERISTICS OF COTTON FIBERS IN BUNDLES, BEFORE AND AFTER PROCESSING

Sample identification	Staple length (in.)	Length distribution* Upper quartile (in.)	Mean (in.)	Coeff. of var. (%)	Tenacity† Flat bundle (g./grex)	Mature fibers (%)	Crystallite orientation‡ (degrees)
S×P							
unprocessed	1 1/2	1.57	1.33	26	4.5	86	30.0
processed		1.56	1.33	26	4.6	86	31.3
Hopi Acala 50							
unprocessed	1 3/32	1.18	0.95	35	4.9	92	25.5
processed		1.20	0.98	32	5.0	88	26.3
Acala 1517							
unprocessed	1 3/32	1.27	1.03	34	3.9	70	30.4
processed		1.27	1.03	29	3.8	66	31.2
Deltapine 14							
unprocessed	1 1/16	1.19	0.95	34	4.0	79	30.8
processed		1.18	0.94	34	4.0	74	30.1
Stoneville 2B							
unprocessed	1 3/32	1.23	1.00	32	4.5	80	26.6
processed		1.19	0.97	32	4.5	74	25.7
Coker 100 Wilt							
unprocessed	1 1/16	1.17	0.97	31	3.8	78	30.5
processed		1.19	0.95	34	3.9	72	32.3
Rowden 41B							
unprocessed	31/32	1.08	0.92	26	4.0	90	28.4
processed		1.13	0.96	25	4.2	87	28.8

* Three length arrays.
† Ten Pressley breaks. 1 g./grex = 1.85 Pressley index.
‡ Angle between maximum and half-maximum intensity of the 002 x-ray diffraction arc.

TABLE II. PHYSICAL PROPERTIES OF INDIVIDUAL FIBERS, BEFORE AND AFTER PROCESSING

Sample identification	Breaking load Mean (g.)	Breaking load Coeff. of var. (%)	Fineness (grex)	Tenacity (g./grex)	Elongation at break Mean (%)	Elongation at break Coeff. of var. (%)
S×P						
unprocessed	6.5	37	1.4	4.9	13.7	32
processed	6.3	33	1.4	4.5	11.1	31
Hopi Acala 50						
unprocessed	6.3	45	1.9	3.3	8.1	38
processed	6.5	43	1.8	3.6	6.5	41
Acala 1517						
unprocessed	4.9	48	1.7	2.9	10.4	39
processed	5.0	45	1.7	3.0	9.7	42
Deltapine 14						
unprocessed	5.3	52	1.9	2.8	10.3	43
processed	5.4	49	1.9	2.9	8.1	46
Stoneville 2B						
unprocessed	5.0	47	1.8	2.7	7.7	40
processed	5.0	48	1.9	2.6	5.9	46
Coker 100 Wilt						
unprocessed	4.9	51	1.9	2.7	9.3	41
processed	5.0	52	1.8	2.8	7.1	48
Rowden 41B						
unprocessed	6.8	48	2.6	2.6	10.0	39
processed	7.6	45	2.6	3.0	8.0	43

same after as before processing, allowing for sample variations and average trends. Since neither breaking load nor fineness were changed, tenacity, which is strength per unit weight-fineness, was unchanged.

The significant difference between the unprocessed and processed cottons is noted in the values for elongation at break. There was a definitely lower elongation at break in the processed fibers of all the varieties; also, the scatter of observations for elongation at break, as measured by the coefficient of variation, was increased. Stretching during processing reduced the average percent elongation of the fibers 1.9%, or approximately one-fifth the percent elongation of the unprocessed fiber. The decrease for Acala 1517 was 7%, while the decrease for the others ranged from 19% to 24%. The elongation at break of textile fibers is probably unimportant in evaluating many textile fabrics since rupture from stress occurs only after fiber properties are altered by long periods of service. That stretching varies also from fiber to fiber is shown by the greater coefficients of variation (Table II) for elongation at break found for processed cotton.

TABLE III. AVERAGE MODULUS IN TENSION

Sample identification	Modulus between 0.2 g. tension and the following: 1 g.* (g./grex / strain ‡)	2 g.* (g./grex / strain ‡)	At break† (g./grex / strain ‡)
S×P			
unprocessed	39	29	34
processed	61	40	41
Hopi Acala 50			
unprocessed	32	31	41
processed	52	56	55
Acala 1517			
unprocessed	25	23	28
processed	48	34	31
Deltapine 14			
unprocessed	35	33	27
processed	42	40	35
Stoneville 2B			
unprocessed	37	38	36
processed	51	45	44
Coker 100 Wilt			
unprocessed	24	24	28
processed	38	37	39
Rowden 41B			
unprocessed	21	23	26
processed	46	45	37

* Average of 40 observations.
† Average of 300 observations.
‡ Elongation per unit length.

In Figure 1 are given curves, which are averages of the seven cottons tested, to illustrate the section of the load-elongation curve altered by processing and the magnitude of the changes. The curves were drawn from average slopes taken between load intervals on curves for individual fibers from the seven cottons. From these curves, it can be seen that the decreased elongation was not uniformly distributed over the whole curve. The processed fiber extended slowly under low loads, and increased in rate as the load approached 2 g. of tension. In contrast, the unprocessed fibers had a period of rapid elongation due to incomplete removal of kinks under the initial tension and to secondary creep under low load. Both unprocessed and processed fibers reached the yield point at approximately the same loads, but with different elongations, and followed similar patterns of increased rigidity slightly above the 2 g. of tension, with approximately the same slopes to rupture.

The shapes of load-elongation curves for individual fibers also indicate that the tension on individual fibers had been different at some stages in the processing into yarns. Many fibers were extended beyond their yield stress, and recovery was incomplete before the tensile tests were made. As a result of the stretching, the normal variability among fibers was increased by the superimposed influences of tensional forces during processing. The tensional forces are expected to vary from loads that are sufficient to rupture fibers to essentially no tension

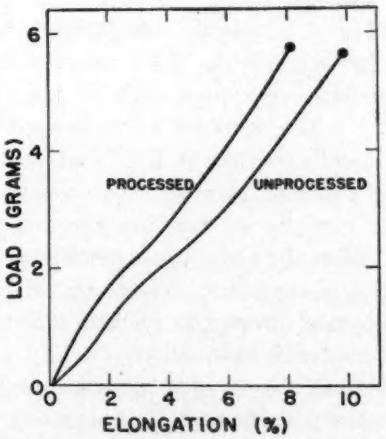

FIG. 1. *Load-elongation curves for unprocessed and processed cotton fibers.*

for fibers that are easily separated and aligned. During the processing, the tension which stretches the fiber also removes kinks and produces a permanent deformation which may be repeated several times as fibers pass through opening, carding, and drawing machines. While this tension is uncontrolled, the procedure can be compared to a process of mechanical conditioning, as described by Hamburger [6]. In both mechanical processing and mechanical conditioning, the load-elongation curve is altered by the application of tension.

The importance of the load-elongation characteristics of textile fibers is indicated by the number of properties of fabrics related to this property of the fiber. Sookne [16] recognized load-elongation measurements as a useful tool in both research and control work, while Hamburger [5] stated that the stress-strain properties measured from the load-elongation curves for fibers are reflected in the abrasion-resistance and elastic performance of textile materials, and Dillon [3] and Ray [12] considered it as a measure of resilience. Several methods are described in the literature [5, 10, 13, 15, 16] for measuring the stress-strain properties of textile fibers, the differences being dependent upon the end-use of the textile fabric to be evaluated. The measure of stress-strain properties considered in the present study is the "average modulus in tension," as taken from load-elongation curves. Average modulus in tension is the ratio of stress to strain due to tension on the fibers when measured from the load-elongation curve at the prescribed loads.

The moduli between 0.2 g. tension and 1 g., 2 g., and "at break" are given in Table III. The value at break is identical with "stiffness," as defined by Smith [15]. The average modulus at break was greater after processing, apparently owing to the lower extension since fiber tenacity was unchanged (Table II). The increase in modulus with processing is usually greater at the lower loads than at break, the amounts varying with different cottons. While the changes in modulus are not consistent with any one of the physical properties of the fibers, the modulus is apparently related to the closely associated physical properties of wall thickness, fineness, and crystallite orientation.

The fact that the changes in elastic properties at low loads are not constant for cottons of different characteristics makes it unreliable to predict fabric characteristics from the properties of these fibers until they are processed. Also, the processed fibers, while more variable in their elongation at break, should represent more closely the characteristics of fibers in the fabric since they represent the fibers immediately before they are woven into the fabric.

Summary

During the mechanical processing of fibers from ginned cotton into 16/2s yarn, tensional forces are applied to the individual fibers which change the shape of the load-elongation curve and reduce the elongation at break. The changes are greater under the low loads than at break. The altered fibers have a greater modulus in tension, the increases in modulus being greater for loads of 2 g. or less than for loads at break. Changes in modulus were not the same for cottons of different fiber properties.

The lower percentage of mature fibers in the length distribution of carded cotton indicates a selective action during the processing which also increases the number of immature fibers in the shorter length groups.

The effects of processing, if any, on length, weight-fineness, tenacity, and crystallite orientation were within experimental errors in the test methods.

Since important properties of the fibers are altered during processing, the extent depending upon the inherent fiber property, fabric characteristics independent of construction effects should be predicted more reliably from properties of the processed than from those of the unprocessed fibers.

Acknowledgment

The authors wish to express their appreciation to the members of the Mechanical Processing Division, who manufactured the yarns; to the members of the Textile Testing Section, who assisted with the routine tests of fiber properties; to Mr. J. J. Creely, who measured the crystallite orientation; and to Mrs. Geraldine C. Humphreys, who made measurements on the load-elongation curves and performed many of the calculations.

Literature Cited

1. Am. Soc. Testing Materials, Committee D-13, Tentative General Methods of Testing Cotton Fibers (D414–49T), in "A.S.T.M. Standards on Textile Materials," 1950, Philadelphia, pp. 250–76.
2. Clegg, G. G., *J. Textile Inst.* **31**, T49–68 (1940).

3. Dillon, J. H., TEXTILE RESEARCH JOURNAL **17**, 207–13 (1947).
4. Grant, J. N., Orr, R. S., and Morlier, O. W., "Breaking Load, Elongation-at-Break, and Related Properties of Cotton Fibers," presented before The Fiber Society, Fontana, N. C., Apr. 27, 1950.
5. Hamburger, W. J., in "A.S.T.M. Standards on Textile Materials," Philadelphia, Am. Soc. Testing Materials, 1948, pp. 491–8.
6. Hamburger, W. J., TEXTILE RESEARCH JOURNAL **18**, 102–13 (1948).
7. Hasling, V. C., private communication.
8. Karrer, E., Grant, J. N., and Orr, R. S., TEXTILE RESEARCH JOURNAL **17**, 314–22 (1947).
9. Krieble, J. G., and Whitwell, J. C., TEXTILE RESEARCH JOURNAL **19**, 556–62 (1949).
10. Meredith, R., *J. Textile Inst.* **36**, T147–64 (1945).
11. Morlier, O. W., Orr, R. S., and Grant, J. N., TEXTILE RESEARCH JOURNAL **21**, 6–12 (1951).
12. Ray, L. G., *ASTM Bull.* No. 176, 46–8 (1951).
13. Schiefer, H. F., Fourt, L., and Kropf, R. T., *ASTM Bull.* No. 144, 17–25 (1947).
14. Segal, L., Creely, J. J., and Conrad, C. M., *Rev. Sci. Instruments* **21**, 431–5 (1950).
15. Smith, H. De W., *Am. Soc. Testing Materials Proc.* **44**, 543–92 (1944).
16. Sookne, A. M., in "A.S.T.M. Standards on Textile Materials," Philadelphia, Am. Soc. Testing Materials, 1948, pp. 498–502.
17. U. S. Bur. Plant Indus., Soils, and Agr. Eng., "Progress Report on Annual Varietal and Environmental Study of Fiber and Spinning Properties of Cottons, 1949 Crop," Beltsville, Md., 1950, 80 pp.
18. Webb, R. W., and Richardson, H. B., "Fiber Measurements of Second-Drawing Sliver Compared with Those of Raw-Cotton in Relation to Yarn Strength and Yarn Appearance," Production and Marketing Administration, Cotton Branch, Nov. 1951.
19. Williams, J. F., Vlases, G., Jr., and Fielding, H., TEXTILE RESEARCH JOURNAL **20**, 719–25 (1950).

(Manuscript received July 14, 1952.)

Development of a Sewability Test for Cotton Fabrics*

E. B. Frederick†

Research and Development Division, Office of The Quartermaster General, Philadelphia, Pennsylvania

Abstract

The development of the seam efficiency test to measure the sewability of a fabric is described. It is shown that this test, which involves the establishment of a ratio between the strength of the original fabric and the strength of the seamed fabric, is more realistic, reproducible, and sensitive than the previous test, which rated a fabric for sewability on the basis of the number of fabric yarns cut per inch during the sewing operation.

Introduction

Some fabrics which meet all of the usual specification requirements cannot be sewn into acceptable garments because of the susceptibility of their yarns to damage by the sewing needle. It appears that the problem is primarily a lack of mobility of the yarns; instead of moving when the needle penetrates the fabric structure, these yarns remain taut and hence are severed.

It has long been recognized that yarn severance detracts from the neatness of garments, since the cut yarns fray during wear and their loose ends appear on the surface of the seam, as shown in Figure 1. Fabric damage by sewing takes on a more serious aspect, however, when it affects the strength of the seam. It is primarily from this standpoint that the Quartermaster Corps has found it necessary to

* This paper was issued as Quartermaster Textile Series Report No. 73.

† Technologist, Textile Materials Engineering Laboratory.

adopt an efficient sewability test for its cotton fabric specifications.

Essentially, the sewability of a fabric, or the degree of its resistance to needle damage, can be determined in two ways. One measure of this property is the proportion of fabric yarns cut by the needle. Another is the loss in fabric strength occasioned by needle damage. The former principle is not new; until recently, a test based on yarn severance appeared in certain military fabric specifications. The particular test used, however, did not approximate actual sewing conditions to the extent necessary for a realistic procedure. The shortcomings of the test became apparent when it failed to detect the poor sewability of a fabric that was so susceptible to needle damage that several manufacturers reported that they could not make garments of acceptable quality from it.

It was proposed that this test be replaced by the seam efficiency test, which is based on strength determinations. This method consists of sewing a seam in the fabric, breaking the fabric at the line of stitching, and establishing a ratio between the original and the seamed fabric strengths. Experience has shown that if this seam efficiency ratio falls below 80%, the fabric has been damaged excessively by the sewing operation.

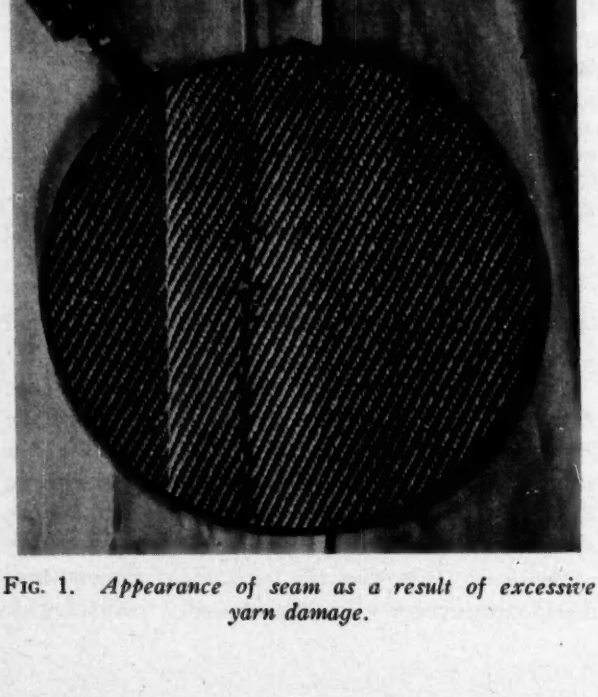

FIG. 1. *Appearance of seam as a result of excessive yarn damage.*

In the evaluation of the seam efficiency test it was found convenient to make, in addition to the strength determinations, a count of the fabric yarns cut in sewing the seam. A much closer correlation was found between yarn severance as obtained in this way and seam efficiency than between yarn severance as measured in the original test and the actual sewing performance of a fabric. This finding suggested that either procedure could be used to determine sewability. Subsequent work on the two methods, however, as described in this report, showed that the seam efficiency test was more realistic, more reproducible, and more sensitive than the yarn severance test, and hence it has been adopted for the evaluation of military fabrics.

Test Methods

Seam Efficiency Test

The details of the seam efficiency test are given elsewhere.* Briefly, the test consists of joining together two cuts of fabric, one 48 in. by 12 in. and the other 48 in. by 8 in., along their length (warpwise) by means of a properly formed 401-LSc-2 seam. The stitch length (number of stitches per inch) and the size and finish of the thread are usually the same as those required by the specification for the end-item in which the fabric is to be used. For heavier fabrics, where the specified thread may not be as strong as the fabric itself, a heavier thread is used. When the seam is sewn, ten pairs of filling breaks (*i.e.*, perpendicular to seam) are made in the sample using a vertical Scott tester. The first of each pair is made in an unsewn portion of the fabric, thus determining the filling breaking strength of the fabric itself. Then, by using guide lines made on the fabric prior to testing, the fabric is placed in the tester so as to break the same filling yarns as before, but with the seam midway between the jaws, thus determining the seamed strength of the fabric. The average of the ten original fabric strengths is then used with the average of the ten seamed strengths to compute seam efficiency according to the equation

$$\text{Seam efficiency} = \frac{\text{seamed fabric strength}}{\text{original fabric strength}} \times 100$$

* Test Method 5110, "Sewability of Woven Cloth: Strength-of-Seam Method," May 15, 1951, from Federal Specification CCC-T-191b, "Textile Test Methods." This is the final test as now conducted. It includes some refinements on the method followed in obtaining the results reported in this paper.

TABLE I. CORRELATION STUDY FABRICS AND SEAM CONDITIONS USED FOR SEAM EFFICIENCY TEST

	Weight (oz./sq. yd.)	No. of mfg. sources	Thread combination Needle	Looper	Stitches per inch	Needle size
Broadcloth	3.2	5	70/3	80/3	14	.036
Poplin	5.0	4	70/3	80/3	14	.036
Oxford	6.5	3	A	A	14	.044
Uniform twill	8.2	3	24/3	60/3	14	.049
Herringbone twill	8.5	10	24/3	60/3	14	.049
Oxford	9.0	3	24/3	60/3	14	.049
Sateen	9.0	3	24/3	60/3	14	.049

Yarn Severance Test

A warpwise seam is made in the fabric, as for the seam efficiency test. The sewing thread is then removed from the seam, and five 1-in. sections of the bottom fabric are cut away to within 1/8 in. of the line of stitching. The warp yarns are then carefully removed to approximately 1/8 in. beyond the line of stitching. During this process, the severed filling yarns in each 1-in. length are counted, and their average is expressed as a percentage of the total number of picks per inch. In Figure 2 is shown a photographic comparison of two fabrics prepared for determination of yarn severance. The upper photograph shows a fabric with little yarn severance, while the lower photograph shows one which has been damaged severely in sewing. Since the fabric yarns most susceptible to needle damage are those running perpendicular to the seam direction, only the filling yarns cut in making a warp seam are counted; warp yarn severance in such a case is usually negligible and almost always significantly less than filling yarn severance. Furthermore, from the standpoint of seamed fabric strength, the cut yarns which run parallel to the seam are of minor importance.

Correlation of the Two Sewability Tests

Procedure

For an analysis of the two sewability tests, seven different fabric constructions, as listed in Table I, were taken from stock at the Philadelphia Quartermaster Depot. Unfortunately, none of the constructions except the herringbone twill were available from a sufficient number of different sources of manufacture to permit a detailed study of each. However, since the materials included covered a rather wide range of the most commonly used military clothing fabrics, they permitted a general analysis of the relative effectiveness of the two sewability tests.

The fabrics were tested as described above, first for seam efficiency and then for yarn severance, using the same seam for each test. The seam conditions used, also shown in Table I, were in some cases the same as those specified for end-items made from the particular material. In other cases they were those required to produce seams stronger than the fabric so that the seam tests would show, not thread strength, but fabric strength at the line of stitching. Sufficient thread tension was used to ensure the proper formation and uniformity of the stitches and to afford a distribution of 40% needle and 60% lower thread in the seam.

Results and Discussion

The results obtained in the two types of sewability tests on the seven fabrics are summarized in Table II.

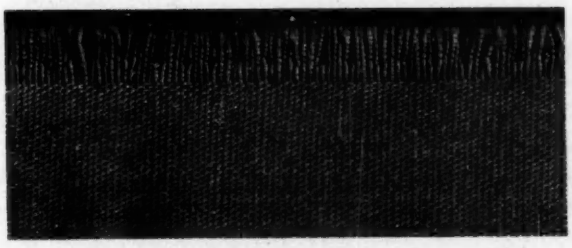

Good sewability

Poor sewability

FIG. 2. *Yarn severance in fabrics of good and poor sewability.*

TABLE II. AVERAGE VALUES OF SEWING CHARACTERISTICS OF ARMY FABRICS

Characteristic	Broadcloth 3.2 oz. (5 contractors)	Oxford 6.5 oz. (3 contractors)	Poplin 5.0 oz. (4 contractors)	Oxford 9.0 oz. (3 contractors)	Herringbone twill 8.5 oz. (10 contractors)	Uniform twill 8.2 oz. (Type I) (3 contractors)	Sateen 9.0 oz. (3 contractors)
Original fabric strength, fillingwise (lbs.)							
Specification requirement	25	50	60	100	85	120	125
Average	29	62	81	92	109	121	153
Minimum–maximum	25–33	52–69	69–90	86–101	81–157	114–136	147–155
Range (% of average)	28	28	26	16	70	18	5
Seamed fabric strength (lbs.)							
Average	18	51	64	85	84	74	134
Minimum–maximum	12–27	46–61	46–75	75–96	56–109	61–84	129–137
Range (% of average)	88	29	46	24	63	4	6
Seam efficiency (%)							
Average	60	83	78	92	78	63	88
Minimum–maximum	41–80	75–87	66–89	88–95	56–97	54–72	88–88
Range (% of average)	66	15	29	8	53	29	0
Filling yarns cut per inch (%)							
Average	14	19	8	2	15	17	2
Minimum–maximum	0–28	10–27	1–13	0–4	4–34	9–26	2–2

This table shows that although all of the fabrics (except 9.0-oz. Oxford) well exceeded, on the average, the specified breaking strength, several of them showed a low seamed strength and consequently a low seam efficiency value. The table also shows that the seam efficiency test is applicable to fabrics over a rather wide range of fabric weights and strengths.*

The significance of the average data in Table II can be demonstrated better if the values for the various contractors on a single fabric construction are shown. This is done in Table III for the broadcloth fabric, which was represented by five contractors. Here it can be seen that four of the five fabrics were subject to yarn severance of from 5% to 28%. It is significant that of the five submissions of broadcloth, the fabrics from manufacturers *D* and *K* showed the highest values for yarn severance and next-to-the-lowest for seam efficiency; these were materials that could not be made into shirts in production sewing because of their poor resistance to needle damage.

In general, the data in Tables II and III indicate a correspondence between the seam efficiency of a fabric and the number of filling yarns severed by the needle. Some exceptions must be made to this observation, however. The type of fabric break obtained at the seam, as illustrated in Figure 3, explains some of these exceptions. A direct break, shown in the upper photograph, is the type normally experienced with fabrics of poor sewability. Such breaks were obtained with fabrics from manufacturers *D* and *K* and, to a lesser extent, *Q* (Table III). Occasionally, however, a low coefficient of friction among the yarns will cause them to slip, as shown in the middle photograph, resulting in seam failure at a

* In exceptional cases, fabrics may be found of such high strength that any thread with which it is practical to sew them will fail instead of the fabrics themselves in the seam strength test. If seam efficiency is computed in such cases (where the seam strength value represents thread strength rather than seamed fabric strength), it will indicate a poorer sewability than the fabric actually has. For fabrics as strong as these, a true seam efficiency value is not only impossible to obtain, but unnecessary. The only important consideration in such fabrics is that the neatness of their seams will not be marred by the appearance of loose ends of the fabric yarns cut during sewing. Hence, where realistic seam efficiency values cannot be obtained because of sewing thread failure, yarn severance is a satisfactory criterion for sewability.

TABLE III. COTTON BROADCLOTH, KHAKI NO. 1, 3.2 OZ.

Characteristic	Manufacturer *I*	*D*	*K*	*C*	*Q*
Original fabric strength, fillingwise (lbs.)	28	27	25	33	31
Seamed strength (lbs.)	12	14	13	27	22
Seam efficiency (%)	41	52	51	82	71
Filling yarns cut per inch (%)	0	22	28	5	13

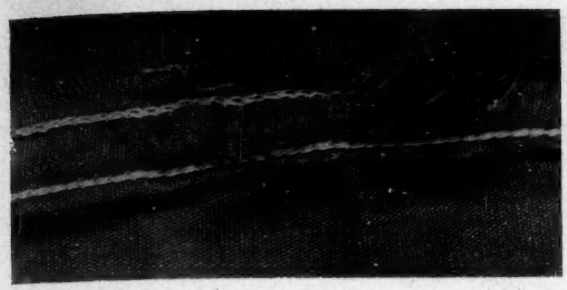

Break

Slippage

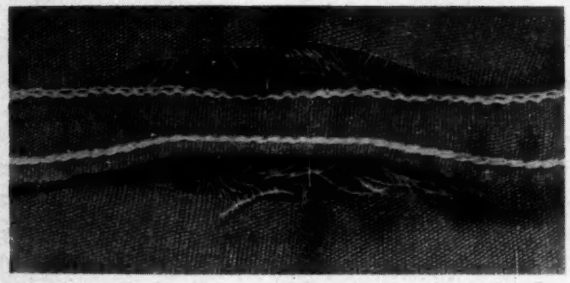

Slippage and break

FIG. 3. *Types of seam failures.*

very low load even though none of the yarns are broken. Such a case is exemplified by the fabric from manufacturer *I*, which showed no filling yarn severance, but at the same time had the lowest seam efficiency (41%) of all the five fabrics in Table III. Under optimum conditions there will be some slippage of the yarns before the break occurs, as shown in the lower photograph of Figure 3. This was the case with the fabric from manufacturer *C* (Table III). These observations indicate that yarn severance is not the only factor determining seam durability, and that, thus, the seam efficiency test, whose results reflect the contribution of other fabric properties such as yarn slippage, is to be preferred as a sewability test.

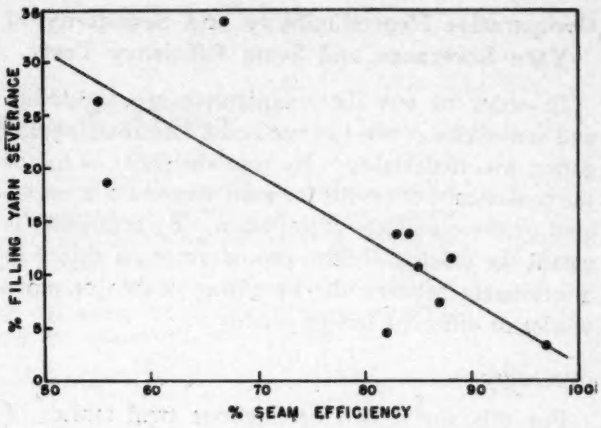

FIG. 4. *Relationship between filling yarn severance and seam efficiency of herringbone twill fabric from different manufacturers.*

The degree of correlation between seam efficiency and yarn severance is also limited by the fact that some fabric yarns are damaged, but not wholly severed, by the needle. It is impossible, by any method depending upon observation alone, such as the yarn severance test, to determine the contribution of these partially severed yarns to lowered fabric strength after sewing. Thus, in the yarn severance test only completely broken yarns are counted. The seam efficiency test, on the other hand, which is based on an actual determination of strength loss, provides a more complete picture of the damage done to the fabric by the sewing operation.

In spite of these known limitations, an attempt was made to correlate the two sewability tests, using as a basis the herringbone twill fabric, which was the only one represented by a sufficient number of different manufacturers (ten) to permit a statistical relationship to be established. The average values for the fabrics from each of the ten manufacturers, which ranged from 97% to 55% for seam efficiency and from 4% to 34% for filling yarn severance, are shown graphically in Figure 4. A rank correlation of these data resulted in a coefficient of $\sigma = .71$. It is thus evident that a realistic method of determining yarn severance is to some degree a measure of fabric sewability, but it cannot be relied upon to the same extent as a test like that for seam efficiency, which is based on an actual measurement of the damage done to the fabric in sewing by means of strength tests.

Comparative Reproducibility and Sensitivity of Yarn Severance and Seam Efficiency Tests

In order to test the comparative reproducibility and sensitivity of the two methods, a further investigation was undertaken. By reproducibility is meant the consistency of results for each procedure as evaluated by the coefficient of variation. By sensitivity is meant the validity of each procedure or its ability to discriminate between the sewability of two or more fabrics of different sewing quality.

Procedure

For this study, two herringbone twill fabrics of different sewing qualities were selected, from which ten sections were cut. Seven specimens were taken from each section for tests of both seam efficiency and yarn severance. The seam efficiency test was the same as that described above. For the determination of yarn severance, unbroken sections of the same seam made for the seam efficiency test were cut from the fabric and the sewing thread was removed. The average number of filling yarns severed, as determined by the method described above, was expressed as a percentage of the total number of filling yarns.

Results and Discussion

The results of these experiments are analyzed in Table IV. The average values in Table IV follow the general trend established by most of the earlier data, in that the fabric with the higher seam efficiency (fabric *P*) also showed less yarn severance. Statistical analysis of the individual values comprising these averages, however, showed that the reproducibility and sensitivity of the seam efficiency test is much better than that of the yarn severance test. The fact that the coefficient of variation of the latter is approximately four times that of the seam efficiency test indicates the much poorer consistency of yarn severance values. Not only is the seam efficiency test the less variable of the two methods, it is also approximately eight times as sensitive, according to this experiment, in discriminating between fabrics of different sewing qualities. The discrimination factor, as shown in the table, is the ratio of the differences of fabric averages to the average variability of the values within each fabric, taking cognizance of the difference among sections.

In order to determine the 95% control limits as a measure of the relative validity of the two tests, five specimen averages were taken from a randomly selected section of fabric *P*. Taking cognizance of the differences among average section values and the average variability of the seven specimens within a section, the limits of error were found to be 10% of the over-all average for the seam efficiency test and 50% for the yarn severance test—that is to say, 95% of the time a given seam efficiency value will be within 10% of the over-all average, whereas a yarn severance value can be off as much as 50% from the over-all average.

TABLE IV. COMPARISON OF SEAM EFFICIENCY AND YARN SEVERANCE METHODS FOR EVALUATING SEWABILITY*

	Seam efficiency (%)	Yarn severance (%)
Average values		
Fabric *P*	82.6	16.8
Fabric *Q*	77.2	19.1
Combined average	80.0	18.0
Reproducibility (including differences among sections)		
Coefficient of variation	13.3	57
Sensitivity		
Discrimination factor	9	1.1
Sensitivity for seam efficiency / Sensitivity for yarn severance	8.2	
Fabric P		
95% control limits (ave. of 5 specimens, 1 section)		
Upper control limit (UCL)	91.4	25.2
Lower control limit (LCL)	73.8	8.4
Limits of error from over-all average (% ave.)		
$\frac{\text{UCL or LCL} - \overline{\overline{X}}\ (100)}{\overline{\overline{X}}}$	10	50

* Ten sections of seven specimens each were tested per fabric.

Summary

The seam efficiency test, as described in this report, is a reliable method for determining the sewability of fabrics. Its effectiveness has been proved in laboratory experiments, and it has stood the test of time as an acceptance procedure. It is more realistic than the yarn severance test, an alternate method of determining sewability, in that it involves reproducing an actual sewing operation. Studies of the comparative reproducibility and sensitivity of the two methods has shown the superiority of the seam efficiency test.

(*Manuscript received August 6, 1952.*)

Letters to the Editor

Short communications in the form of Letters to the Editor are intended to provide prompt publication of significant new research results and to permit an exchange of views on papers previously published in the Journal. These communications are not submitted to formal review as are research papers, and the editors do not assume any share of the author's responsibility for the information given or the opinions expressed. When work previously published in the Journal is the subject of critical comment, the authors of the original paper are given an opportunity to submit a reply, which will be published concurrently when possible.

The Homogeneous Degradation of Cellulose

Hercules Powder Company
Experiment Station
Wilmington, Delaware
June 26, 1952

To the Editor
Textile Research Journal

Dear Sir:

I have read the paper "Cellulose Studies: Part XVIII: The Homogeneous Degradation of Cellulose in Phosphoric Acid," by Bauer and Pacsu (Textile Research Journal 22, 397 (1952)) with a great deal of interest. The facts uncovered by these workers are undoubtedly important. However, the whole interpretation hinges on the question whether or not native cellulose is molecularly dispersed in 85% phosphoric acid.

In this connection, I fear that my opinions are misrepresented by a quotation lifted out of context: "Each molecule is molecularly dispersed and only occasionally is associated with one of its neighbors. Any such association, if formed, is soon broken by thermal agitation." (In "Cellulose and Cellulose Derivatives" (E. Ott, editor), New York, Interscience Publishers, Inc., 1943, p. 855.) This was a very general statement in a section devoted to cellulose derivatives, and was qualified in the same paragraph as follows: "The arguments against the existence of micelles in most solutions will, however, be outlined." Later, on p. 890, dealing specifically with phosphoric acid-cellulose solutions, I stated, "Seemingly, cellulose of any chain length may be dissolved in HCl or H_2SO_4 solutions, but only the lower-molecular-weight products are soluble in H_3PO_4 solutions." I do not feel that this can support the premise that any cellulose dispersion in phosphoric acid is a true solution.

I would like to recommend strongly to workers in the field of homogeneous cellulose hydrolysis that they apply independent checks to their solutions to make sure that they are molecularly dispersed. As criteria for the absence of remnants of the cellulose crystalline structure such as those demonstrated in acid hydrolyzates of cellulose by Hock, Morehead, Rånby, and others, I suggest the use of high-speed centrifugation, flow birefringence, electron microscopy, and light scattering. In efforts I have made to secure reasonably good solutions of cellulose in phosphoric acid, I was forced to resort to the use of regenerated cellulose.

I have discussed these points with Prof. Pacsu and Dr. Bauer, and I believe that they concur in the suspicion that their solutions contained undispersed material.

H. M. Spurlin

T. R. I. Annual Meeting

THE TWENTY-THIRD ANNUAL MEETING of Textile Research Institute will be held in the Main Ballroom, Hotel Commodore, New York City, on Monday and Tuesday, November 17 and 18, 1952. The program for the meeting follows.

Monday, November 17

Chairman: James H. Wakelin, Director of Research, T. R. I.

9:00 A.M.—Registration

10:00 A.M.—Morning Session

"The Elasticity of Cotton," by Helmut Wakeham, T. R. I.

"Studies on the Resilience and Crease-Resistance of Fabrics," by R. G. Stoll, Celanese Corporation of America

12:30 P.M.—Luncheon

2:00 P.M.—Afternoon Session

"Fiber-Forming Phenomena with Certain Proteins," by E. H. Mercer, Commonwealth Scientific and Industrial Research Organization, Australia (Visiting Fellow at T. R. I.)

"Fundamental Improvements in Regenerated Cellulose Fiber Structure," by Nicolas Drisch and Leo Soep, Comptoir des Textiles Artificiels, Paris, France (paper to be given by Dr. Soep)

4:00 P.M.—Meeting of T. R. I. Board of Trustees

Tuesday, November 18

Chairman: John H. Dillon, Director, T. R. I.

10:00 A.M.—Morning Session

"Studies of Aging in Worsted Processing," by Harris M. Burte and Richard O. Steele, T. R. I. (paper to be given by Dr. Steele)

"Radioactive Tracer Techniques in Textile Research," by Howard J. White, Jr., T. R. I.

"Factors Influencing Clothing Comfort," by O. C. Wetmore, Textile Research Division, Textile Fibers Department, E. I. du Pont de Nemours & Company

Luncheon—Special program to be announced later

Exhibits, West Ballroom

Anderson Machine Shop, Inc.	Yarn uniformity testers
Brabender Corporation	Conditioning ovens
Brookfield Engineering Company	Viscometers
Brush Development Company	Yarn uniformity testers
Carbide and Carbon Chemicals Company	Dynel
Custom Scientific Instruments, Inc.	Abrasion tester
E. I. du Pont de Nemours & Company, Inc.	Fibers
Hart Moisture-Meters, Inc.	Moisture measuring instruments
Instron Engineering Corporation	Tensile strength tester
Osgood Engineering Company	Optical instruments and electronic moisture indicators
Tennessee Eastman Company	New fibers
Thwing-Albert Instrument Company	Tensile tester
Uster Corporation	Yarn uniformity testers
Virginia-Carolina Chemical Corporation	Vicara